Further Studies of Dothistromin Toxin Genes in the Fungal Forest Pathogen *Dothistroma septosporum*

A thesis presented in partial fulfillment of the requirements

for the degree of Master of Science in Biochemistry

at Massey University, Palmerston North, New Zealand

Zhilun Feng

2007

ABSTRACT

The fungal pathogen *Dothistroma septosporum* is the main causal agent of *Dothistroma* (red-band) needle blight, which is a devastating foliar disease of a wide range of pine species. Dothistromin is a difuranoanthraquinone toxin produced by *D. septosporum* and is considered as a possible virulence factor for the disease. Based on the similarity of chemical structure between dothistromin and aflatoxin (AF) /sterigmatocystin (ST) precursors, nine putative dothistromin biosynthetic genes have been identified, which are homologous to their corresponding genes in the AF/ST gene clusters. However, in contrast to all 25 AF biosynthetic genes tightly clustered in one region (70-Kb) of the genome, the dothistromin gene clusters are located on a 1.3-Mb chromosome and separated into three mini-clusters along with non-dothistromin genes.

The *dotC* gene, located in the mini-cluster 1, is predicted to encode a major facilitator superfamily (MFS) membrane transporter involved in secretion of dothistromin. In this work, by constructing DotC-eGFP fusion protein containing mutants, the subcellular localization of the DotC protein was determined to be mainly targeted to the plasma membrane. The biological function of the *dotC* gene was characterized by targeted gene disruption. The *dotC* gene disrupted mutants showed a significant reduction of dothistromin production in both the medium and mycelium. In addition, the exponential growth of *dotC* null mutants was inhibited when exogenous dothistromin was presented and these mutants also displayed more sensitivity than the wild type strain to exogenous dothistromin. The results indicated that the DotC protein is a membrane associated protein and might have a role in dothistromin production and be involved in secretion of exogenously supplied dothistromin toxin.

Two novel dothistromin biosynthetic genes, *norA/B* and *verB* (partial sequence), were identified by using degenerate PCR and *D. septosporum* genomic library screening. The putative NorA/B and VerB are postulated to encode a dehydrogenase and a desaturase, respectively and are similar to AF/ST genes. These findings further confirmed that the dothistromin shares biosynthetic pathway steps with AF/ST.

ACKNOWLEDGEMENTS

First and foremost, I would like to gratefully acknowledge my supervision Dr Rosie Bradshaw for her constant encouragement and guidance during this research. Thanks for your kindness and patience to make the last two and half years be the wonderful and inspiring time in my life.

It is a pleasure to thank my lab colleagues. Thanks for Shuguang always ready with helpful technical support and advice. Thanks for Ping sharing her knowledge to give me an easy beginning in the lab. Thanks for Arne kindly providing GFP and microscopy technical support. Thanks for Naydene for her ELISA support and English help. Thanks for Yanan and Justine, it was so happy to work together in the "fungaljungle".

I would also like to thank Dr Kathryn Stowell for giving me very useful advice when I first stepped into the IMBS. Thanks for Kathy Hamilton arranging my study course. Many thanks for other staff working in the IMBS, who gave me help over the duration of my studies.

Finally I would like to thank my parents and my wife. With your understanding and encouraging, I could easily stay by myself in Palmy, which is a quiet and small town far away from Auckland and China.

ABBREVIATIONS

ABC transporter	ATP-binding cassette transporter
AF	aflatoxin
amp^r	ampicillin resistance
bp	base pair
cm	centimeter
°C	degree celsius
dATP	deoxyadenosine triphosphate
DMSO	dimethyl sulphoxide
DNA	deoxyribonucleic acid
DNase	deoxyribonuclease
dNTP	deoxynucleotide triphosphate
Doth	dothistromin
Fig.	figure
g	gram
GFP	green fluorescent protein
eGFP	enhanced green fluorescence protein
IPTG	isopropyl-β-d-thiogalactoside
Kb	kilobase pair
L	litre
M	molar
Mb	megabase
MFS transporter	major facilitator superfamily transporter
ml	milliliter
mM	millimolar
OD_{600}	optical density at 600 nm
ORF	open reading frame
RNA	ribonucleic acid
RNase	ribonuclease
rpm	revolutions per minute
SDS	sodium dodecyl sulfate
ST	sterigmatocysin
TMD	transmembrane domain
µl	microlitre
µM	micromolar
µg	microgram
UV	ultraviolet
v/v	volume per volume
WT	wildtype
w/v	weight per volume
X-Gal	5- bromo-4-chloro-3-indolyl-β-D-galactopyranoside
~	approximate

TABLE OF CONTENTS

List of Figures

List of Tables

CHAPTER ONE: INTRODUCTION

1.1 DOTHISTROMA NEEDLE BLIGHT AND *DOTHISTROMA SEPTOSPORUM*

Dothistroma (red-band) needle blight is a devastating foliar disease of a wide range of pine species. The fungal pathogen *Dothistroma septosporum* (Barnes *et al.*, 2004), which infects and kills pine needles, is the main causal agent of this notorious disease. Premature defoliation caused by this fungus has resulted in complete failure of some ponderosa pine plantings in the U.S.A and the *Pinus radiata* pine plantations of several countries such as New Zealand, Chile and Australia have also suffered severe economic losses (Gibson, 1972). The aim of this section is to give a brief overview of the pathological and epidemiological features of this disease.

1.1.1 Dothistroma needle blight: the red band blight

Dothistroma needle blight has its predominant symptom in distinct brick-red bands (1-3mm wide) around the needles that can be observed within weeks of infection and can sometimes still be seen after the needles have died, earning its common name: red band needle blight (Fig. 1.1). The red color is due to production of the mycotoxin dothistromin by the fungus (Shain and Franich, 1981). After the fungus infects via the stomata, initial symptoms appear as water-soaked lesions on the needles. Black fruiting bodies develop at these infection sites, which then are surrounded by a red band in later stages of the disease. Adjacent to those red bands are areas of yellow necrotic tissue and sometimes a dark green tissue that contains highly lignified cells flanking the yellow region (Franich *et al.*, 1986). The end of the needle beyond the band dies and eventually the whole needle may develop extensive necrosis (browning) and drop prematurely

(Edwards and Walker, 1978). Severe levels of disease can lead to tree death.

Figure 1.1: Infected pine needles.

A

B

A. Infected needles with red bands.

B. Some infected needles develop extensive necrosis in a pine tree.

Dothistroma needle blight is an economically significant disease in many species of *Pinus*, particularly in *Pinus radiata* D.Don, which has a crucial role in plant resources, such as wood. The most serious impacts of the disease upon economic losses are reduction of wood yield since defoliation of needles normally retards growth of those pines rather than mortality (Gibson, 1972). The severity of the disease appears to be related to a favorable climate in the southern hemisphere where the pest and host trees are exotics. Therefore, countries such as New Zealand, Australia, Chile and Kenya, where commercial pine plantations are predominantly monocultures of susceptible hosts, have suffered huge economic losses (Gibson, 1972; Ivory, 1967; Vanderpas, 1981). For instance, *Pinus radiata* makes up approximate 90% of the 1.8 million hectares of managed tree plantations in New Zealand and the forest industry contributed to 11.2% of New Zealand's total export earnings in 2005 (www.maf.govt.nz/statistics). Dothistroma needle blight has been recorded in most parts of the north island of New Zealand and some parts of south island (Otago, Nelson) as well (Bulman. *et al.*, 2004). Thus, the disease indeed has been a serious threat and had significant impacts to forest industry of New Zealand although the exact economic losses are hard to estimate. In the

northern hemisphere where the host trees are native, a few outbreaks of needle blight have been reported in the USA since the 1960s and sporadic outbreaks reported in Europe. However, Woods *et al.* (2003) reported the disease had increased in the northern hemisphere recently. They found the disease symptoms in 93% of 700 stands of young (less than 20 years) lodgepole pines (*Pinus contorta var. latifolia*) covering 21,000 hectares in northwest British Columbia, Canada. Mortality was seen in 6.2% of the surveyed area and even in over 50-year-old lodgepole pine trees. They suggested that a local increase in summer precipitation appeared to be responsible for the outbreak of this severe disease (Woods *et al.*, 2005).

1.1.2 *Dothistroma septosporum*: the causal agent of blight

The taxonomy of the causal agent of blight has had a confused history. In 1941, Hulbary described the red band fungus in the USA and named it as *Dothistroma pini* Hulbary (Bradshaw, 2004; Gibson, 1972). This was the most common name used to describe this fungus in early studies. Recently, Barnes and co-workers analyzed a total of 32 isolates of *Dothistroma* pathogens from various locations in 13 countries representing a global distribution. They compared DNA sequences for four different regions of the genome in those isolates and they concluded that red band blight of *Pinus* is caused by two distinct species: *D. septosporum* and *D. pini*. The former fungus has a worldwide distribution and is the causal agent of the blight that has damaged plantations of *Pinus radiata* in the southern hemisphere, while the other, *D. pini*, is restricted to the North-Central USA. Therefore, the name *D. pini* used in the early research is actually now *D. septosporum* in most cases (Barnes *et al.*, 2004).

1.1.3 The infection process

Asexual conidiospores from the black fruiting bodies are the most important spore form for dispersal of the fungus and account for the movement of the pathogen over short distances. Spores land on needles of susceptible hosts and then penetrate through the

stomatal pores (Gilmour, 1981; Karadzic, 1989). After penetration, the hypha is confined almost exclusively to the mesophyll and spread only a few millimeters from the site of penetration. The host cells collapse after 32-114 days and needle symptoms and stromata (fruiting bodies) appear (Ivory, 1972; Peterson, 1973).

Environmental conditions affect the incidence of the disease. Water appears to be essential for the dispersal of conidia. This is confirmed by some previous studies, which indicated the maximum conidial dispersal took place under light rain or heavy mist conditions (Dubin and Walper, 1967; Peterson, 1973). Light is thought to be another factor to influence the infection. Low light intensity dramatically reduced the development of symptoms of the disease although the germination of conidia and early growth was not affected (Gadgil and Holden, 1976). Temperature is less important than humidity and light, as the disease can be developed between 5°C and 26 °C. Gadgil (1984) determined the optimal conditions for infections as 20°C / day and 12 °C / night at continuous leaf wetness and a minimum light intensity of 133W/ m^2.

1.1.4 Current methods of disease control

Aerial spraying of copper-based fungicides and breeding resistant trees are the two current main methods to control this disease. Since the 1970s, two fungicides, copper oxychloride and cuprous oxide have been widely accepted with their effective biological function of inhibiting germination of spores at relatively low cost (Gibson, 1974). Whyte (1976) has examined the benefits of spraying those chemical agents; his results showed that the final wood yield of infected 13-year-old *P. radiata* was 30-40 m^3 / hectare more from a sprayed area than from an untreated area. The other way to control the disease is breeding *D. septosporum* resistant strains of *P. radiata.* Some species have been found with natural resistance to *D. septosporum* such as *P. sylvestris* (Gibson, 1974). In addition, the resistance to *D. septosporum* is variable even within the same species (Peterson, 1984). Resistant strains may reduce mean strand infection by 15% and lower cost by 56% compared with chemical sprays (Carson, 1989). These

strains can be used in areas with high infection risks. However, it is reported that the resistant strains have a relatively lower wood yield in low infection risk areas (Dick, 1989).

1.2 DOTHISTROMIN TOXIN

Dothistromin is a difuranoanthraquinone toxin produced by *D. septosporum* (previously called *D. pini*) as well as by several *Cercospora* species including the peanut pathogen *C. arachidicola* (Bassett *et al.*, 1970; Stoessl and Stothers, 1985). This toxin is considered a fungal secondary metabolite and thought to be a possible virulence factor for the disease. Several dothistromin biosynthetic genes have been characterized based on its dramatic structural similarity to the potent carcinogen aflatoxin's precursors and further studies on this toxin will be carried on in this project.

1.2.1 General features of dothistromin

Dothistromin is a polyketide, which was first extracted from *D. septosporum* and was subsequently isolated from several *Cercospora* species and *Mycosphaerella laricina*. This toxin, distinctively red in color, was isolated from lesions of infected pine needles and from cultures (Bassett *et al.*, 1970). Shain and Franich (1981) injected purified dothistromin into pine needles and reproduced the symptoms of disease. This experiment suggested a critical role for dothistromin as a pathogenicity factor in Dothistroma needle blight. Host defences to invading pathogens usually contribute to the symptoms of disease. This also can be seen in Dothistroma needle blight. Previous research indicated that dothistromin is broken down in the needle tissue to oxalic acid and CO_2, with only 10-20% of the toxin remaining after 24 hours. However, the necrotic lesion still continues to expand although most of the dothistromin has been degraded. This suggests that damage of the needle is due to the plant's defense response rather than direct toxicity of dothistromin (Franich *et al.*, 1986). Furthermore, in *P.*

radiata, the defense response to *D. septosporum* has been observed even in the absence of dothistromin (Hotter, 1997). A recent study found that a dothistromin-deficient mutant geminated on the pine needle surface and fruiting bodies were observed on a necrotic needle which had been inoculated with the dothistromin deficient mutant (Barron, 2006). In view of those findings, the dothistromin seems like a possible virulence factor rather than a pathogenicity factor.

Light and oxygen are required for dothistromin biosynthesis. Previous studies showed that dothistromin probably reacts with oxygen molecules and generates reactive oxygen species (ROS). Youngman and Elstner (1984) have illustrated that dothistromin produces ROS superoxide and hydrogen peroxide and can cause lipid peroxidation and breakdown of photosynthetic pigments. Another possibility of the mode of action of dothistromin is that it specifically interacts with cellular components that function only in the light (Debnam *et al.*, 1994). However, since the dothistromin is rapidly degraded in the presence of light, the role of light in the dothistromin toxicity is far more confused.

The toxicity of dothistromin to humans has been investigated. Evidence has shown that dothistromin has significant mutagenic activity in an Ames assay but mutagenic activity is weak (Elliott *et al.*, 1989; Ferguson *et al.*, 1986). Interestingly, Skinnider *et al.* (1989) found that dothistromin induces a dose-dependent increase in sister-chromatid exchange frequency in Chinese hamster ovary cells and human lymphocytes. To forestry workers, wearing protective clothing is recommended when working in infected areas, particularly in wet weather.

1.2.2 Biochemical aspects of dothistromin

Using spectroscopic and crystallographic methods, the structure of dothistromin has been illuminated (Bear *et al.*, 1972; Gallaghe and Hodges, 1972). As shown in Fig. 1.2, the chemical structure of dothistromin is remarkably similar to versicolorin A and B,

aflatoxin (AF) precursors, produced by *Aspergillus parasiticus*. In a further study of the biosynthesis of dothistromin, C^{13} nuclear magnetic resonance (NMR) illustrated that the labeling pattern in the bistetrahydrofurano side chain is identical to that found in aflatoxin and sterigmatocystin (ST, a precursor of AF, the carcinogenic mycotoxin produced by *A. nidulans* (Shaw *et al.*, 1978). Moreover, several precursors of AF were detected in the culture filtrates of dothistromin-producing species (Danks and Hodges, 1974). Combining this evidence, it was proposed that dothistromin shares biosynthetic pathway steps with AF/ST.

Figure 1.2: Chemical structures of aflatoxin B_1, versicolorin A, versicolorin B, and dothistromin.

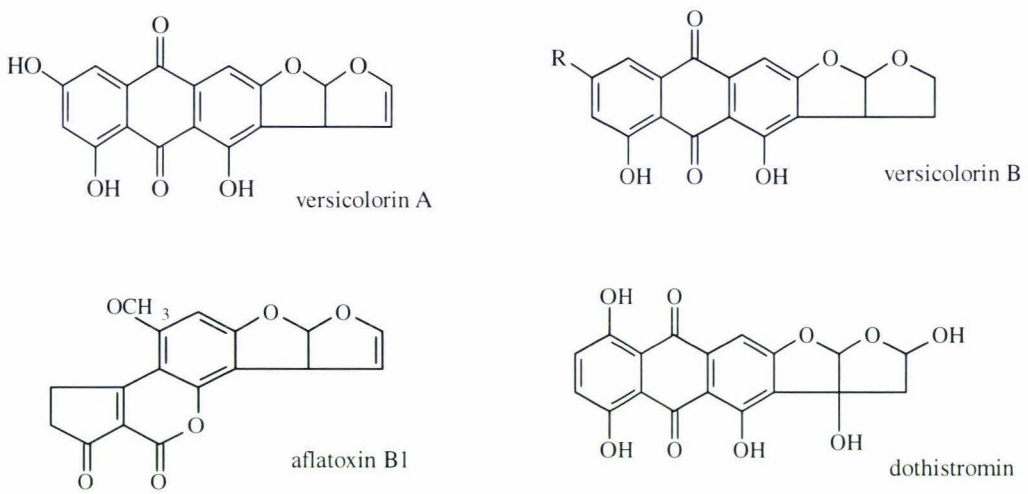

1.2.3 Dothistromin biosynthetic gene clusters

1.2.3.1 Fungal gene clusters of AF/ST

Fungal toxin biosynthesis genes are generally clustered together and key regulatory genes are often involved in the cluster (Yu *et al.*, 2004a; Yu and Keller, 2005; Yu *et al.*, 2004b). Research has been carried out on gene clusters for AF and ST biosynthesis in

Aspergillus species because of their serious impact upon food contamination. In 1979, Bennett isolated two mutants *aflM* (*ver*-1) and *aflD* (*nor*-1) of *A. parasiticus* that were blocked in aflatoxin biosynthesis and accumulated the brightly colored compounds versicolorin and norsolorinic acid, providing a detectable phenotype for identification screening (Bennett, 1979). Genetic analysis showed that genetic linkage did exist between the *aflM* (*ver*-1) and *aflD* (*nor*-1) genes with the regulatory gene *aflR* in cosmid clones and provided the first clue to identify the aflatoxin pathway gene cluster (Skory *et al.*, 1993; Trail *et al.*, 1995). The latest finding shows that 25 aflatoxin pathway genes are clustered in an 70-Kb *A. parasiticus* region of genomic DNA along with four sugar utilization genes (Yu *et al.*, 2004b). While, in the ST gene cluster, most ST genes are orthologues of AF genes, they are arranged in a different order (Fig. 1.3; Keller and Hohn, 1997).

1.2.3.2 Dothistromin gene clusters

Based on the similarity of the biosynthesis pathway between dothistromin and aflatoxin, aflatoxin genes were used as hybridization probes to identify dothistromin genes from a *D. septosporum* genomic library. For example, clone λCGV1 (mini-cluster 1, Fig. 1.3) selected from *D. septosporum* genomic library showed a strong hybridization to the probe *aflM* (*ver*-1). The λCGV1 clone contains 13.3 Kb of *D. septosporum* genomic DNA, with five predicted genes: *dotA*, *dotB*, *dotC*, *dotD* and *ddhA* (Bradshaw *et al.*, 2002).

Figure 1.3: Synteny comparison of gene clusters.

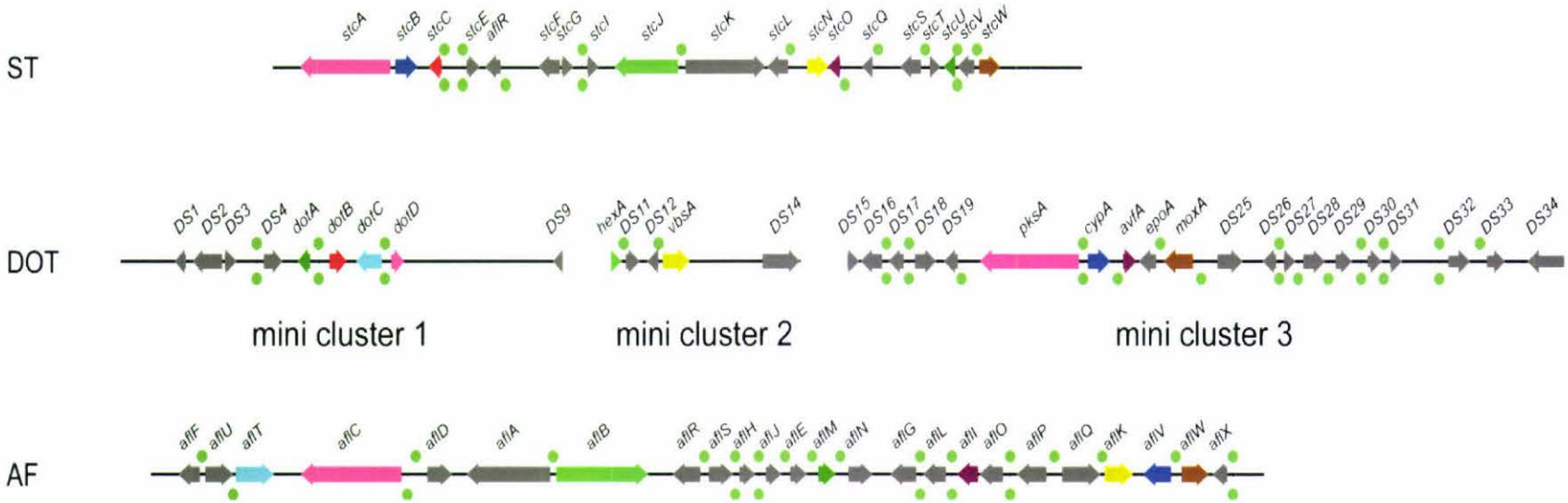

The three dothistromin mini-clusters are compared with the *A. nidulans* sterigmatocystin (ST, Accession No. ENU 34740) and *A. parasiticus* aflatoxin (AF, Accession No. AY371490) gene clusters. Genes predicted to have similar functions in the three fungi are in the same color. Putative AflR (regulatory protein) binding sites in promote regions of the genes are indicated with stemmed balls: those above the genes indicate the sequence $TGGN_5CGR$ and those beneath the genes indicate the sequence $TGGN_{11}CGR$. The numbers of binding sites in the individual regions are not shown.

This figure was prepared by S. Zhang (Zhang *et al.*, 2007)

In addition, using *aflC* (*pksA*) gene from *A. parasiticus* as a hybridization probe, the λ KSA clone (mini-cluster 3) was isolated from a *D. septosporum* genomic library. Five other genes were identified in this clone: *pksA*, *cypA*, *avfA*, *epoA* and *moxA* (Bradshaw *et al.*, 2006). Moreover, using degenerate PCR (primers designed by alignment of Vbs polypeptide sequences from *Aspergillus* species), the *vbsA* gene was identified on a 14-Kb contig (mini-cluster 2) along with a partial fragment of the *hexA* gene at one end (Zhang *et al.*, 2007).

The arrangement of all identified dothistromin biosynthetic genes and adjacent non-dothistromin genes is shown in Fig. 1.3 and their putative functions are listed in Table 1.1. Comparing the dothistromin genes with AF/ST gene clusters, the dothistromin genes are located on a 1.3-Mb chromosome and separated into three mini-clusters instead of being tightly clustered in one region (70-Kb) of the AF/ST genes (Zhang *et al.*, 2007). These results suggest that the regulation of dothistromin biosynthesis could be different to AF/ST. Except the *epoA* gene, all the other dothistromin genes have orthologs in AF/ST gene clusters.

Of the dothistromin biosynthetic genes mentioned above, the *dotA* (encoding a ketoreductase), *pksA* (encoding a polyketide synthase) and *vbsA* (encoding a versicolorin B synthase) genes were mutated by targeted gene replacement. The results illustrated that all the three genes were critical for the toxin biosynthesis (Bradshaw *et al.*, 2002; Bradshaw *et al.*, 2006; Zhang *et al.*, 2007). However, mutation of the unique *epoA* gene (encoding an epoxide hydrolase) of dothistromin genes did not show any effect on the toxin synthesis (Jin, 2005).

In the mini-cluster 1, the *dotC* gene is predicted to encode a major facilitator superfamily (MFS) transporter (Bradshaw *et al.*, 2002) to secrete the toxin. From the putative function, the *dotC* gene is actually not a dothistromin biosynthetic gene and its biological function will be characterized in this research.

Table1.1 Characterization of genes identified in the three dothistromin gene mini-clusters.

Gene	Size[1] (aa)	Putative function (domain)[2]	Highest BLAST match[3]	Genbank accession no.	Species	Indicative E-value	*A. parasiticus* AF cluster		*A. nidulans* ST cluster	
							Probable homolog[4]	% aa identity	Probable homolog[4]	% aa identity
DS1	271	unknown	UG	AACS01000171	*Coprinopsis cinerea*	9e-08				
DS2	646	chitin synthase	UG	AE017346	*Cryptococcus neoformans*	8e-10				
DS3[5]	157	unknown	UG	XM_001227301	*Chaetomium globosum*	1.6				
DS4 (*ddhA*[5])	469	UDP-N-acetyl-D-mannosaminuronate dehydrogenase	UG	AP007161	*A. oryzae*	1e-110	-	-	-	-
dotA	263	ketoreductase	*stcU*	EAA61594	*A. nidulans*	2e-112	*aflM* (M91369)	80.2	*stcU* (L27825)	79.1
dotB	414	oxidase	UG	XM_743185	*A. fumigatus*	5e-59	-	-	*stcC* (U34740)	24.0
dotC	602	toxin pump	UG	XM_749669	*A. fumigatus*	8e-141	*aflT* (AF268071)	31.2	-	-
dotD	322	thioesterase	*pksP*	XM_001261234	*Neosartorya fischeri*	4e-67	*aflC* (L42766)	34.8	*stcA* (U34740)	37.9
DS9[6]	71	cytoskeleton assembly protein	*SLA2*	AJ884600	*Xanthoria parietina*	8e-16	-	-	-	-
hexA[6]	321	fatty acid synthase	*hexA*	AY510454	*A. nomius*	1e-20	*aflA* (AF391094)	48.8	*stcJ* (AN7812)	41.3
DS11	304	unknown	UG	AP007174	*A. oryzae*	3e-33	-	-	-	-
DS12	262	unknown (DUF1772)	UG	AP007159	*A. oryzae*	1e-30	-	-	-	-
vbsA	643	versicolorin B synthase	*vbs*	AY510454	*A.nomius*	0.0	*aflK* (AF169016)	72.0	*stcN* (AN7812)	69.1
DS14	702	potassium channel	*toka*	AJ510245	*N. crassa*	2e-116	-	-	-	-
DS15[6]	228	unknown	UG	XM_001217330	*A. terreus*	9e-26	-	-	-	-
DS16	482	unknown	*AocAR*	AB240531	*A. oryzae*	9e-46	-	-	-	-
DS17	274	unknown	UG	XM_387929	*Gibberella zeae*	1e-20	-	-	-	-
DS18	498	unknown (PCI)	UG	AP007167	*A. oryzae*	4e-176	-	-	-	-
DS19	356	unknown (SURF1)	UG	XM_959428	*N. crassa*	2e-98	-	-	-	-
pksA	2399	polyketide synthase	*pksA*	AY510452	*A. flavus*	0.0	*aflC* (AAS66004)	54.8	*stcA* (EAA61613)	57.0
cypA	511	averufin monooxygenase	*stcB*	XM_676001	*A. nidulans*	0.0	*aflV* (AAS66022)	59.3	*stcB* (EAA61612)	59.8

Gene	Size[1] (aa)	Putative function (domain)[2]	Highest BLAST match[3]	Genbank accession no.	Species	Indicative E-value	*A. parasiticus* AF cluster		*A. nidulans* ST cluster	
							Probable homolog[4]	% aa identity	Probable homolog[4]	% aa identity
avfA	301	oxidase	*aflI*	AY371490	*A. parasiticus*	3e-73	*aflI* (AAS66010)	47.8	*stcO* (EAA61613)	43.7
epoA	420	epoxide hydrolase	*EPH2*	DQ443738	*A. niger*	4e-93	-	-	-	-
moxA	626	hydroxyversicolorone monooxygenase	*moxY*	AY510454	*A. nomius*	0.0	*aflW* (AAS66023)	55.1	*stcW* (EAA61592)	59.0
DS25	575	amino acid permease	*Agp2*	XM_001267393	*Neosartorya fischeri*	9e-139	-	-	-	-
DS26	345	unknown (YqcI_YcgG)	UG	XM_391678	*G. zeae*	1e-97	-	-	-	-
DS27	196	unknown	UG	XM_391679	*G. zeae*	5e-84	-	-	-	-
DS28	523	MFS multidrug transporter	UG	XM_391680	*G. zeae*	1e-169	-	-	-	-
DS29	300	unknown	UG	XM_741940	*A. fumigatus*	0.75	-	-	-	-
DS30	348	unknown (NmrA)	UG	XM_387985	*G. zeae*	2e-30	-	-	-	-
DS31	231	translation elongation factor	*stcT*	XM_675984	*A. nidulans*	1e-47	-	-	*stcT* (ENU34740)	41.1
DS32	529	methionine permease	UG	XM_001267118	*Neosartorya fischeri*	0.0	-	-	-	-
DS33	458	unknown	UG	XM_677390	*A. nidulans*	7e-75	-	-	-	-
DS34[6]	889	unknown (DUF1785, Piwi, PAZ)	UG	AACS01000213	*Coprinopsis cinerea*	2e-88	-	-	-	-

[1] The size of the peptide was predicted from the putative genes.

[2] Putative function was based on BLAST search at NCBI (restricted to fungal data) and the putative domains were from the Pfam database. The putative domains or Pfam family IDs are in brackets.

[3] Best match from BLAST search at NCBI (restricted to fungal data) (UG: unnamed gene).

[4] Genbank acession numbers are in brackets.

[5] Pseudogenes with stop codons within open reading frames.

[6] Partial genes.

This table was prepared by S. Zhang (Zhang *et al.*, 2007).

1.3 MEMBRANE TRANSPORTERS IN FILAMENTOUS FUNGI

In nature, filamentous fungi are constantly exposed to a wide variety of toxic compounds originating from various sources. Survival of microorganisms in natural environments is favoured by the capacity to produce compounds toxic to competing organisms and the ability to resist the effects of such toxic compounds (Del Sorbo *et al.*, 2000; Stergiopoulos *et al.*, 2002). The accumulation of toxicants in cells is affected by two integral membrane protein families: the ATP-binding cassette (ABC) and the major facilitator superfamily (MFS) of transporters. In fungi, these transporters provide protection against toxic compounds present in their natural habitat or prevent the cytoplasmic accumulation of toxic secondary metabolites produced by the fungus itself (Nelissen *et al.*, 1997; Pao *et al.*, 1998). In addition, in plant pathogenic fungi these transporters may act as virulence or pathogenicity factors if they mediate secretion of virulence factors or antagonize plant defense compounds during pathogenesis (deWaard, 1997). Furthermore, ABC and MFS transporters also provide protection against synthetic compounds, such as fungicides (deWaard, 1997; Reimann and Deising, 2005).

1.3.1 ABC transporters

ABC transporters are one of the largest protein families known to date, operating in a wide range of organisms from bacteria to man (Higgins and Linton, 2001). They are located in the outer plasma membrane or in membranes of intracellular compartments, such as endoplasmic reticulum, peroxisomes, and mitochondria. ABC transporters can bind and hydrolyze nucleotide triphosphates (mainly ATP) to generate energy for transporting solutes across cell membranes. This can occur even against an electrochemical gradient and thus the ABC transporters are regarded as primary active transporter systems (Azzaria *et al.*, 1989). ABC family permeases are in general multicomponent transporters, capable of transporting both small molecules and macromolecules in response to ATP hydrolysis (Bauer *et al.*, 1999; Del Sorbo *et al.*,

2000).

ABC transporters of fungi typically contain two intracytoplasmic regions, which both harbor a nucleotide-binding fold (NBF) for binding and hydrolysis of ATP and two prevalently hydrophobic regions, each containing six transmembrane domains (TMDs, Fig. 1.4A). These transporters are encoded by a single gene. The NBFs of ABC transporters are distinguished by the conserved Walker A and Walker B motifs (Ames *et al.*, 1989; Walker *et al.*, 1982).

ABC transporters from filamentous fungi are capable of providing protection against natural toxic compounds and fungicides. For instance, several ABC transporter genes from *A. nidulans*, such as *atrA, atrB, atrC* and *atrD*, have been defined. Expression of these genes is up-regulated by a range of natural and synthetic toxic compounds. Functional analysis by gene replacement of *atrB* in *A. nidulans* demonstrated that *atrB* is involved in protection against compounds from all major classes of fungicides and natural toxic compounds (Del Sorbo *et al.*, 1997). In addition, Gardiner and coworkers reported that the ABC transporter gene in the sirodesmin biosynthetic gene cluster of *Leptophaeria maculans* is not essential for sirodesmin production but facilitates self-protection (Gardiner *et al.*, 2005).

1.3.2 MFS transporters

MFS transporters comprise one of the largest protein families and exist from bacteria to higher eukaryotes. The MFS transporters are single-polypeptide secondary carriers capable only of transporting small solutes in response to chemiosmotic ion gradients (Pao *et al.*, 1998).

A typical MFS is composed of 400-800 amino acids residues and has a molecular mass of 45-90 KDa. It consists of 12-14 TMDs arranged into two homologous halves, joined together by a large cytoplasmic loop between TMDs 6 and 7. An additional two TMDs

emerge at the C-terminal domain linked by a cytoplasmic loop between TMDs 12 and 13 if the transporter is composed of 14 TMDs (Pao *et al.*, 1998). Unlike ABC transporters, MFS proteins do not have characteristic signature. Mutational analysis with respect to function of MFS proteins suggests that the N-terminal domain is primarily involved in proton translocation while the C-terminal domain participates in substrate binding and recognition (Griffith *et al.*, 1992).

MFS transporters are involved in secretion of host-specific toxins, which was firstly reported by Pitkin *et al.* (1996). In the maize pathogen *Cochliobolus carbonum*, the *tox*A gene encodes a MFS transporter, which has 10-13 predicted TMDs and secretes the host-specific cyclic tetrapeptide HC-toxin. Two copies of *tox*A gene flank the gene cluster required for synthesis of the HC toxin. Mutants with a single-disrupted copy of *tox*A still produce the HC-toxin and are virulent on maize. All attempts to obtain knockout mutants for both copies of *tox*A were unsuccessful. This finding suggests that the protein encoded by *tox*A is involved in self-protection against the HC-toxin and is essential for survival and virulence on host plants of HC-toxin producing strains. In addition, in the fungal genus *Cercospora*, *cfp* (cercosporin facilitator protein) encodes another putative MFS transporter. Over-expression of *cfp* in *C. kikuchii* up-regulates production and secretion of cercosporin. Gene disruption of *cfp* results in dramatically reduced cercosporin production and virulence, and increases sensitivity to the toxin. Transfer of the *cfp* gene to a cercosporin-sensitive fungus increases its resistance to the toxin (Upchurch *et al.*, 2002).

Furthermore, most of the genes involved in trichothecene biosynthesis by *Fusarium spp.* are assembled in a gene cluster. In *F. sporotrichioides*, *Tri12*, an MFS gene encoding a transporter with 14 TMDs, is located in this cluster. Mutants of *S. cerevisiae* transformed with *Tri12* showed decreasing sensitivity to trichothecene. Strains of *F. sporotrichioides* with disrupted *Tri*12 produced less trichothecene and were more sensitive to this compound. Therefore, these results indicate that *Tri*12 acts as a trichothecene transporter and has a role in self-protection of *F. sporotrichioides* against

trichothecenes (Alexander *et al.*, 1999). In contrast with *Tri*12, the MFS gene *afl*T, which is located in aflatoxin biosynthetic gene cluster , does not have a significant role in aflatoxin secretion (Chang *et al.*, 2004).

MFS transporters also have other functions. *Bcmfs*1 is another MFS gene from *Botrytis cinerea* and encodes a protein with 14 predicted TMDs. The *Bcmfs*1 disrupted mutants have an increased sensitivity to the plant defence compound camptothecin and the toxin cercosporin. Over expression mutants of *Bcmfs*1 display an increased tolerance to these toxins and to structurally unrelated fungicides, such as sterol demethylation inhibitors (DMIs) as well. These findings demonstrate that *Bcmfs*1 is a multidrug transporter (Hayashi *et al.*, 2002).

1.3.3 DotC, a putative MFS transporter

The *dotC* ORF lies 0.72kb from *dotB* in dothistromin biosynthetic cluster and is predicted to encode a hydrophobic 585-amino acid-protein. The analysis of the DotC amino acid sequence shows 25% identity to those of several other fungal MFS transporters, such as the *tox*A gene in *C. carbonum* and the *afl*T gene in *A. parasiticus* (Bradshaw *et al.*, 2002) The study of the structure of the DotC protein reveals it has 14 predicted TMDs, which is a typical feature of MFS transporters (Del Sorbo *et al.*, 2000). Therefore, the *dotC* gene is suspected to encode a MFS transporter. The significance of studying *dotC* is that the gene may be the prime target for future disease control since some MFS proteins have self-protection function that allows the producer organism to resist its own toxin and even unrelated fungicides.

Figure 1.4: Schematic representation of ABC and MFS transporters.

A

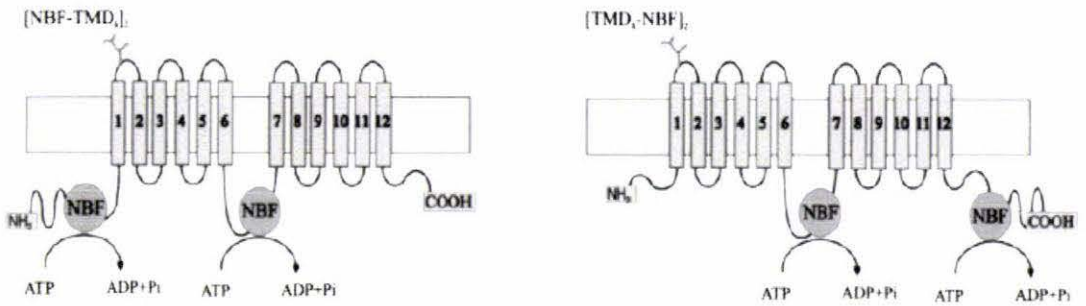

B

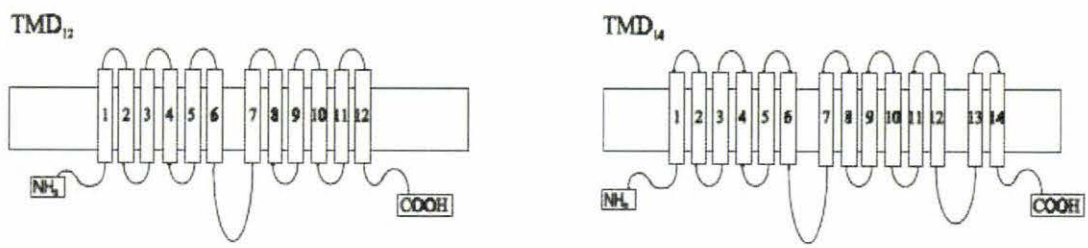

A: ABC transporter with the [NBF-TMD6] 2 and [TMD6-NBF] 2 topology.

B: MFS transporters with 12 and 14 TMDs.

The TMDs are indicated in boxes and are numbered (Stergiopoulos *et al.*, 2002).

1.4 GREEN FLUORESCENT PROTEIN

The green fluorescent protein (GFP), isolated from jellyfish *Aequorea victoria*, was cloned and sequenced in 1992 (Prasher *et al.*, 1992) and firstly used as a reporter gene in 1994 (Chalfie *et al.*, 1994). Purified GFP, a protein of 238 amino acids, absorbs blue light (maximally at 395 nm with a minor peak at 475 nm) and emits green light (peak emission at 509 nm). The fluorescence of GFP only requires UV or blue light and oxygen, unlike other reporters (such as luciferase and β-glucuronidase) that rely on

cofactors and substrates for activity. It can be used without invasive techniques for *in vivo* observation within individual cells or in whole organisms interacting with environments in real time. Fusion of GFP to a protein rarely affects the proteins activity or mobility, and GFP is nontoxic in most cases. Therefore, with such a low threshold for use, GFP has been applied extensively from prokaryotes to eukaryotes throughout the biological sciences.

1.4.1 Applications of GFP

Numerous studies have been reported in successfully using the GFP. The most common application of GFP remains as a reporter of gene transcription or a protein of interest. GFP fused with cellular polypeptides can be used to examine the subcellular location and to chase protein sorting and dynamic subcellular processes over time (Walker *et al.*, 1999). Tenreiro and coworkers (Tenreiro *et al.*, 2000) fused the *Azr*1 gene (encoding a MFS transporter) in *Saccharomyces cerevisiae* with *gfp* and observed the distribution of the *AZR*1-GFP fusion protein by fluorescence microscopy; the results indicated that *AZR*1 was a plasma membrane protein. More examples using GFP as a reporter in fungi, such as in observation of cellular localization of cercosporin resistance proteins in *Cercospora nicotianae* and multidrug resistance protein 1 of *Leishmania parasites*, were reported by Chung *et al.* (2002) and Dodge *et al.* (2004) respectively.

Besides protein fusions, GFP can also be applied to visualize a whole-organism (Du *et al.*, 1999) or for transcriptional probes, in which GFP is linked to an environmental or stress sensitive promoter and serves as an indicator when the condition of the environment or stress level is changed (Albano *et al.*, 2001). In some cases, the GFP can provide a screening method to rapidly sort cells by observation of green fluorescence using microscopy (Yuk *et al.*, 2002).

1.4.2 GFP improvements

Although GFP is a facile and low-cost marker, the limitations of wild type GFP still have been considered. The GFP was isolated from *A. victoria* that lives in cold water; it tends to misfold at temperatures over 37°C. Additionally, the GFP requires up to two hours from transcription to functional fluorescent protein and thus makes it difficult to monitor early developmental events. Furthermore, GFP has a low turnover rate and many biological species autofluoresce at the same wavelength as GFP; therefore, the background noise can impact the visualization of GFP, especially when the expression protein of interest is low (March *et al.*, 2003; Zimmer, 2002).

For solving these problems in filamentous fungi, modified forms of *gfp* with optimized codon usage of GFP (such as synthetic GFP, sGFP and enhanced GFP, eGFP) have been developed that can be efficiently translated in fungi and increase the GFP protein fluorescence. The sGFP has a S65T amino acid substitution and eGFP has a double amino acid substitution of P64L and S65T. The S65T substitution causes a "red shift" in excitation maxima from 395 and 475 nm to 488 nm and has detection near 508 nm, which is suitable for observation using special filters of fluorescence microscopy (Lorang *et al.*, 2001). Many studies have confirmed that the sGFP and eGFP can be successfully applied in fungal biology research, such as in the symbiotic basidiomycete fungus *Hebeloma cylindrosporum*, sGFP was efficiently expressed as a marker and could be modulated under different environmental conditions (Rekangalt *et al.*, 2007). Muller *et al.* (2006) used eGFP as a reporter in *H. cylindrosporum* and found uniform distribution of fluorescence in the hyphae and no significant background signal in control hyphae. In the study of dothistromin genes, the eGFP was applied to examine gene expression by fusing it with the *dotA* and under control of the *dotA* promoter. The green fluorescence was observed highly concentrated in young mycelia of transformed *D. septosporum* mutants, which was consistent with real-time PCR results that showed the *dotA* gene expressed at high levels during the onset of exponential growth (Schwelm *et al.*, 2007). In addition, the eGFP was also successfully used for tracking the *D.*

septosporum infection process with dothistromin deficient mutants (Barron, 2006).

1.5 TARGETED GENE DISRUPTION

Targeted gene disruption provides a powerful method for characterization of gene function by a reverse genetic approach (Capecchi, 1989). This technology depends on homologous recombination reactions that occur between the transfected DNA (targeted vector) and the host genome. In the early form, this technique required the replacement of a targeted open reading frame (ORF) by a selectable marker using PCR to obtain the 5' and 3' ends of the targeted ORF, and then using restriction digestion and ligation to introduce the selectable marker to construct the vector, following by transformation of the vector into host genome (Bradshaw *et al.*, 2002). A few developments for gene disruption resulted in more facile and more efficient methods to construct the targeted vector, such as PCR-mediated methods without the use of DNA ligase and plasmid vectors (Kuwayama *et al.*, 2002), using a group II intron (targetron) vector containing a retrotransposition-activated selectable marker (Zhong *et al.*, 2003), and even a method based on non-homologous end-joining in *Neurospora* strains (Ninomiya *et al.*, 2004). In this project, a relatively easy and efficient recombination cloning technology: MultiSite Gateway system (Invitrogen) will be used for targeted gene disruption.

The MultiSite Gateway system is based on the *Escherichia coli* bacteriophage lambda integrase/*att* system, which facilitates the cloning of multiple DNA fragments. As shown in Fig. 1.5A, firstly, specific *att*B sites are flanked to three DNA fragments by PCR, usually, the "A", "B" and "C" represent the 5' element of the target gene, the selective marker and 3' element of the target gene, respectively; then the PCR products are cloned into three donor vectors bearing the corresponding *att*P sites catalyzed by BP clonase; finally, recombination between all *att*L sites with their corresponding *att*R sites is catalyzed by the LR Clonase. The LR recombination combines the three entry clones and the destination vector to create a construct with the three inserts in an oriented order

(Fig. 1.5B).

This method eliminates the use of restriction endonuclease and ligase. The *E. coli* transformants can be easily screened by using a positive (kanamycin /ampicillin resistance) and a negative (the cytotoxic *ccd*B gene) selection, which does not allow the growth of by-products and any intact donor or destination vectors.

Figure 1.5: MultiSite Gateway.

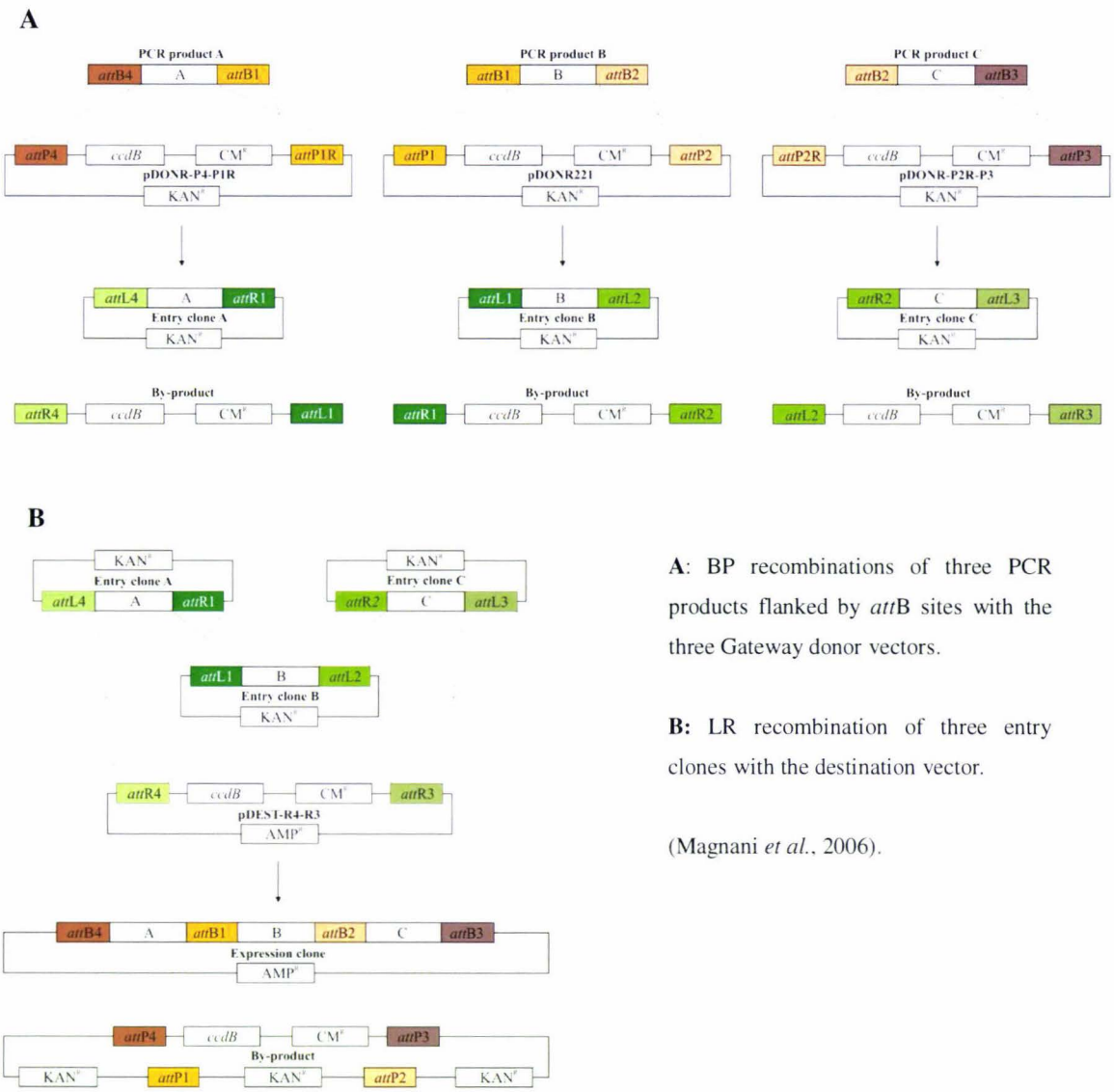

A: BP recombinations of three PCR products flanked by *att*B sites with the three Gateway donor vectors.

B: LR recombination of three entry clones with the destination vector.

(Magnani *et al.*, 2006).

1.6 AIMS AND OBJECTIVES

The first aim of this project is to obtain a fusion gene containing *gfp* and the *dotC* gene. Using GFP as a marker, the localization of the DotC protein can be observed under microscopy. If the GFP protein is observed tightly association with cell membrane, it indicates that DotC protein is associated with the cell membrane as well. This expected finding will support the hypothesis: the *dotC* gene encodes an MFS transporter, which is an integral membrane protein.

The second aim of this project is to achieve a mutant blocked in the synthesis of DotC protein via targeted gene disruption. This mutant will allow direct assessment of the role of the DotC protein, by examining toxin production and secretion, toxin resistance, and the sporulation rate. However, if the *dotC* gene functions the same as the *tox*A in *C. carbonum*, no mutant would be obtained since the fungus may lose its self-protection mechanism and be killed by its own toxin. This problem could be solved by using growth conditions which totally inhibit dothistromin production.

The third aim is to identify novel dothistromin biosynthetic genes by using degenerate primers, derived from the consensus amino acid sequences of the AF/ST biosynthetic proteins. Based on the known sequences, the probes can be designed to screen the *D. septosporum* genomic library to find any positive clones, in which unknown dothistromin biosynthetic genes are located.

CHAPTER TWO: MATERIALS AND METHODS

2.1 FUNGAL, BACTERIAL STRAINS AND PLASMIDS

Table 2.1 Fungal, bacterial strains and plasmids

Strains or plasmid	Relevant characteristics	Source or reference
Fungal strains		
Dothistroma septosorum		
NZE8 (wild type)	Single spore isolate, laboratory strain.	
NZE10 (wild type)	Single spore isolate, laboratory strain.	
***dotC-gfp* transformants**		
FJT70 (DG1*)	*dotC* ::*egfp*::*hph*, derivative of NZE8	This study
FJT71 (DG18*)	*dotC* ::*egfp*::*hph*, derivative of NZE8	This study
FJT72 (DG21*)	*dotC* ::*egfp*::*hph*, derivative of NZE8	This study
FJT73 (DG41*)	*dotC* ::*egfp*::*hph*, derivative of NZE8	This study
FJT74 (DG48*)	*dotC* ::*egfp*::*hph*, derivative of NZE8	This study
FJT75 (DG78*)	*dotC* ::*egfp*::*hph*, derivative of NZE8	This study
FJT76 (DG97*)	*dotC* ::*egfp*::*hph*, derivative of NZE8	This study
FJT77 (DG103*)	*dotC* ::*egfp*::*hph*, derivative of NZE8	This study
***dotC* disrupted transformants**		
FJT15 (DCKDM93*)	*dotC* knockout; pR260, derivative of NZE10	This study
FJT16 (DCK3*)	*dotC* knockout; pR260, derivative of NZE10	This study
FJT19 (DCK44*)	*dotC* ::*hph*, derivative of NZE10 (3' single cross-over)	This study
FJT41 (DCK46*)	*dotC* ::*hph*, derivative of NZE10 (ectopic)	This study
FJT42 (DCKDM90*)	*dotC* ::*hph*, derivative of NZE10 (ectopic)	This study
FJT43 (DCK12*)	*dotC* ::*hph*, derivative of NZE10 (ectopic)	This study
FJT79 (DCK18*)	*dotC* ::*hph*, derivative of NZE10 (ectopic)	This study
FJT80 (DCK39*)	*dotC* ::*hph*, derivative of NZE10 (ectopic)	This study
***Escherichia coli* strains**		
XL-1 Blue	*sup*E44 *hsd*R17 *rec*A1 *end*A1 *gyr*A46 *thi rel* A1 lac$^-$ F' [proAB$^+$ lacI^q Δ (lacZ) M15 Tn10 (tet^r)]	(Bullock *et al.*, 1987)
Top 10	F$^-$ *mcr* A Δ(*mrr-hsd* RMS-*mcr* BC) Φ80 (*lacZ*)ΔM15 Δ *lac* X74 *rec* A1 *deo*R *ara*D139 Δ(*ara-leu*)7697	Invitrogen

Plasmids		
Strains or plasmid	**Relevant characteristics**	**Source or reference**
pAN7-1	6.8 kb Hygromycin^R, Ampicillin^R	(Punt and van den Hondel, 1992)
pBluescript II KS plus vector	Ampicillin^R, lacZ' (3.0 Kb)	Stratagene
pDONR P4-P1R	4.77kb Cm^R, Kanamycin^R, *ccd*B gene	Invitrogen
pDONR P2R-P3	4.77kb Cm^R, Kanamycin^R, *ccd*B gene	Invitrogen
pDEST R4-R3	4.43kb Cm^R, Ampicillin^R, *ccd*B gene	Invitrogen
pGEMT-easy	Ampicillin^R, lacZ' (3.0 Kb)	Promega.
pPN81	*egfp* gene, hph cassette (5.7Kb)	(Schwelm, 2007)
pR225	*hph* gene in pDNOR 221	(Teddy, 2004)
pR260	*dotC* disruption vector	This study
pR261	*att*B4-5' element-*att*B1	This study
pR262	*att*B2-3' element-*att*B3	This study
pR263	*dotC-gfp* in pGEMT-easy vector	This study
pR264	*dotC-gfp* in pBluescript II KS plus vector	This study
pR265	*dotC-gfp-hph* in pBluescript II KS plus vector	This study
pR266	700 bp of norA/B from DegePCR in pGEMT-easy	This study
pR267	100 bp of *VerB* from DegePCR in pGEMT-easy	This study
pR268	13 Kb *NorB* containing clone isolated from genomic library	This study

*: alternative names in brackets.

2.2 GROWTH AND MAINTENANCE OF CULTURES

Recipes for growth media and other reagents are shown in Appendix I and II.

2.2.1 Growth and maintenance of *E. coli* cultures

E. coli cultures were grown on LB agar plates or in LB broth, supplemented with appropriate antibiotics when required, at 37°C overnight. Plates were sealed with parafilm and stored at 4°C. For long-term storage, the selected *E. coli* cells (grown overnight in LB broth with shaking) were mixed with 50% (v/v) sterile glycerol to reach a final concentration of 15% (v/v) glycerol and stored at –80°C.

2.2.2. Growth and maintenance of *D. septosporum* cultures

2.2.2.1 General growth and maintenance of *D. septosporum* cultures

A 0.25 cm^2 section of mycelium, cut with a scalpel from the edge of a *D. septosporum* colony, was placed in the centre of a 90 mm petri dish containing approximately 25 ml of medium. *D. septosporum* cultures were grown on DM, DSM or PDA plates sealed with parafilm at 22°C for 14-21days. Plates were then stored at 4°C for short-term storage. For long-term storage, mycelia were stored in 15% (v/v) sterile glycerol at -80°C.

2.2.2.2 Single spore purification

A genetically pure colony of *D. septosporum* was isolated as the follows. The spores were collected with a sterile loop of MilliQ water brushed over a sporulating colony (growing on DSM), then streaked across a new DSM plate. The plate was turned and streaked again from the end of previous streak three times, flaming the loop between each streak. This plate was incubated at 22°C approximately 10 days until a single colony was grown up to a sufficient size to repeat the streaking process. After two rounds of streaking, a single colony was isolated and said to be pure. Generally, to obtain purified transformants, those cultures were grown on DSM plates containing appropriate selection supplements.

2.2.2.3 Growth and harvest of *D. septosporum* mycelia

For inoculum, two 5 mm diam. plugs of *D. septosporum* mycelia were cut from the edge of *D. septosporum* colonies (grown for 14-28 days on DM at 22°C) using a sterile cork borer and transferred to a 1.5 ml microcentrifuge tube containing 0.6 ml sterile MilliQ water. The mycelia were ground using a sterile plastic pestle.

For solid media (usually DM agar plates), 150 µl of macerated mycelium suspension was dispensed onto DM plates covered with a sterile 90 mm diam. cellophane disc on the media surface. The suspension was spread across the cellophane's surface evenly with a sterile glass spreader. Plates were sealed with parafilm and incubated at 22°C for 10-14 days. After incubation, mycelia were removed from the surface of cellophane using sterile tweezers or a spatula and stored in a microcentrifuge tube at -20°C or freeze-dried at -80°C by the Dura-Dry™ corrosion resistant freeze-dryer. However, collecting mycelia for PCR screening of *D. septosporum* transformants, each transformant was subcultured onto a single point on the surface of cellophane in DM plates (~20 transformants per plate). After 14 days growth, the whole colony of each transformant was removed from the surface of cellophane and divided into two parts using sterile scalpel and forceps. The smaller part of mycelia was sub-cultured into another DM plate and incubation at 22°C; the larger part of mycelia was freeze-dried to extract its genomic DNA (Section 2.3.1), which was treated as the template for further PCR screening.

For liquid media (usually LDB broth), 100 µl of macerated mycelium solution was inoculated into a 125 ml flask containing 25 ml LDB broth. Alternatively, 50-100 µl spore suspension (~1-3× 10^5 conidia/ml) was used for inoculation in the above LDB broth (refer to Section 2.13 for the method of harvesting conidia). All flasks were incubated at 22°C for 7-10 days with shaking (150 rpm). The mycelia were harvested by a vacuum harvester (BioRad), in which a sterile 5 cm disc of Whatman paper was used to filter liquid broth and collect mycelia. The mycelia of each flask were transferred into a 15 ml falcon tube and freeze-dried. The filtrate from each flask was also collected into a sterile 15 ml falcon tube and stored at -20°C for further ELISA assays, when required.

2.3 DNA MANIPULATION

2.3.1 DNA isolation from *D. septosporum* cultures: CTAB Method

This method is based on the CTAB (hexadecyltrimethylammonium bromide) DNA extraction method developed by Doyle and Doyle (1987) for isolating plant DNA. It has been successfully used for preparation of *D. septosporum* genomic DNA for Southern hybridization (Jin, 2005). Thus, this method was applied in this research to prepare genomic DNA for Southern hybridization and for PCR screening of *D. septosporum* transformants in this project.

The freeze-dried mycelia were ground to a fine powder with liquid nitrogen in a sterile mortar and pestle. The fine powder (for Southern hybridization, approximately 80-100 mg in each tube) was transferred to microcentrifuge tubes containing CTAB buffer (600 µl) and 2 µl of RNaseA (10 mg/ml). This mycelia suspension was mixed thoroughly and then incubated at 37°C for 10 minutes; followed by incubation at 65°C for 1 hour. When the incubation was finished, the tubes were left at the room temperature for cooling down, and 600 µl of chloroform was added to the tube. The suspension was mixed thoroughly by vortexing and centrifuged at 15,700 × g for 5 minutes. The upper phase was subsequently transferred to a new microcentrifuge tube; a further 600 µl of chloroform was added and mixed thoroughly by inverting the tubes several times, then centrifuged at 15,700 × g for another 5 minutes. The upper phase was transferred to a new microcentrifuge tube; one volume of isopropanol was added to the tube and the completely mixed solution was incubated at room temperature for 2 minutes, and then centrifuged at 15,700 × g for 2 minutes. The pellet was washed three times in 1 ml 80% ethanol and centrifuged at 3,300 × g for 20 seconds after each wash. After the last round of washing, ethanol was removed by a P200 pipette. The microcentrifuge tube was left to air-dry, then the DNA was resuspended in TE buffer or water.

2.3.2 Isolation of plasmid DNA from *E. coli*

Plasmid DNA was isolated from *E. coli* cells using the QIAGEN plasmid minikit (≤ 20 μg plasmid DNA) or QIAGEN plasmid midikit (≤ 100μg plasmid DNA) according to the manufacturer's instructions.

2.3.3 Agarose gel electrophoresis of DNA

DNA samples were mixed with loading dye before loading into the gel. DNA fragments were size fractionated by electrophoresis through a 0.7%-1.2% (w/v) agarose gel in 1×TBE buffer at 60-100 volts. After electrophoresis, the agarose gel was stained in 0.01% ethidium bromide for 15 minutes with mild shaking. The gel was de-stained in water for 5 minutes and observed under short wave UV light and photographed.

2.3.4 Agarose gel purification of DNA fragments

DNA samples were fractionated through a 0.7% - 1.0% (w/v) agarose gel in 1× TBE buffer. After staining in ethidium bromide, the DNA was observed under long wave UV light. The desirable DNA fragments were excised using a clean scalpel and transferred to a microcentrifuge tube. The DNA was then recovered using the QIAquick gel extraction kit (Qiagen) according to the manufacturer's instructions. The extracted DNA was confirmed to be the correct size by gel electrophoresis.

2.3.5 Determination of DNA concentration by fluorometric assay

DNA samples were quantified using a "Hoefer DyNA Quant 200" (Amersham Biosciences) fluorometer. The fluorometer was firstly calibrated to 100 by adding 2 μl (100 ng/μl) calf thymus DNA standard to 2 ml of fluorometer working solution in a cuvette before testing. Once the reading of the calibration was stable, 2 μl of sample DNA was added to 2 ml of fresh working solution for concentration testing. The reading on the fluorometer was recorded as the concentration of DNA in ng/μl.

2.4 DNA LIGATION AND CLONING

2.4.1 Restriction endonuclease digestion of DNA

Restriction endonuclease digestion was performed according to the manufacturer's instructions. The incubation time usually was one hour and could be extended to overnight in some cases, such as DNA digestion of genomic DNA for Southern blotting and some ligation reactions. After digestion, the digested DNA was examined by agarose gel electrophoresis.

In this project, restriction endonucleases were also used for screening of transformants after transformation of *E. coli* competent cells with constructed vectors. After transformation, each colony was clearly marked and picked up using a pipette and then transferred into a 0.2 ml PCR tube, which containing 6 µl LB broth. An aliquot of 3 µl of above cell suspension was then mixed with 8 µl "green buffer" (Appendix II) in a new PCR tube and the tube was put in a boiling water bath for 30 seconds to release DNA. After the cell suspension was cooled to room temperature, the tube was centrifuged briefly to pellet cells. Then 8 µl of supernatant was transferred to another PCR tube, 2 µl of restriction endonuclease buffer (containing 1 µl of enzyme, 1 U/µl; 1 µl 10 × reaction buffer) was added and left at the recommended temperature (according to the manufacturer's instructions for different enzymes) for 30 minutes. Since the digestion map of the vector was already known, the enzyme chosen here was an enzyme which could provide a clear digestion pattern. After enzyme digestion, DNA samples were run through a 1% agarose gel (Section 2.3.3), 2 µl of RNaseA (10 mg/ml) could be added to each sample before loading to eliminate the background causing by RNA. By comparing the digestion pattern of each transformant with the expected digestion map, the positive transformants could be determined.

2.4.2 Standard ligation reactions

Ligation reactions were set up in 10- 20 µl volumes with the required insert/vector ratio (usually 3:1), final concentration of 1 × ligation buffer and 1 µl of 3 U/µl T4 ligase (Roche). The reaction solutions were mixed well and incubated at 4°C overnight.

When the pGEM®-T Easy vector (Promega) was used in the ligation reaction, the purified PCR products were generally used directly according the manufacturer's instructions. However, if Platinum® *Taq* DNA Polymerase High Fidelity (Invitrogen) was used for PCR, the purified PCR products had an "A" (dATP) added before ligation using the following method. The total volume of the reaction system was 20 µl, which contained 15 µl of purified PCR products, 2 µl of 10 × Taq polymerase reaction buffer (Invitrogen), 0.8 µl of dATP (5 mM, Invitrogen), 1 µl of Taq DNA polymerase (5 U/µl, Invitrogen), 0.7 µl $MgCl_2$ (50 mM, Invitrogen) and 0.5 µl MilliQ water. The reaction solution was mixed briefly and incubated at 70°C for 30 minutes.

When the vector was prepared using only single enzyme digestion, the vector was dephosphorylated to prevent self-ligation in the subsequent ligation reaction. Shrimp alkaline phosphatase (SAP, Roche) was used in this dephosphorylation reaction according to the manufacturer's instructions.

2.4.3 Gateway recombination reactions

(Using the MultiSite Gateway™ Three-Fragment Vector Construction Kit, Invitrogen)

2.4.3.1 BP recombination

The 5'element and 3'element of the target gene were amplified by PCR using Platinum® *Taq* DNA Polymerase High Fidelity (Invitrogen). In previous research (Teddy, 2004), it was reported that recombination between circular DNA (plasmid containing PCR

products with *att*B sites) and the donor vector was more efficient than between linear DNA (PCR products with *att*B sites) and the donor vector. Thus, the PCR products (the 5'element and 3'element of the target gene) were ligated into the pGEM®-T Easy vector (Promega) before BP recombination. The inserted 5' element and 3' element were subsequently verified with DNA sequencing (Section 2.7) to confirm that correct DNA fragments had been cloned into the pGEM®-T Easy vector. BP recombination reactions were set up according to the manufacturer's instructions in 10 µl volumes with the appropriate vector: insert ratio. Approximately 150 ng of DONR vector was added and approximately 120 ng of pGEM®-T Easy vector with inserts along with 2 µl of 5× BP clonase reaction buffer, 2 µl of BP clonase enzyme mix and added TE buffer (pH 8.0) to 10 µl. All mixtures were briefly vortexed and then incubated at 25°C overnight. The reaction was stopped and the mixture was cleaned using a QIAquick PCR purification kit (Qiagen) to remove enzyme and salts instead of adding proteinase K to stop the reaction as recommended in the manufacturer's instructions. This modification to the protocol was based on the results of optimization studies carried out by Jin (2005).

2.4.3.2 LR recombination

LR recombination reactions were set up in 20 µl volumes according to the manufacturer's instructions. In general, 60 ng of DESTINATION vector was added and approximately of 60-80 ng (20-25 pmol/µl) of each entry clone along with 4 µl of 5× LR clonase reaction buffer, 4 µl of LR clonase enzyme mix and TE buffer (pH 8.0) to a final 20 µl volume. All mixtures were briefly vortexed and incubated at 25°C overnight. Then the reaction was stopped and mixture was cleaned by QIAquick PCR purification kit (Qiagen).

2.5 TRANSFORMATION

2.5.1 Transformation of *E. coli* competent cells

2.5.1.1 Preparation of competent cells and transformation by electroporation

The Top10 *E. coli* cells were purified by streaking with a sterile loop on an LB plate. One single colony was picked up by a sterile loop and inoculated into 5 ml LB broth in a 15 ml test tube and incubated at 37°C overnight with shaking. The next day, 50 µl of the above cell suspension was inoculated into 500 ml LB broth in a 2 L flask at 37°C with shaking. Once the OD reading of the LB broth reached to 0.5-1.0 (OD_{600}), the flask was chilled on ice for 20 minutes. The *E. coli* cells were harvested by centrifuging at 4,080 × g (5000 rpm, GSA rotor) for 10 minutes at 4°C. The pellet was washed twice by resuspending with 0.5 L ice-chilled sterile water and centrifuging at the same speed as above. After two rounds of washing steps, the cells were washed again with 20 ml ice-chilled 10 % (v/v) glycerol and centrifuged at 4,302 × g (6000 rpm, SS34 rotor). Finally, the cells were resuspended in 4 ml ice cold 10 % (v/v) glycerol and an aliquot 120 µl cells were transferred into each microcentrifuge tube and stored at -80°C.

For transformation, the Gene Pulser (Bio-Rad) was set at 25 µF, 2.5 kV and 200 Ω. An aliquot (40 µl) of competent *E. coli* cells was transferred into an ice-cold 0.2 cm cuvette and mixed with 2 -5 µl (depends on the total volumes of the ligation reaction) ligated DNA or 1 µl plasmid DNA (1 ng/µl). The cuvette was wiped with clean paper to avoid any water remaining on the cuvette and air bubbles were eliminated from the above solution by a 2 µl tip. The mixture then was pulsed at these settings and the mixture was immediately mixed with 0.7 ml of non-selective LB broth in a microcentrifuge tube, and then incubated at 37°C for 1 hour with shaking. Three aliquots (of 20 µl, 50 µl and 100 µl) of the cell sespension were spread onto selective LB agar plates and incubated at 37°C overnight.

2.5.1.2 Transformation by $CaCl_2$ competent cells

An aliquot (200 µl) of $CaCl_2$ competent *E. coli* cells (supplied by Masters student, H. Jin) were mixed with 2 µl ligated DNA or 1 µl plasmid DNA (1 ng/µl) and the mixture was left on ice for 40 minutes. The mixture was then heat shocked at 42°C for 2 minutes and placed on ice for 2 minutes. Next, 1 ml non-selective LB broth was added, following by incubation at 37°C for 1 hour with shaking. The cells were subsequently plated on appropriate selective LB agar plates and incubated overnight at 37°C.

2.5.2 Transformation of *D. septosporum*

The protocols used to prepare competent protoplasts and to achieve fungal transformation were based on the methods developed by Yelton *et al.* (1984), Oliver *et al.* (1987) and Vollmer and Yanofsky (1986). The methods were further optimized by Bradshaw (1997), Seconi (2001) and Teddy (2004).

2.5.2.1 Preparation of competent *D. septosporum* protoplasts

Two 5 mm diam. plugs of *D. septosporum* mycelium were ground in 0.6 ml sterile MilliQ water. The ground mycelia solution (100 µl) was then dispensed onto DM plates covered with a 90 mm diam. cellophane disc on the media's surface. The plates were sealed with parafilm and incubated at 22°C for approximately 7 days (no more than 10 days). After incubation, each cellophane along with mycelia was transfererred into another petri dish containing approximately 10 ml of filter-sterilized Glucanex (Novozymes Switzerland, 10 mg/ml in OM buffer). The mixture was incubated at 30°C for 12-16 hours with shaking at 80-100 rpm. After incubation, 5 µl of the mixture was placed onto a glass slide to check the enzyme digestion by microscopy. Once protoplasts were observed, the mixture was filtered through a sterile Mira cloth into a sterile 15 ml corex tube and overlaid with 4 ml of ST buffer very carefully. The tube was centrifuged at 4°C for 5 minutes at 5,860 × g (Rotor SS34). After centrifugation, the protoplasts

formed a white layer between the OM and STC buffer and the interface was removed into another fresh corex tube and subsequently washed four times with 5 ml STC buffer by centrifuging at 5,860 × g (Rotor SS34) for 5 minutes at 4°C. Finally the protoplast pellet was resuspended in 50 µl STC buffer and stored on ice.

The concentration of the protoplasts was determined by counting with a haemocytometer. The working concentration of protoplasts was 9.6×10^7 to 1.25×10^8 protoplasts / ml in this project.

2.5.2.2 Transformation of *D. septosporum* protoplasts

For each transformation, 80 µl of ~1.0×10^8 protoplasts / ml in STC buffer along with 20 µl 40% Polyethyleneglycol (PEG) 6000 were mixed with 5 µg DNA and incubated on ice for 30 minutes. Then 900 µl 40% PEG 6000 solution was added to the above solution, mixed very carefully, and then incubated for a further 20 minutes at room temperature. An aliquot of 100 µl of the DNA/protoplasts/PEG solution was mixed with 5 ml DM top agar at 50°C in a 15 ml corex tube and spread onto a DMSuc plate (20 ml DMsuc per plate). The plates were incubated at 22°C overnight and then overlaid with another 5 ml DM top agar that contained hygromycin B (Sigma) to make an overall concentration of 70 µg/ml in the whole plate.

Parallel with the above transformation process, controls were set up as follows. Aliquots (100 µl) of undiluted, 10^{-1}, 10^{-2}, 10^{-3} and 10^{-4} dilutions of the protoplast sample were grown on DMSuc plates without hygromycin B selection to verify the viability of the protoplasts used in the transformation. A negative control was carried out with protoplasts only (no DNA) using the same transformation procedure described above. Aliquots (100 µl) of undiluted protoplasts (no DNA) were spread on a DMSuc plate with hygromycin B selection to confirm the sensitivity of the protoplasts to hygromycin B. A positive control was carried out using 5 µg pAN7-1 DNA (containing *hph* gene) mixed with protoplasts and PEG; 4 aliquots (100 µl) were spread on DMSuc plates with

hygromycin B selection to examine the transformation frequency.

2.6 AMPLIFICATION OF DNA BY THE POLYMERASE CHAIN REACTION

2.6.1 Normal oligonucleotide primers and degenerate primers

All the primers were ordered from Invitrogen (http://www.invitrogen.com). Each primer was resuspended in sterile MilliQ water to a final stock concentration of 200 μM and stored at -20°C. The stock primers were diluted to a working concentration of 10 μM for PCR reactions and 3.2 μM for sequencing reactions. Table 2.2 shows the primers used in this study.

Table 2.2 Sequencing and PCR primers

Primer	Primer location	Sequence (5'to 3')	Source /reference
100downdotC-Rep3	AF448056 16668 -16688	TTGTGGCGAATCAGGATCCA	This study
3'hph3032	*hph* cassette	GTCTGCTGCTCCATACAAGC	(Teddy, 2004)
3' hph fwd1	*hph* cassette	TCTTCCACACCACCGGAGATTC	(Teddy, 2004)
3'hphout	*hph* cassette	TCCTTGAACTCTCAAGCCTACAG	(Teddy, 2004)
5'hph2672	*hph* cassette	ATCTTAGCCAGACGAGCG	(Teddy, 2004)
5'hph rev2	*hph* cassette	TATCGGCGAGTACTTCTACACA	(Teddy, 2004)
5'hphout	*hph* cassette	GAATCTCCGGTGTGGAAGA	(Teddy, 2004)
5'dotD RACE	AF448056 20973 - 20995	TAGACGGCGAGGTCGCGAGAGAT	(Jin, 2005)
DCSE1	AF448056 17535 -17552	GAGAGACCTTGCAAGATC	This study
DgNorA-fwd1	Degenerate primer	GGCAACTTCATHGAYRYNGCNAA	This study
DgNorA-fwd2	Degenerate primer	GATGTNGCNAAYTTYTAYCARGG	This study
DgNorA-rev3	Degenerate primer	GTAGTRAARTCCCACATRTGNACRTA	This study

Primer	Primer location	Sequence (5'to 3')	Source /reference
DgNorA-rev4	Degenerate primer	CCGATCACIGGRAA IACRTAIGG	This study
DgVerB-fwd1	Degenerate primer	CACCARAARTAYGGNGAYACNGT	This study
DgVerB-fwd2	Degenerate primer	TACTTYAAYATGGCNATHTTYGA	This study
DgVerB-rev3	Degenerate primer	TTATGAATNGCRTCNACCCANGG	This study
DgVerB-rev4	Degenerate primer	TGGCCTGGNACNGCNGGRTACAT	This study
dotC3'fwd	pR260	GGGGACAGCTTTCTTGTACAAAGTGG GCACTCCAGACCAAGATCAAGCAGA	This study
dotC3'rev	pR260	GGGGACACCTTTGTATAATAAAGTTG GTCTGCATCGTGCGGTTGTACCTGT	This study
dotC5'fwd	pR260	GGGGACAACTTTGTATAGAAAAGTTGA TCTTACGATGCGACTCGATGTGTG	This study
dotC5'rev	pR260	GGGGACTGCTTTTTTGTACAAACTTG CGGATCCTTCTCGGACAAGTTGTCG	This study
DotcSE 920	AF448056 19376 - 19394	CGGTACTGGTTGTTGTGA	This study
dotCzf1	AF448056 20288 - 20312	ATCTTACGATGCGACTCGATGTGT	This study
dotCzf2	pR265	TCCTCGCCCTTGCTCACCATGGACTTTT GGGCCTTCTCCA	This study
dotCzf3	pR265	TGGAGAAGGCCCAAAAGTCCATGGTG AGCAAGGGCGAGGA	This study
egfp rev	pPN81	AGAAGATGGTGCGCTCCT	(Schwelm, 2007)
Inv-NorAfwd1	pR268	GACTCACTGCTCGGACTCTC	This study
Inv-NorArev1	pR268	GTCATTGCCATACGTCGAAG	This study
Inv-VerBfwd1	pR267	ATTCTCCGAAAGCGAGGGCA	This study
Inv-VerBrev1	pR267	AACAGCATGCGTGACCGCAA	This study
M13 fwd	-	GCCAGGGTTTTCCCAGTCACGA	Perkin Elmer
M13 rev	-	GAGCGGATAACAATTCACACAGG	Perkin Elmer
MF4151P3	AF448056 18636 - 18657	GGACCAGAGGAACATACTTGG	(Monahan, 1998)
MF4152P2	AF448056 17256-17278	CTATCATTGTCGCTTCGTAACG	(Monahan, 1998)
NorAfwd1	pR268	GAGAGTCCGAGCAGTGAGTC	This study
NorArev1	pR268	CTTCGACGTATGGCAATGAC	This study
NorBclufwd1	pR268	ATGCGAGCGTAGCAGACTGATGT	This study
NorBclufwd2	pR268	ACATGAGAGGGTCTACTCGT	This study
NorBclufwd3	pR268	TATGACGAGTCGCGCAAGTT	This study
NorBclufwd4	pR268	CGTGACCTCATCGATTTGCT	This study
NorBclufwd5	pR268	ACTAGACGGTGCTGGAGCAT	This study

Primer	Primer location	Sequence (5'to 3')	Source /reference
NorBclufwd6	pR268	CTATGCTTGATGCGTTTGAG	This study
NorBclufwd7	pR268	ATGGTGTTGTCGTTGGAAGC	This study
NorBcluRev1	pR268	GATACCGTTTCCGGTGGTGGATTA	This study
NorBcluRev2	pR268	GAATTCATCAATCCACGCCA	This study
NorBcluRev3	pR268	GAATAGCCTGACGTCTCATC	This study
NorBcluRev4	pR268	CACTTGCTGTACCAGCTCCA	This study
NorBcluRev5	pR268	ATAGTAGAGACTCTGCCGTC	This study
NorBcluRev6	pR268	GATTGCTCTCGAATGCAACG	This study
NorBcluRev7	pR268	ACTCTGAGAGCCCATGCTCA	This study
NorBclugap	pR268	TCGAATAGCGTCCCACTGAG	This study
NorBseqRev1	pR268	ACCGAATGAGAGATTCCG	This study
NorBseqRev2	pR268	GATGAGATTGTGCTTGCG	This study
pPN81 2978rev	pPN81	TCTCAACTCCGGAGCTGA	This study
RT-gfpfwd	pPN81	GCCATGCCCGAAGGCTA	(Schwelm, 2007)
RT-gfprev	pPN81	CATGCCGAGAGTGATCCC	(Schwelm, 2007)
SP6	-	TTTAGGTGACACTATAGAATAC	Promega

H: A+T+C; Y: C+T; R: A+G; N: A+G+T+C

2.6.2 Reagents and cycling conditions for basic PCR

PCR reactions were set up on ice and in a total volume of 20 µl in 0.2 ml PCR tubes. The components added to each reaction were: 2 µl of 10 × *Taq* polymerase buffer (Invitrogen), 0.8 µl of 50 mM $MgCl_2$ (Invitrogen), 1 µl of 5 mM dNTPs, 0.1 µl of *Taq* DNA polymerase (10 U/µl, Invitrogen), 1 µl of 10 µM primers, 1-3 ng of plasmid DNA template or 3-10 ng of genomic DNA template and proper volumes of sterile MilliQ water to 20 µl.

The PCR reaction solution was mixed briefly and the tube was placed in a thermal cycler (Master cycler gradient; Eppendorf). The reaction was started at a denaturation step lasting for 2 minutes at 94°C, then 30 cycles of denaturation at 94°C for 30 seconds, annealing at 58°C for 30 seconds (the annealing temperature was adjusted depending on primers used and specificity wanted) and extension at 72°C for 1 kb/minute (based on expected product size). The whole process was completed with a final 10 minutes extension step at 72°C.

2.6.3 Optimization of PCR conditions

Usually, when using DNA polymerase, too much free magnesium ion may produce a variety of unwanted products and promote misincorporation, and too little free magnesium ion will result in little or no PCR product. Moreover, too many dNTPs may also lead to unwanted mismatches during the amplification process. In order to increase the accuracy of PCR, the reaction conditions were optimized by adjusting the concentrations of magnesium and dNTPs. Thus, the final concentration of magnesium in one reaction was reduced to 1 mM or 1.5 mM and dNTPs concentration was decreased to 0.1 μM. In addition, Platinum® *Taq* DNA Polymerase High Fidelity (Invitrogen) with proofreading function was used when required and the cycles of PCR decreased to 20 to minimize misincorporation errors in some cases.

2.6.4 Touchdown PCR and inverse PCR

2.6.4.1 Touchdown PCR

Touchdown PCR is a method of PCR used to minimize amplification of nonspecific sequence by primers. The temperature at which primers anneal during a cycle of PCR determines the specificity of annealing. The earliest steps of a touchdown polymerase chain reaction cycle have high annealing temperatures. The annealing temperature is decreased in increments for every subsequent cycle. The primer will anneal at the highest temperature that it is able to tolerate. Thus, the first sequence amplified is the one between the regions of greatest primer specificity; it is most likely that this is the sequence of interest. These fragments will be further amplified during subsequent rounds at lower temperatures, and will swamp out the nonspecific sequences to which the primers will bind at those lower temperatures. The whole procedure of touch down PCR used in this project is shown in Table 2.3.

Table 2.3 The procedure of touchdown PCR.

Step	Temperature	Lasting time	Cycles
1	94°C	2 minutes	1
2	94°C 66°C 72°C	30 seconds 40 seconds 1 minute/kb (base on expected product size)	3
3	94°C 63°C 72°C	30 seconds 40 seconds 1 minute/kb (base on expected product size)	3
4	94°C 60°C 72°C	30 seconds 40 seconds 1 minute/kb (base on expected product size)	3
5	94°C 57°C 72°C	30 seconds 40 seconds 1 minute/kb (base on expected product size)	3
6	94°C 54°C 72°C	30 seconds 40 seconds 1 minute/kb (base on expected product size)	3
7	94°C 51°C 72°C	30 seconds 40 seconds 1 minute/kb (base on expected product size)	3
8	94°C 48°C 72°C	30 seconds 40 seconds 1 minute/kb (base on expected product size)	12
9	72°C	5 minutes	1

The initial and the final annealing temperatures depended on the primers used in PCR.

2.6.4.2 Inverse PCR

A limitation of standard PCR is that 5' and 3' flanking regions of the target DNA fragment must be known. Inverse PCR is a variant PCR that can be used to determine the flanking sequences when only one internal sequence of the target DNA is known. Based on the known internal sequence, two primers were designed at each end of this fragment with outward direction. The genomic DNA of NEZ8 was digested with different restriction enzymes (~800 ng DNA for each reaction, Section 2.4.1) for 5 hours and the cleaved DNA fragments of each enzyme were purified individually by the QIAquick PCR purification Kit (Qiagen). The purified DNA fragments were then ligated using T4 DNA ligase (Roche, Section 2.4.2). The PCR was subsequently carried out with the above two primers using 2 µl of the ligation solution as the templates. The PCR products were selected to ligated into the pGEM®-T Easy vector (Promega, Section 2.4.2) and the DNA sequence of this inserted fragment was finally obtained (Section 2.7).

2.6.5 *E. coli* colony PCR

E. coli colony PCR was used to screen *E. coli* transformants using the colony cells directly as templates. A sterile P2 pipette tip was used to pick up the colony cells by gently touching at the colony surface, too many cells could inhibit the PCR. The cells were suspended in the working solution used for a basic PCR; the total volume was usually reduced to 15 µl. The initial step of PCR program was one cycle of 3 minutes at 96°C to release the cell components, followed by 30 cycles the same as the basic PCR described above.

For screening large numbers of transformants, the transformants were pooled into groups (5-10 colonies in one group). Each colony was marked very clearly. A few cells from each colony in one group were pooled together in a 0.2 ml PCR tube containing 10 µl sterile MilliQ water. All the PCR tubes were submerged in boiling water for 3

minutes and centrifuged at 13,000 rpm (Eppendorf, Centrifuge 5415R) for 1 minute. The supernatant then was used as the template for PCR screening of those transformants. Once positive results were found in one group, each colony of this group was then checked individually by *E. coli* colony PCR to identify which one had the positive product.

2.6.6 Purification of PCR products

PCR products were purified by the QIAquick PCR purification Kit (Qiagen) according to the manufacturer's instruction.

2.7 DNA SEQUENCING

Before sequencing, plasmid DNA was purified by a commercial plasmid extraction kit (Section 2.3.2) and its concentration was determined by the Fluorometer (Section 2.3.5). In each sample, 300 ng plasmid DNA and 3.2 pmol primer were mixed with MilliQ water to reach a final 15 μl of the testing solution. All samples were sent for sequencing at Allan Wilson Centre Genome Analysis Centre, the Institute of Molecular BioSciences of Massey University.

2.8 HYBRIDISATION OF DIG-LABELED PROBES TO BLOTS

2.8.1 DIG labeling of DNA probe

Digoxigenin-11-2'-deoxy-uridine-5'-triphosphate, alkali-labile (DIG-11-dUTP, Roche) was used to label the DNA probes for Southern blotting by PCR according to the manufacturer's instructions. DNA probes for hybridisation to colony blots were labelled with DIG-11-dUTP using a DIG-random priming labelling kit (Roche) according to the manufacturer's instructions.

2.8.2 Southern blotting (Capillary)

The DNA blotting method used in this project was based on the method described by Southern (1975). DNA for Southern blotting was prepared using the CTAB method (Section 2.3.1) and digested with restriction endonucleases (Section 2.4.1). Digested DNA was separated by gel electrophoresis (Section 2.3.3) through a 0.8% agarose gel and run at low voltage (1-2 volts/cm) overnight at 4 °C. The gel was stained in ethidium bromide for 15 minutes, observed under short wave UV light and photographed with a ruler alongside the gel. If the target DNA was over 5 Kb, in order to be able to transfer high molecular DNA to membrane, the DNA was depurinated by submerging the gel in 250 mM HCl for 8 minutes with shaking at room temperature. Then, the DNA was denatured in denaturing solution for 2 × 15 minutes at room temperature with shaking. The gel was neutralized by washing twice in neutralising solution for 20 minutes per wash. Before placing on the blotting apparatus, the gel was soaked in 20 × SSC for 15 minutes. The blotting apparatus was constructed as described in the DIG application manual for filter hybridization (Roche). After blotting overnight, the apparatus was disassembled and the Hybond-N^+ membrane (Amersham) was treated with shortwave UV light for 3 minutes in the UV crosslinker (Ultralum) to crosslink the DNA to the membrane then air-dried.

2.8.3 Preparing colony lifts

For preparing colony lifts to be hybridized, the method used in this project was basically accorded to the DIG application manual for filter hybridization (Roche). Usually, the *E. coli* cells were first serially diluted to determine which dilution could achieve approximately 800-1000 colonies in one LB agar plate. The diluted *E. coli* cells were spread evenly on LB agar plates (with appropriate selection) and incubated at 37°C overnight. After incubation, the agar plates containing colonies were cooled to 4°C for 30 minutes. A 90 mm diam. nylon membrane disc was then carefully placed onto the agar surface of each cooled plate. The membrane disc was left on the plate for 5 minutes

and clear marks made both on plate and on the NON-colony membrane side to mark the orientation of the membrane relative to the plate. The membrane was then transferred onto another fresh LB agar plate (with the colony side facing up) using tweezers and incubated for 4 hours at 37°C. After incubation, each membrane was placed onto a 12 × 12 cm^2 Whatman paper, which already had been soaked in the denaturation solution, with the colony side facing up for 15 minutes. The membranes were then removed to another stack of Whatman papers containing the neutralization solution and incubated for 15 minutes. The membranes were subsequently equilibrated on 2 × SSC containing Whatman papers for 10 minutes and briefly air-dried on a clean Whatman paper sheet. The DNA was finally cross-linked to the membrane using the UV crosslinker (Ultralum, Section 2.8.2)

2.8.4 Probe concentration determination

To determine suitable probe concentration in the hybridization buffer, a series of probe dilutions were prepared as follow: 1/5, 1/25, 1/125, 1/625, 1/3125 and 1/15625. An aliquot of 2 µl each dilution was spotted onto a 7×4 cm nylon membrane. After briefly air drying, DNA was fixed to the membrane using the UV crosslinker (Ultralum, Section 2.8.2). The detection procedures are described in Section 2.8.6. A sample result shows in Fig. 2.1. Since the pure probe was used for detection in this step, considering the efficiency of probe incorporation during the hybridization, the working concentration of probe was usually used with the one grade (five times) higher concentration than the lowest concentration which had been detected. As shown in Fig. 2.1, the lowest dilution (1/15625) can be clearly observed, thus the working probe concentration is the 1/3125 dilution. In the experiment, if total volumes of the hybridization buffer are 20 ml, then 6.4 µl (20 ml / 3125= 6.4 µl) of probe will be added into the hybridization buffer (method based on the instruction manual of DIG High Prime DNA Labeling and Detection Starter Kit II, Roche).

Figure 2.1: A sample result of probe concentration determination

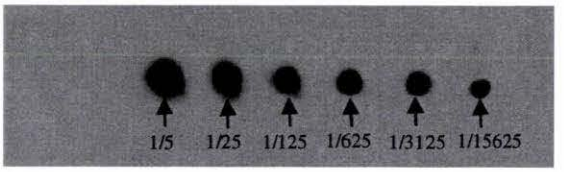

2.8.5 Hybridization of DIG labeled probe

The membranes to be hybridized were placed in a hybridization tube and 25 ml of DIG Easy Hyb solution (Roche, approximately 10 ml/100 cm^2 of membrane) was added to the tube. A mesh was usually used to separate the membranes. The membranes were then placed in a rotary oven at 42 °C and pre-hybridized for one hour. The probe was denatured by heating for 10 minutes in a boiling water bath and plunging immediately into ice. The cooled probe solution was subsequently transferred into the pre-hybridization solution (avoiding direct contact of the concentrated probe with the membranes). Mixing the solution briefly, the membranes were incubated at 42°C in a rotary oven overnight.

After hybridization, excess (un-hybridized) probe was washed off. The membranes were removed from the hybridization tube with forceps, and washed twice (5 minutes each washing) in 400 ml of low stringency buffer (wash solution I) in room temperature with shaking. Then the membranes were washed twice (15 minutes each washing) in 400 ml of high stringency buffer (wash solution II) at 68 °C in a water bath with constant shaking.

2.8.6 Immunological detection

After stringent washes, the membranes were rinsed briefly (2-5 minutes) in buffer I (refer to recipe in Appendix II) and then incubated for 30 minutes in buffer II (blocking solution, approximately 150 ml for a A4-sized membrane) with shaking at room temperature. The Anti-DIG-AP (Roche) was added directly into buffer II to reach a final

1/ 10,000 (v/v) dilution and the membranes were incubated for another 30 minutes with shaking. The membranes were washed twice (15 minutes each) in buffer I and then equilibrated for 5 minutes in buffer III. The membranes were then placed inside an A4 copysafe pocket (OfficeMax) and CSPD lumigen (Roche) was dispensed evenly over the membrane surface of DNA side by using a 200 µl pipette. The excess solution was squeezed out by gently wiping a clean towel paper over the pocket surface. The copysafe pocket was sealed and placed into the 37°C room for 10 minutes. The membrane was then exposed to X-ray film (Kodak) for 20 minutes to 1 hour. The X-ray film was finally developed by an automated developer (100 Plus Automatic X-ray Processor, All Pro Imagining).

2.8.7 Stripping blots

The membrane can be stripped of DIG-labeled probe and rehybridized to a different probe after chemiluminescent detection. The membrane was firstly rinsed in double distilled water thoroughly for 5 minutes and then washed twice (15 minutes each) in stripping buffer at 37°C. Finally, the membrane was rinsed in 2 × SSC for 5 minutes. The membrane can be stored in 2 × SSC for rehybridization.

2.9 DOTHISTROMIN ISOLATION FROM MYCELIUM OF *D.SEPTOSPORUM*

Freeze-dried *D. septosporum* mycelia (approximately 50-80 mg) were placed in a 1.5 ml microcentrifuge tube. Each sample had three replicates. An aliquot of 600 µl of acetone was added to the tube. The mycelia suspension was mixed thoroughly and incubated on a shaking platform overnight. The next day, the tube was centrifuged at 13,000 rpm (Eppendorf, Centrifuge 5415R) for 2 minutes and the supernatant was transferred into another microcentrifuge tube. This was left in the fume cupboard and the acetone allowed to evaporate completely. The process was repeated three times by adding 600 µl

acetone to the mycelia to ensure thorough extraction. The toxin was finally re-suspended in 100 µl DMSO for further ELISA assay.

2.10 QUANTIFICATION OF DOTHISTROMIN (ELISA METHOD)

The concentration of the dothistromin produced by *D. septosporum* in liquid media was measured using the competitive ELISA method described by Jones *et al.* (1993).

For preparing the DOTH-MSA conjugated plates, microtitre wells (96 wells plate) were coated with 100 µl of DOTH-MSA conjugate (supplied by Bill Jones, HortResearch), which was diluted 3000-fold with 1% phosphate-buffered saline (PBS). The plates were covered with gladwrap and incubated at 37°C for 3 hours. After incubation, the plates were washed five times with PBST (filled fully of each well) and 400 µl of BSA was subsequently added to each well. The plates were incubated for another 3 hours at 37°C. The dothistromin (DOTH) added on the plate competed with the dothistromin in the test samples to interact with a peroxidase labeled monoclonal antibody (per 10C12). The substrate solution could detect the antibody remaining bound to the plate after washing. Therefore, the more dothistromin in the test samples, the less antibodies bond to dothistromin fixed onto the plate, and the less substrate reacted with the antibodies. The BSA mix was used to block the remaining protein-binding sites on the micro-well surface. After incubation, the plates were washed once with PBST. The plates were stored at 4°C and washed with PBST just once before use.

Ten standards were prepared by adding 1 µl of the standard stock solutions (supplied by Naydene Barron) to 1 ml of dilution buffer and broth (1000-fold dilution). The dothistromin concentration of the 1000-fold diluted standards was as follows: 0, 3.9, 7.8, 15.6, 31.2, 62.5, 125, 250, 500 and 1000 ng/ml.

For test samples, the filtrates were prepared as described in section 2.2.2.4. An aliquot

(200 µl) of each sample was mixed with 200 µl of working buffer to make a 2-fold dilution (usually three replicates for each sample). DMSO added in this step was to compensate the effect of DMSO in the standards. If test samples required further dilutions, the working buffer and broth was used to obtain those dilutions.

Standards and test samples (100 µl of each) were pre-incubated at 37°C for 1 hour with 100 µl of peroxidase-labeled monoclonal antibody, per 10C12 (30,000-fold in dilution buffer) in new microtitre plates. Each standard and test sample was loaded in three different wells to make the replicates. After one hour incubation, 100 µl of the test samples and standards were then transferred to the washed DOTH-MSA microtitre plates and incubated at 37°C for 3 hours. The DOTH-MSA plates were then washed six times with PBST to remove any free labeled peroxidase. The peroxidase labeled monoclonal antibody was detected by adding 200 µl of freshly prepared substrate to each well. The plates were covered in tinfoil and shaken gently at room temperature for 30 minutes to get a color reaction. The reaction was stopped by adding 50 µl of 4 M H_2SO_4 to each well after incubation. Absorbance was measured at 490 nm with reference at 595 nm in a Anthos labtec HT2, Version 1.21E ELISA plate reader.

2.11 OBSERVATION OF GFP EXPRESSION IN *D.SEPTOSPORUM* CULTURES

2.11.1 Fluorescence microscopy

D. septosporum cultures (including WT and mutants) were inoculated as described in Section 2.2.2.1. After approximate 7 days incubation, the colonies of *D. septosporum* were observed by fluorescence microscopy (Olympus SZX12) and photos were taken using an Olympus DP70 microscope digital camera. The spore suspension of each sample was prepared as described in Section 2.13 and observed by fluorescence microscopy (Olympus BX51).

2.11.2 Confocal microscopy

D. septosporum cultures were inoculated in LDB broth for 5-7 days (Section 2.2.2.3). An aliquot of 5 µl of mycelia suspension was dropped upon a microscope slide and then covered with a 22×22 mm cover glass (Esco). All samples were observed by fluorescence miscroscopy (Olympus BX51) firstly and then subjected to confocal microscopy (Leica 6000B).

2.12 GROWTH RATE ANALYSIS

DM agar plates were used for inoculating each strain tested in this experiment. Nine 3 mm diam. agar plugs were cut from the edge of one-month-old colonies using a sterile cork borer for each strain. Three plugs were inoculated onto one DM plate. All the plates were sealed with parafilm and incubated at 22°C for four weeks. The diameter of each colony was measured along two different axes. In some colonies with irregular shape, both long axis and short axis were measured and the average value was taken.

2.13 OBTAINING *D. SEPTOSPORUM* CONIDIA AND QUANTIFICATION

Two 5 mm diam. plugs of *D. septosporum* mycelia were cut from the edge of *D. septosporum* colonies using a sterile cork borer and transferred to a 1.5 ml microcentrifuge tube containing 0.6 ml sterile MilliQ water. The mycelia were ground by a sterile plastic pestle. The macerated mycelium solution (150 µl) was then dispensed onto DSM plates and spread across the surface of the media with a sterile glass spreader. Plates were sealed with parafilm and incubated at 22°C for 10-14 days. After incubation, conidia were harvested from the multiple growing colonies on the DSM plates firstly by dispensing 4 ml of sterile MilliQ water onto the plates. Then, the conidia were suspended in the water by gently scrubbing with a sterile glass spreader across the

colony surface and with shaking the plate briefly. The conidia suspension was finally pipetted into microcentrifuge tubes and stored at -80°C.

For conidia quantification, an alternative method for harvesting conidia was used in this project. Five mm diameter agar plugs from a one-month-old culture were used to inoculate the test plates. All 6 replicate plugs of each strain were inoculated onto DSM plates and three plugs from the same strain were inoculated onto one DSM plate. Meanwhile, a different inoculation method was carried out as follows: three colonies on each DSM plate, including one wild type, one ectopic and one mutant, at least 5 replicates for each sample. All plates were incubated at 22°C for 3 weeks. After incubation, two plugs of mycelia (5 mm diameter) were cut from the leading edge of each colony at an opposite position, placed into 200 µl 0.1% Tween-20 (diluted in sterile MilliQ water) and vortexed for one minute. The concentration of conidia was quantified using a haemocytometer.

2.14 DOTHISTROMIN RESISTANCE ASSAY

DM media was used for preparing the plates in this experiment. The dothistromin was firstly dissolved in DMSO as a stock solution to make a final concentration of 1.4 mM. The final dothistromin concentrations in the testing plates were 0 µM, 0.14 µM, 1.4 µM and 14 µM respectively, in which the dothistromin was diluted with DMSO from the stock solution and calibrated to the same volume (200 µl of different concentration dothistromin solutions in 20 ml molten DM agar). Five replicate plates were set up for each different dothistromin concentration. Four 3 mm diam. mycelia plugs (one WT, two *dotC* disrupted mutants and one ectopic mutant) were transferred onto each above DM plate. All plates were sealed with parafilm and inoculated at 22°C up to four weeks. The diameter of each colony was measured at 6, 14, 20, and 27 days after inoculation.

CHAPTER THREE: DOTC-EGFP MUTANTS

3.1 INTRODUCTION

The *dotC* gene, located in the dothistromin biosynthetic gene cluster, is the gene of particular interest in this research. This gene is proposed to encode a major facilitator superfamily (MFS) membrane transporter, which may participate in secreting the dothistromin toxin and/or as a self-protection function for the fungus to resist its own toxin. In order to verify the cellular localization of the DotC protein, the *dotC* gene was fused with the enhanced green fluorescence protein gene (*egfp*), which can be efficiently translated in fungi and increases the GFP protein fluorescence. After transforming the fusion *dotC-egfp* gene to *D. septosporum*, the localization of the protein DotC can be observed by the green fluorescence under microscopy.

3.2 CONSTRUCT THE DOTC-EGFP CONTAINING VECTOR

The overall process for cloning the *dotC-egfp* fusion gene containing vector is outlined in Figs. 3.1 and 3.2.

3.2.1 Obtaining the *dotC-egfp* fusion gene

The *dotC-egfp* fusion gene was obtained using a three-step PCR. In the first step, a 3 Kb DNA fragment (including the *dotC* ORF and a 1.1 Kb promoter region of the *dotC* gene) was amplified by PCR from *D. septosporum* strain NZE8. The primers used were the forward primer (dotCzf1) and the reverse primer (dotCzf2), which was designed as a long primer containing the terminal part of the *dotC* gene and the initial part of the *egfp* gene (Fig. 3.1).

In the second step, a 800 bp *egfp* gene was amplified by using primers dotCzf3/pPN81 2978rev. The pPN81 plasmid (containing the *egfp* gene, plasmid map in Appendix V) was used as the template. The sequences of primer dotCzf2 and primer dotCzf3 were exactly complementary to each other. When designing primers dotCzf2 and dotCzf3, the stop codon of the *dotC* was eliminated to allow translation read-through into *egfp*.

In the third step, the above two rounds of PCR products were firstly purified using a QIAquick PCR purification kit (Qiagen) and then combined as templates in this round PCR using primers dotCzf1 and pPN81 2978rev. The final PCR product was the *dotC-egfp* fusion fragment, which was approximately 3.8 Kb long. The nucleotide sequence of the four primers is shown in Table 2.2 and the precise location of these primers is indicated in Appendix III. Since the final PCR product was going to be precisely expressed as its corresponding fusion protein, in order to minimize misincorporation errors during the PCR, Platinum® *Taq* DNA Polymerase High Fidelity (Invitrogen) was used in all PCR reactions and the cycles of PCR decreased to 20 (Section 2.6.3). PCR conditions were further optimized by reducing the concentration of magnesium (1.5 μM as the final working concentration) and dNTPS (0.1 μM as the final working concentration).

Figure 3.1: Schematic diagram shows the procedure obtaining a *dotC-egfp* fusion gene.

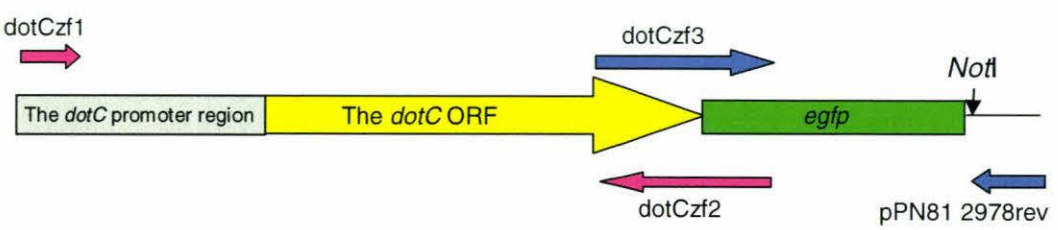

The first round PCR: Primers dotCzf1 /dotCzf2 using genomic DNA as template to obtain the *dotC* fragment (~3 Kb). The second round PCR: Primers dotCzf3/pPN81 2978rev using plasmid pPN81 as template to amplify the *gfp* fragment (~0.8 Kb). The third round PCR: Primers dotCzf1 and Primer pPN81 2978rev using a mixture of the above two rounds of PCR products as template to achieve the *dotC-egfp* fusion gene (~3.8 Kb).

Figure 3.2: The overall process for cloning the *dotC-egfp* vector.

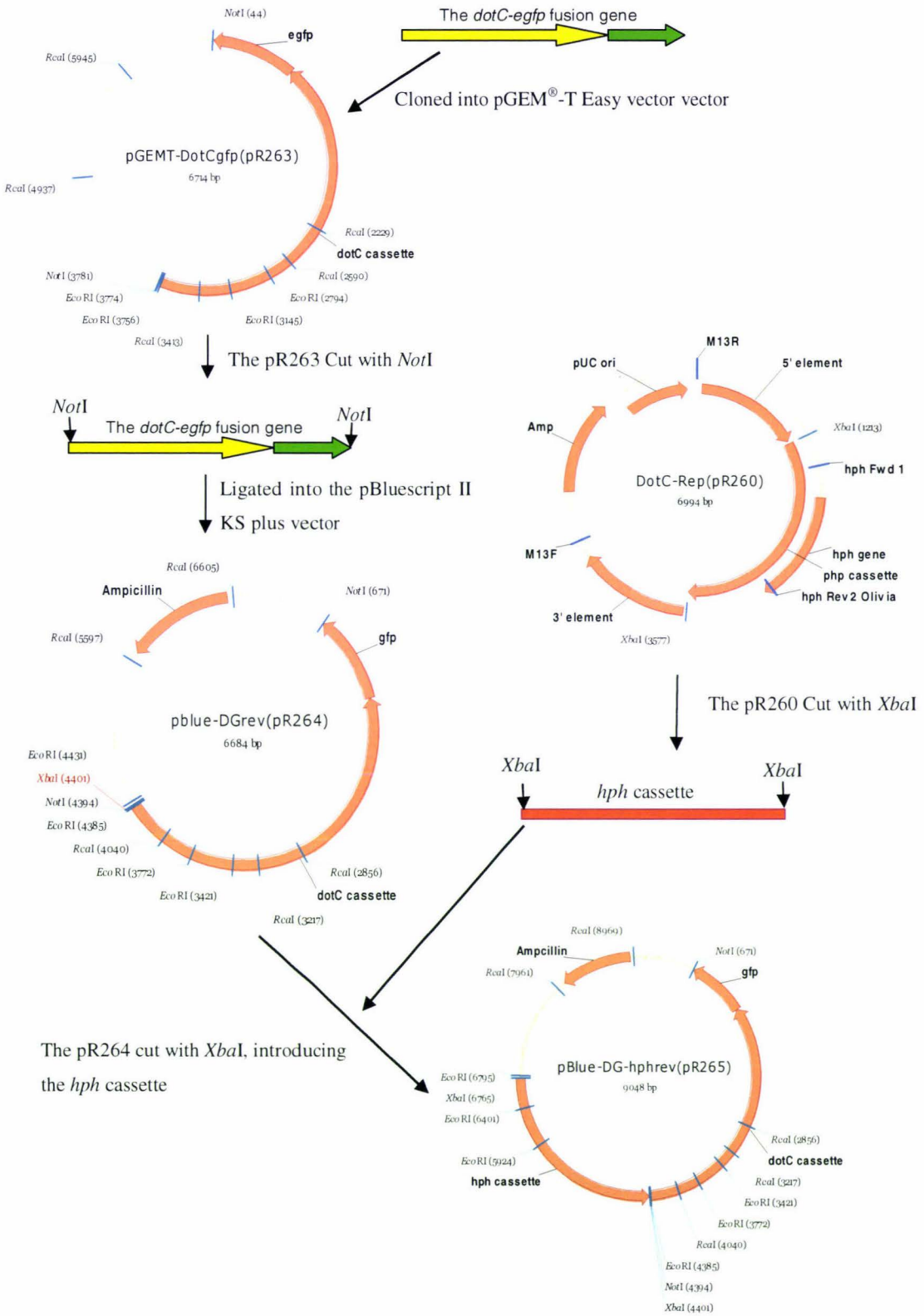

3.2.2 Cloning the *dotC-egfp* fusion gene into the pGEM®-T Easy vector

Initial attempts were carried out to clone the *dotC-egfp* fusion gene into pPN81 vector directly (the pPN81 contains hygromycin B resistance gene, *hph,* which can be used as a selectable marker for fungal transformation). Two vectors were finally obtained, which contained independently amplified *dotC-egfp* genes. Unfortunately, DNA sequencing results showed several nucleotide mismatches occurred in the PCR amplified *dotC-egfp* gene and some of the mismatches resulted in amino acid changes in the *dotC* ORF. This cloning method required a relatively high amount of insert DNA and had no blue-white selection for screening the transformants. As mentioned in Section 3.2.1, the PCR product yield was usually quite low when the reaction reduced to 20. In order to improve the efficiency of this cloning process, one more efficient cloning system, pGEM®-T Easy vector (Promega), was subsequently applied in this project.

Since Platinum® *Taq* DNA Polymerase High Fidelity (Invitrogen) was used in the PCR reactions, an "A" tail (dATP) was added to the 3' ends of the fusion PCR product to increase ligation efficiency with the pGEM®-T Easy vector (Section 2.4.2). After purification of those "A" tail attached PCR products, they were ligated into the vector as described in Section 2.4.2. Then, 5 µl ligation solutions were transformed to $CaCl_2$ competent *E. coli* cells (XL-1 Blue) as described in Section 2.5.1.2.

Hundreds of transformants were obtained on LB Amp plates after transformation. In the subsequent PCR screening, seventy transformants were initially pooled into 14 groups (5 transformants in one group) and screened for the existence of the *dotC* fragment (Section 2.6.5). Eventually three individually purified transformants (No. 15, 18 and 21) were found that clearly contained the *dotC* gene using a rapid PCR-screen with primers dotCzf1/ dotCzf2 (Fig. 3.3B).

The plasmid DNA was subsequently isolated from the three transformants and digested with *EcoR*I and *Rca*I to determine the insertion pattern (Fig. 3.3C). The results showed

that the plasmids 15 and 21 had the correct digestion pattern as expected for a *dotC-egfp* insert. Therefore, the plasmid DNA of No.15 (pR263) was selected and sent for DNA sequencing to verify whether the *dotC-egfp* fragment had been precisely amplified by PCR. The sequencing results indicated that one nucleotide (WT: TTCA***C***CTCG; fusion gene: TTCA***T***CTCG) was not consistent with the *D. septosporum* genomic DNA sequence from the database. This nucleotide alteration (the precise position is shown in Appendix III) was located in the coding region of the *dotC* and resulted in an amino acid change (Threonine→Isoleucine). This mismatch was compared with the two previous *dotC-egfp* fusion gene-containing vectors constructed in this research (the *dotC-egfp* fusion gene was cloned into the vector pPN81). DNA sequencing results showed that this "mismatch" had happened in the same position in each vector. Since the *dotC-egfp* fragment in those three different vectors were amplified by PCR independently (in different time and different PCR conditions), the "mismatch" was unlikely due to the PCR amplification error but more likely due to an error in the database sequence. Thus, the pR263 was used for the further cloning process.

Figure 3.3: Checking the plasmid pR263 with PCR and enzyme digestion.

A. The plasmid map of pR263.

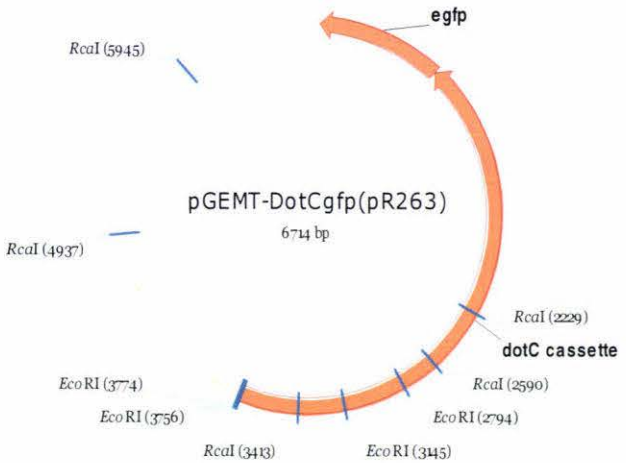

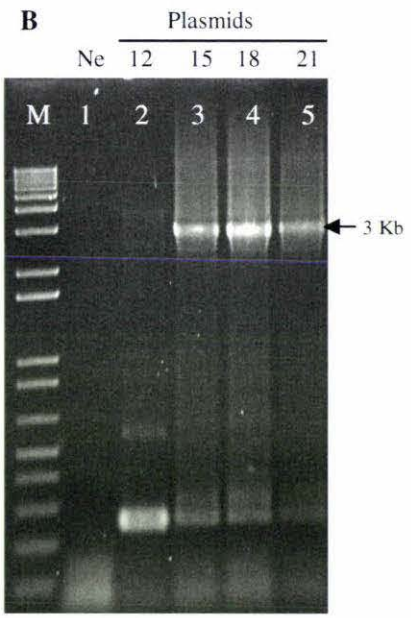

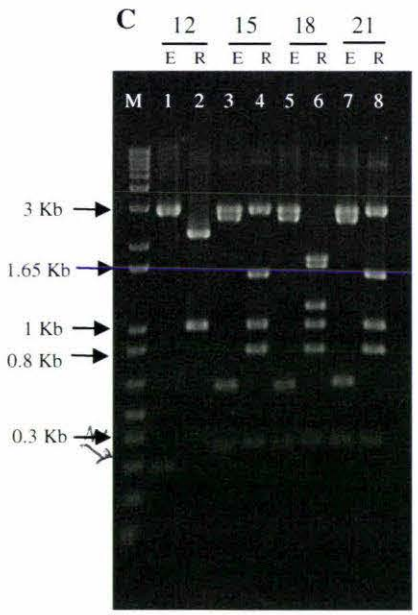

B. The PCR results checking the existence of the *dotC* fragment. Lane M: 1 Kb$^+$ ladder; lane 1: negative control without DNA template; lane 2: plasmid 12; lane 3: plasmid 15; lane 4: plasmid 18; lane 5: plasmid 21. Using primers dotCzf1/ dotCzf2, the PCR results showed that only plasmid 15, 18 and 21 had the expected 3 Kb products.

C. The enzyme digestion results. From Fig3.3A, *EcoR*I digestion was expected to give four fragments (~0.35 Kb, 0.6 Kb, 2.8 Kb and 3 Kb); and *Rca*I sites digestion five fragments (~0.36 Kb, 0.8 Kb, 1 Kb, 1.5 Kb and 3 Kb). Thus, only plasmid 15 and 21 fit to this digestion pattern. E: *EcoR*I; R: *Rca*I

Lane M: 1 Kb$^+$ ladder;

lane1: plasmid 12/*EcoR*I; lane 2: plasmid 12/*Rca*I;

lane3: plasmid 15/*EcoR*I; lane 4: plasmid 15/*Rca*I;

lane5: plasmid 18/*EcoR*I; lane 6: plasmid 18/*Rca*I;

lane7: plasmid 21/*EcoR*I; lane 8: plasmid 21/*Rca*I;

3.2.3 Cloning the *dotC-gfp* fusion gene and the *hph* gene into the pBluescript II KS plus vector

Once the DNA sequence of the *dotC-gfp* fusion gene in pR263 was confirmed without any amplification errors, a vector suitable for fungal transformation was constructed. The *hph* gene is a selectable marker (encoding hygromycin B resistance) that functions in *D. septosporum*. Unfortunately, the pR263 vector did not provide a suitable restriction site for introducing the *hph* gene directly. Therefore, the vector pBluescript II KS plus (plasmid map in Appendix V) was chosen to accomplish this cloning process, since it can provide the desirable restriction sites for cloning both the *dotC-egfp* and *hph* genes (see Fig. 3.2 flow diagram).

3.2.3.1 Cloning the *dotC-egfp* fusion gene into the pBluescript vector

The pBluescript vector (~ 1.5 µg) was cut with the restriction enzyme *Not*I and then treated with SAP (Roche) to prevent self-ligation (Section 2.4.1). The reaction mixture was cleaned by the QIAquick PCR purification kit (Qiagen) after the digestion and the dephosphorylation steps.

The *dotC-egfp* fragment was cut out of pR263 using *Not*I, then gel-purified, ligated into the prepared pBluescript vector and transformed into *E. coli* (Section 2.3.4, Section 2.4.2, Section 2.5.1.1 and Section 2.6.5). The primers dotCzf1/ dotCzf2 were used for pre-screening by PCR. The transformants with correct PCR products were single-cell purified, plasmids isolated and subsequently re-confirmed by PCR and enzyme digestion for determining the insert direction. Fig. 3.4B shows the isolated plasmid pBlue-DGrev (pR264) had the *dotC* fragment (3 Kb). Fig. 3.4C shows the plasmid pR264 cut with *Eco*RI and *Rca*I and this digestion results fit to the expected digestion pattern. The digestion result also indicated that the *dotC-egfp* fragment was cloned into the pBluescript vector in a reverse direction.

Figure 3.4: Checking the plasmid pBlue-DGrev (pR264) with PCR and enzyme digestion.

A. The plasmid map of pR264.

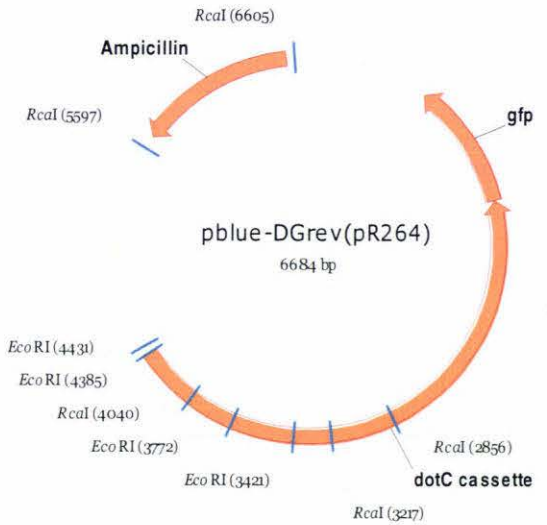

B

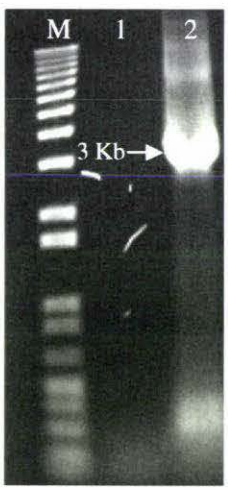

C

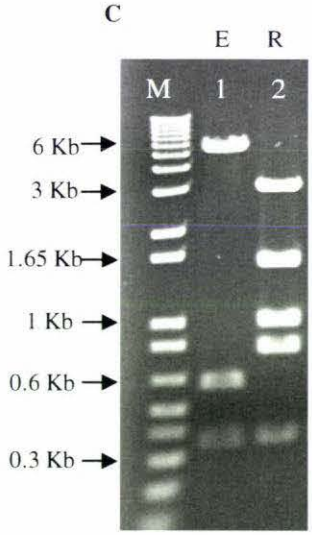

B. The PCR results checking the existence of the *dotC* fragment in pR264. Lane M: 1 Kb$^+$ ladder; lane 1: negative control without DNA template; lane 2: plasmid pR264. Using primer set dotCzf1 and dotCzf2 in the PCR, the 3 Kb band confirmed that the *dotC* fragment had been cloned into pR264.

C. The enzyme digestion results. Lane M: 1 Kb$^+$ ladder; lane 1: pR264/*EcoR*I; lane 2: pR264/*Rca*I. According to the digestion map shown in Fig. 3.4A, three fragments were expected after *EcoR*I digestion: 0.35 Kb, 0.6 Kb and 5.7 Kb (plus a 46 bp fragment too small to see); and five fragments (0.36 Kb, 0.8 Kb, 1 Kb, 1.6 Kb and 2.9 Kb) from *Rca*I digestion, this result was exactly consistent with Fig. 3.4A.

E: *EcoR*I; R: *Rca*I

3.2.3.2 Cloning the *hph* gene into the pBlue-DGrev (pR264)

All cloning steps were similar to the Section 3.2.3.1 except using the restriction enzyme *Xba*I instead of *Not*I (see Fig. 3.2). The insert *hph* fragment was cleaved from the DotC-Rep (pR260, refer to Fig. 4.4) plasmid DNA by *Xba*I. The pBlue-DGrev (pR264) was cut with *Xba*I as well and treated with SAP (Roche). Fig. 3.5B shows the PCR results that confirmed the two replicates of new plasmid pBlue-DG-hphrev (pR265) containing both the *dotC* fragment (lane 1 and 2) and the *hph* fragment (lane 3 and 4). Enzyme (*EcoR*I) digestion results (Fig. 3.4C) confirm that the pR265 is the correct vector, which has the expected digestion pattern and also indicate the direction of the inserted *hph* fragment (Fig. 3.5A).

Figure 3.5: Checking the plasmid pR265 with PCR and enzyme digestion.

A. The plasmid map of pR265.

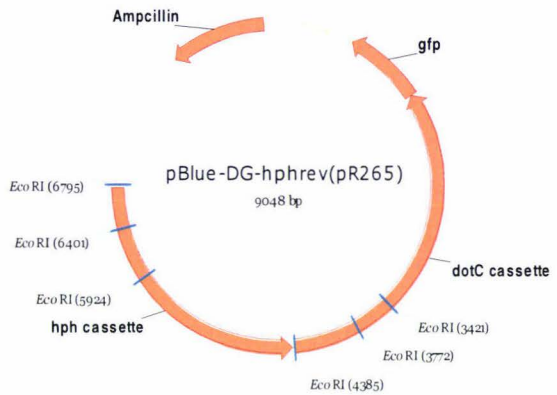

B

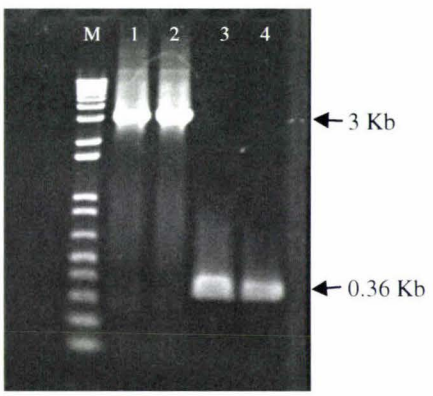

C

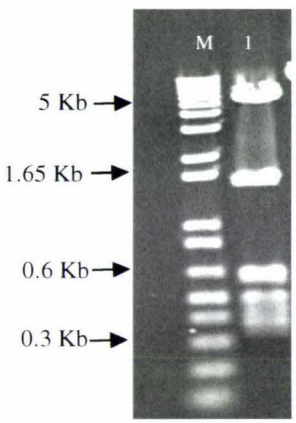

B. The PCR results checking the existence of the *dotC* and *hph* fragment in pR265.

Lane M: 1 Kb^+ ladder;

Lane 1and 2: PCR products using primer set dotCzf1 and dotCzf2; the two replicates of pR265 confirmed a 3 Kb *dotC* fragment had been cloned already.

Lane 3 and 4, PCR results showed the two replicates of pR265 had *hph* fragment as well, the primer set used here was 5'hph2672 and 3'hph3032 (located in the *hph* cassette and gave an expected ~0.36 Kb PCR product).

C. The enzyme digestion results to re-confirm the plasmid pR265.

Lane M: 1 Kb^+ ladder; lane 1: pR265/*EcoR*I;

According to Fig. 3.5A, six fragments are expected after *EcoR*I digestion: 0.35 Kb, 0.39 Kb, 0.48 Kb, 0.6 Kb, 1.5 Kb and 5.7 Kb; a smear can be observed around ~0.4 Kb region since the 0.35 Kb and 0.39 Kb fragments are too close.

3.3 TRANSFORMATION OF THE pR265 VECTOR INTO *D. SEPTOSPORUM*

3.3.1 *D. septosporum* protoplasts mediated fungal transformation

The pBlue-DG-hphrev vector (pR265) was transformed into *D. septosporum* wild type strain NZE10 using the protoplast mediated method (Section 2.5.2).

The first attempts at transformation had failed due to poor protoplast regeneration: less than 20 colonies had regenerated even under non-selective conditions. In order to solve this problem, all buffers and media were replaced and experiments were carried out to examine critical factors preventing the regeneration of the protoplasts (See details in Appendix IV). Finally, the stock 40% PEG was found to be inhibitory to protoplast regeneration. When fresh-prepared 40% PEG was used in transformation, hundreds of small transformants were observed after 7 days incubation at 22°C. After 14 days incubation, a few transformants continued to grow up to a size of approximately 5-10 mm. These larger colonies were likely to contain vector integrated into the genome, as opposed to having transient expression of resistance from an extrachromosomal plasmid. Of those transformants, 103 colonies were sub-cultured into fresh hygromycin-containing DM plates (20 colonies per plate), with cellophane on the surface of agar. After two weeks incubation, 24 colonies out of the 103 transformants were eventually grown up to a size of approximately 15×15 mm.

3.3.2 Screening of *dotC-egfp* mutants by PCR

In those 24 transformants, the colony of each transformants was divided into two parts using sterile scalpel and forceps. The smaller part of mycelia was sub-cultured into

another DSM plate and incubation at 22°C; the larger part of mycelia was freeze-dried and its genomic DNA extracted using the CTAB method (Section 2.3.1). The isolated DNA of each transformant was directly used as the template for further PCR screening.

The primer set used in the PCR screening was DCSE1/egfp rev. (Fig. 3.6A). If the *dotC-egfp* gene had been integrated into wildtype *D. septosporum* genome, the PCR product should be ~0.52 Kb DNA fragment and would also confirm that the *dotC* and e*gfp* were still linked together after transformation. PCR results showed that 23 transformants out of 24 had the expected products (results not shown). After observing the colonies of those 23 transformants under UV microscopy (Olympus SZX12), 8 transformants (FJT70-77) with relatively strong fluorescence (Ref to Fig 3.8) were chosen to be purified as described in Section 2.2.2.2. Fig. 3.6B shows the same PCR reactions described above to re-confirm those 8 transformants after purification. The results showed that all eight integrated mutants had the fusion *dotC-egfp* fragment.

Figure 3.6: Screening of *dotC-egfp* mutants by PCR.

A. The primer set used in the PCR screening and their approximate location

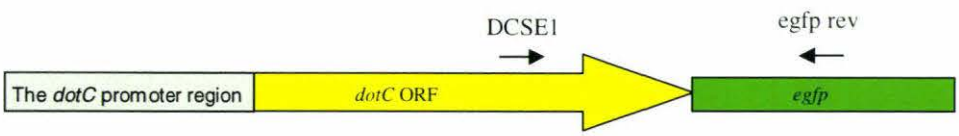

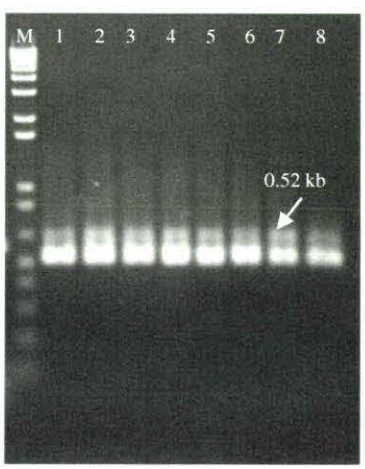

B. The PCR results confirming that the 8 single-spore purified mutants had the integrated *dotC-egfp*.

Lane M: 1 Kb^+ ladder;

The negative was set up without DNA template (not shown in this figure).

lane1: FJT70; lane2: FJT71;

lane3: FJT72; lane4: FJT73;

lane5: FJT74; lane6: FJT75;

lane7: FJT76; lane8: FJT77;

The results showed that all 8 mutants had the expected results (a 0.52 Kb product).

3.3.3 **Confirmation of the integration of *egfp* by Southern blotting analysis**

Although green fluorescence was observed in the 8 transformants, Southern blot hybridization was also applied to further confirm the integration of *dotC-egfp* into the *D. septosporum* genome.

The genomic DNA of four *dotC-egfp* mutants (FJT73, FJT74, FJT75 and FJT76) and WT (NZE10) was extracted as described in Section 2.3.1 The isolated DNA was then purified using a PCR purification kit (Qiagen) for further enzyme digestion. One DIG-labelled hybridization probe was a 420 bp partial *egfp* ORF fragment, which was amplified by PCR with primers RT-gfp fwd and RT-gfp rev using plasmid pPN81 as the template. Another probe, which amplified with primers DotCSE920 and MF4152P2 using NZE10 genomic DNA as the template, was designed to detect the *dotC* fragment (details see Section 4.3.2). Approximately 2 μg purified genomic DNA of each mutant and WT was digested with enzyme *Xho*I, then run in the agarose gel overnight. The details of Southern hybridization are described in Section 2.8.

The vector pR265 was expected to integrate into the *D. septosporum* genome randomly, thus the hybridization patterns of those mutants could not be predicated beforehand. The enzyme *Xho*I was chosen here since there is only one digestion site (out of the *dotC-egfp* fusion region) in the pR265 (Fig. 3.7A). If whole copies of pR265 had integrated into *D. septosporum* genome in tandem, the copy number of the *egfp* could be estimated based on the intensity of the hybridization bands of each mutant. Fig. 3.7A shows the approximate location of probes used in this experiment and the *Xho*I digestion site; Fig. 3.7B is the gel photo checking the status of *Xho*I digested genomic DNA of each strain. As shown in Fig. 3.7B, no band was observed in the WT, since no *gfp* fragment existed in WT *D. septosporum* strain. The mutants FJT73, FJT74, FJT75 and FJT76 all had the *egfp* fragment, which was consistent with the PCR screening

results in Section 3.3.2. In addition, although all strains had the same amount of DNA loaded into the gel, FJT73 and FJT75 had stronger hybridization bands than other two mutants, indicating multiple copies of the *dotC-egfp*. Based on the hybridization results using the *dotC* probe (Fig. 3.7D); the ~8.7 Kb band of WT was the only band which could be predicted before hybridization in this blotting analysis. Since there is only one copy of *dotC* in WT (Section 4.3.2), the copy number of integrated *dotC-egfp* fragment in mutants can be roughly estimated by comparing with the WT. The FJT74 had similar band intensity with the WT, thus copy number was considered as one. Moreover, for FJT74, there was one band in Fig. 3.7C of the *gfp* hybridization and two bands in Fig. 3.7D of the *dotC* hybridization, this result indicated that the *dotC-egfp* fragment had integrated into *D. septosporum* genome out of the *dotC* region. The FJT75 had two bands in both in Fig. 3.7C and Fig. 3.7D; this result suggested that the *dotC-egfp* fragment had integrated in two different regions and with multiple copies (~4 copies in total). The FJT76 had two weak bands in Fig. 3.7C and only one band in Fig. 3.7D, the copy number of *dotC-egfp* fragment might be one and the vector could be integrated into the genome randomly. Because the fragment size between two *Xho*I sites in WT (8.7 Kb) is very close to the vector (9 Kb), although the FJT73 had only one strong band both in Fig. 3.7C and Fig. 3.7D, it was still uncertain to conclude that the *dotC-egfp* fragment had integrated the original *dotC* region in tandem. However, there was no doubt that FJT73 had the vector integrated into the genome with multiple copies (~4 copies).

Figure 3.7: Southern blotting results.

A: The approximate location of probes used in Southern blotting and the XhoI sites

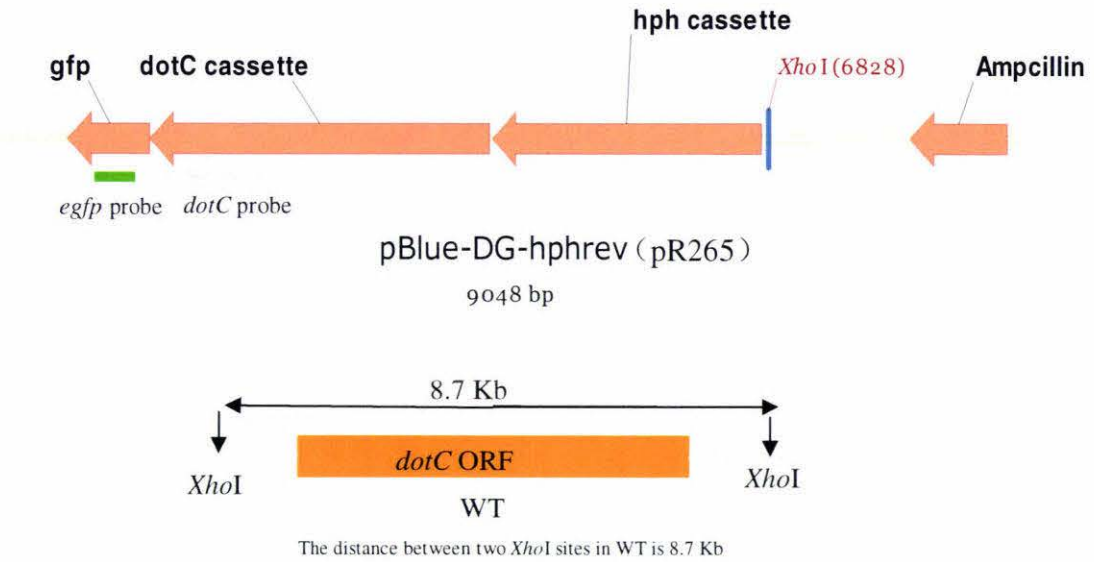

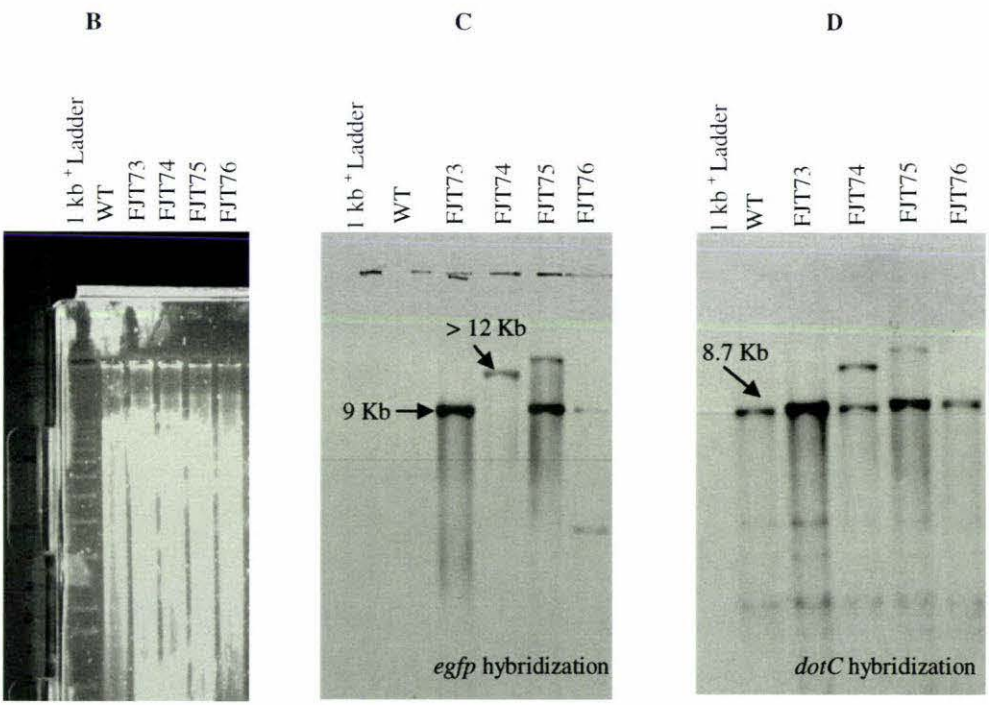

B. Southern blot gel

C. Southern hybridization X-ray film with *egfp* probe

D. Southern hybridization X-ray film with *dotC* probe

3.4 OBSERVATION OF THE DOTC-EGFP MUTANTS

In addition to observing the DotC-eGFP fusion protein, the radial growth rates of *dotC-egfp* integrated mutants and WT were also measured to check that the introduced construct did not adversely affect the fungus.

3.4.1 Growth rate of the *dotC-egfp* integrated mutants

The radial growth rates of the *dotC-egfp* integrated mutants (FJT73-76) and WT (NZE10) were measured as described in Section 2.12. The results are shown in Table 3.1. The radial growth of each mutant compared to the WT was analyzed by an unpaired T-test (http://www.graphpad.com/quickcalcs/ttest1.cfm). From the results shown in Table 3.1, the FJT73 mutant grew much faster than the WT from day 5 to day 28. The FJT74 grew faster than WT in the early stage (day 5), however, from day 18 to day 28, it grew slower than the WT. Similar to FJT74, the FJT75 showed faster growth rate than the WT till to day 18, while, it grew slower than the WT at day 28. FJT76 had a faster growth rate than the WT by the end of day 18, however, eventually the FJT76 showed no growth difference to the WT at the end of day 28. Overall there is no consistent trend to suggest that the presence of the *dotC-egfp* fusion gene affects growth rate.

Table 3.1 Radial growth of *dotC-egfp* integrated mutants

Strains	5days	11days	18days	24days	28days
	Mean ± SD (mm)	Mean ± SD (mm)	Mean ± SD (mm)	Mean ± SD (mm)	Mean ± SD (mm)
NZE10 (wild type)	3.68 ± 0.24	7.27 ± 0.76	13.33 ± 0.67	19.52 ± 1.53	22.76 ± 1.58
FJT73	*5.40 ± 1.18	*11.37 ± 1.82	*17.12 ± 1.64	*22.37 ± 1.83	*24.89 ± 1.79
FJT74	*4.35 ± 0.20	7.45 ± 0.59	13.36 ± 0.49	*17.54 ± 1.38	*20.64 ± 1.12
FJT75	*4.64 ± 0.60	*7.98 ± 0.66	*14.17 ± 0.96	18.26 ± 1.15	*20.61 ± 1.23
FJT76	*4.52 ± 0.57	*9.36 ± 0.80	*14.74 ± 1.50	20.27 ± 1.66	22.36 ± 1.37

All strains had 9 replicates;

*: indicates the data statistically significant when comparing mutants with wild type within each column.

3.4.2 Observation of the colonies and spores of the *dotC-egfp* integrated mutants

The colonies of all the *dotC-egfp* integrated mutants were checked under the fluorescence microscope to determine the expression of the eGFP protein (Section 2.11.1). Fig. 3.8 shows green fluorescence emitted from the colonies of the FJT73 and FJT75 mutants. The green fluorescence of each colony was concentrated mainly in the actively growing margins of the colony. FJT75 showed stronger fluorescence than the FJT73 under same exposure time. The WT colony did not show any image under this exposure time.

Figure 3.8: The green fluorescence of the FJT73 and FJT75 colonies.

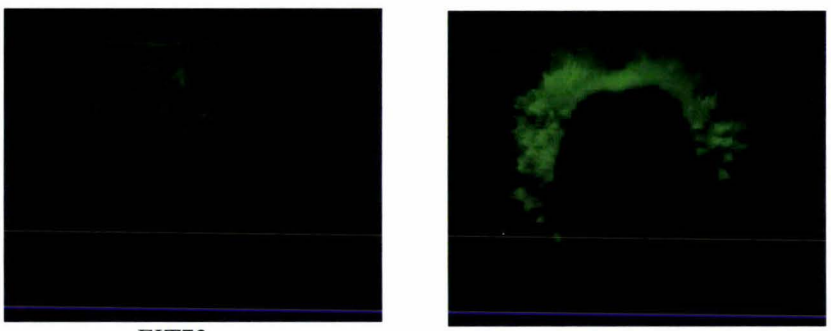

FJT73 FJT75

The spore suspension of each strain was observed under fluorescence microscopy (Section 2.11.1) to confirm whether the green fluorescence was stably expressed in each *dotC-egfp* mutant. In Fig. 3.9, The WT strain can only be seen under longer exposure time. A mutant (FJT22), in which a constitutively-expressed e*gfp* gene (vector pPN82) was transformed into the *D. septosporum* genome without *dotC* fusion, is shown as a control (Schwelm, 2007). In this strain, the eGFP protein has very bright fluorescence and can be observed throughout the spore. The spores did not show strong green fluorescence in FJT73, 74 and 76, even though the Southern results showed that FJT73 had multiple *egfp* copies. The fluorescence in FJT75 was unevenly distributed, which indicated the heterogeneity of GFP expression.

Figure 3.9: WT and e*gfp* containing mutants under normal microscopy.

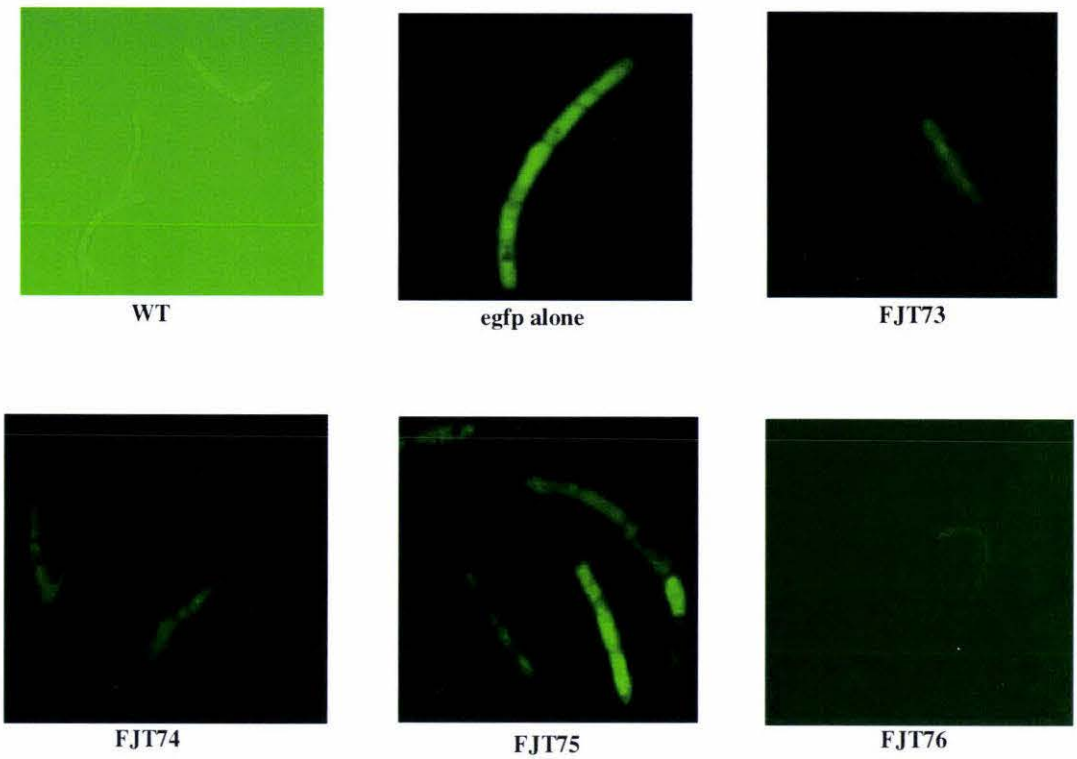

3.4.3 Observation of the mycelia of the *dotC-egfp* integrated mutants by confocal microscopy.

The method for preparation of cultures to be examined was described in Section 2.11.2 and spore suspensions of each sample were used for inoculation. FJT73 and FJT75 were selected for confocal microscopy observation (Fig. 3.10). The green fluorescence of FJT75 is located at the edge of each hypha, which suggests that the DotC is associated with the plasma membrane. In addition, quite a few strong green fluorescence dots can be observed in some hyphae but not all of them. These dots are localized within the cytoplasm and formed a circular structure, which suggested that the DotC of FJT75 could also be localized in vesicles (small) or vacuoles (large). Comparing to FJT75, the green fluorescence of FJT73 is mainly located at the margin and septa of each hypha and only a few fluorescent vesicles can be observed. Two cross sections are also shown

for FJT73 at the two dashed lines level. The white arrows point out a cross section of the hyphae. Here it can be seen that green fluorescence formed a hollow circle, which indicated that the DotC-eGFP fusion proteins were targeted to the plasma membrane in FJT73. From the Southern blot results, the different GFP distribution pattern between FJT73 and FJT75 was possibly due to the different vector integration pattern or/and different copy numbers. Some hyphal compartments lacked of fluorescence, indicating heterogeneity of GFP expression.

Figure 3.10: Mycelia of the FJT73 and FJT75 under confocal microscopy.

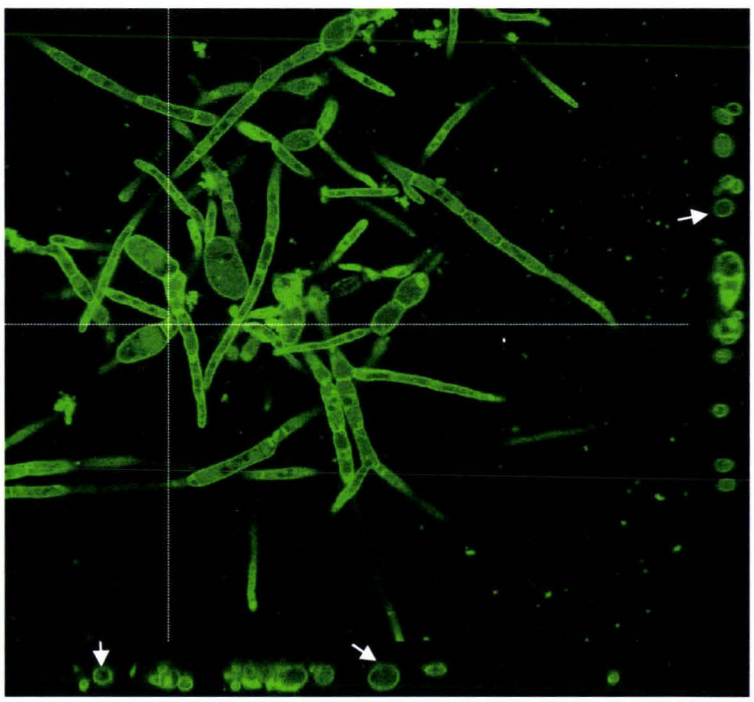

FJT73

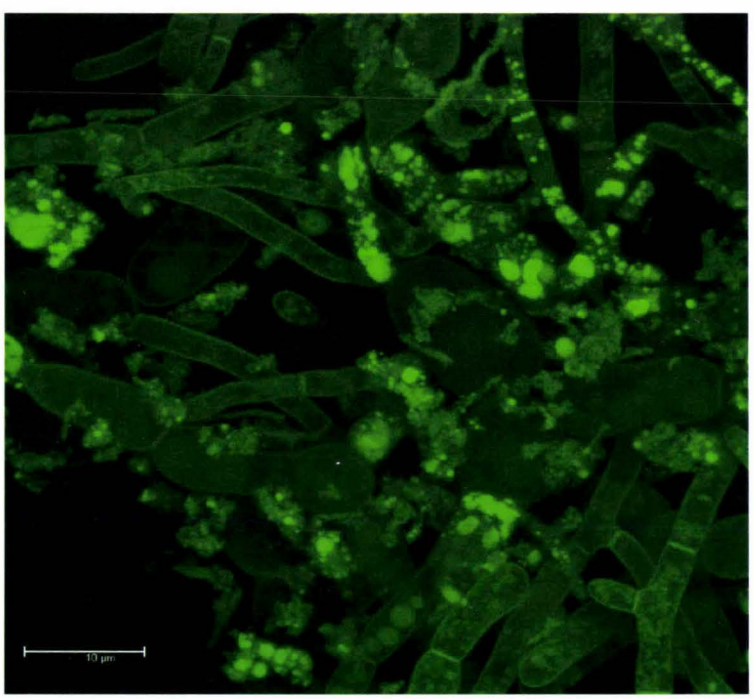

FJT75

FJT73: The green fluorescence is mainly located at the margin and septa of each hypha. Two cross sections are shown the two dashed lines level. The white arrows point out the cross section of the hyphae. The green hollow circle indicates that the DotC was targeted to the plasma membrane.

FJT75: Quite a few strong green fluorescence dots can be observed in some hyphae. Due to the low resolution of the FJT75 image, the cross sections are not shown.

3.5 DISCUSSION

3.5.1 Obtaining the *dotC-egfp* gene containing vector (pR265)

The method used for obtaining the vector pR265 was described in Section 3.2. Although the whole process seems more complicated than directly cloning the *dotC-egfp* fusion gene into the vector pPN81, the advantages of this method were:

1) The pGEM®-T Easy vector has reliable ligation efficiency and less insert is needed. In order to minimize misincorporation errors, the cycles of PCR reactions were reduced to 20. This relatively low PCR product yield worked well when cloning into the pGEM®-T Easy vector.

2) The pGEM®-T Easy vector has blue-white selection function, which is easy for transformants screening. In the original method, the pPN81 vector did not provide this preliminary screening method.

3) The pGEM®-T Easy vector can be directly used for cloning. There is no need to prepare the vector.

The foremost aim of this part was to obtain a *dotC-egfp* fusion gene without any amplification errors. The PCR optimization resulted in a lower PCR product yield than usual. Therefore, the pGEM®-T Easy vector provided an easy and quick method for cloning and verifying the DNA sequences of the *dotC-egfp* fragment. Once the correct fusion gene was obtained, the rest of the cloning steps would not impact on the sequence of this fusion gene.

3.5.2 Fungal transformation

In fungal species, the cell wall usually blocks the entry of DNA into the cell. To conquer this problem, the protoplast is introduced into the fungal transformation system; it had

its cell wall completely removed by enzyme digestion and becomes very sensitive to osmotic stress (Bradshaw, 2006). The PEG/protoplasts mediated *D. septosporum* transformation method is a sophisticated method, which optimized by Bradshaw (1997), Seconi (2001) and Teddy (2004).

There were 23 transformants out of 24 stable hygromycin-resistance colonies that were identified with the *dotC-egfp* fusion fragment by PCR. By observing the colonies under UV light, at least eight transformants had relatively strong green fluorescence. Four of these transformants were further confirmed by Southern blotting analysis, they all had the integrated *egfp* fragment although with different number of copies. The overall transformation frequency was quite high.

3.5.3 GFP observation in *dotC-egfp* integrated mutants

The *dotC* gene is located in dothistromin biosynthetic cluster and has 25% identity of its amino acid sequence identity to other fungal MFS transporters, such as the *aflT* gene (Bradshaw *et al.*, 2002). The analysis of the putative DotC protein reveals it has 14 predicted TMDs, which is a typical feature of MFS transporters (Del Sorbo *et al.*, 2000). Therefore, the *dotC* gene is postulated to encode a MFS transporter targeted in the plasma membrane and involved in dothistromin secretion. In this study, the DotC controlled eGFP was successfully expressed in *D. septosporum* and thus the DotC localization could be observed using GFP as a marker.

In *dotC-egfp* integrated mutants, GFP was firstly observed by checking the colonies under a fluorescence microscope. The fluorescences were mainly observed at margin of the colonies (Fig. 3.8) and this phenomenon was also found in the *dotA-egfp D. septosporum* mutants by (Schwelm *et al.*, 2007). In Schwelm's research, real-time PCR analyses indicated that the expression of dothistromin biosynthetic gene *dotA* occurred at an early stage of growth. This result was consistent with their observation of DotA controlled GFP highly concentrated at the growing margin of the colony. However, the

real-time result showed that *dotC* is constitutively expressed over time and has no correlation with *dotA* expression. The constitutively expressed *dotC* is inconsistent with the expression of DotC controlled GFP mainly at the edges of the colonies. As mentioned in chapter one, expression of GFP requires oxygen; this is why difficulties were encountered when using GFP in the studying of anaerobes (Tsien, 1998). Considering the oxygen metabolism in these growing mycelia, enhanced GFP at the colony margin might reflect the more active metabolism occurring in the young hyphae. Alternatively, there may be some post-transcriptional control of *dotC* which means the protein is not constitutively produced.

The confocal image of FJT73 provided strong evidence suggesting that DotC is associated with the plasma membrane. An analysis using pTARGET program (a computational method to predict the subcellular localization of proteins) suggested that the native DotC protein was predicated to be a plasma membrane protein with 100% confidence (Schwelm, 2007); this was consistent with the results obtained in this research. In addition, fluorescent dots were also observed in some hyphal compartments in both strains, particularly in FJT75. Based on their shape, they are postulated to be vesicles or vacuoles. The *dotC* is a putative MFS transporter encoding gene, previous researchers reported that some MFS transporters were located in the vacuolar membrane (Chiou and Bush, 1996; Shimazu *et al.*, 2005). These findings could suggest that the DotC also has relationship with the vacuolar membrane. However, in Schwelm's research, green fluorescent vesicles were also observed in DotA-controlled GFP mutants. By using FM4-64, which stained endocytic vesicles and vacuolar membranes, he found that these dots indeed overlapped with FM4-64 stained endocytic components. Therefore, he suggested that these dots represent the DotA controlled GFP targeted to organelles but which kind of organelles was uncertain. Since *dotA* is a putative ketoreductase gene and has no relationship with the cell membrane, the bigger green fluorescence dots observed in *dotC-egfp* mutants are more likely the vacuoles just containing the DotC-eGFP proteins (possibly are going to be degraded due to overproduction by the multiple copies of integrated DotC-eGFP proteins). The smaller

dots could be the vesicles involved in protein sorting. Although the pTARGET program gave a hint that the native DotA protein was predicted to be located at peroxisomes; more solid experimental evidence is needed to support those hypotheses.

Similar research has been carried out to examine the subcellular localization of aflatoxin biosynthetic enzymes. Lee *et al.* (2004) reported that Nor-1 and Ver-1 were primarily localized to the cytoplasm and OmtA was possibly located to vacuoles. In addition, the VBS was found that distributed throughout the cytoplasm and concentrated in ring-like structures surrounding nuclei (Chiou *et al.*, 2004). However, the relationship between the enzymes' function and subcellular localization was unclear.

It is uncertain why there was heterogeneity of GFP expression in hypha. The possible reason might be due to an impaired ability of some cells to express *gfp* and the fusion constructs (Chung *et al.*, 2002). However, the membrane localization of the DotC-eGFP does support the hypotheses that DotC is a membrane transporter protein.

CHAPTER FOUR: *DOTC* GENE DISRUPTION

4.1 INTRODUCTION

The putative *dotC* gene is proposed to encode a MFS transporter and may participate in secreting the dothistromin toxin and/or as a self-protection function for the fungus to resist its own toxin. In chapter 3, the localization of the DotC protein was observed under confocal microscopy using GFP as a marker. The results indicated that the DotC-GFP fusion proteins were mainly targeted to the plasma membrane of *D. septosporum*. To continue studying the biological functions of the *dotC* gene, targeted gene disruption provides a powerful method by a reverse genetic approach. A *dotC* gene disruption vector was constructed and the phenotypes of *dotC* gene-disrupted mutant(s) were characterized after this disruption vector was transformed into wild type *D. septosporum*.

4.2 CONSTRUCT THE DOTC GENE DISRUPTION VECTOR

The *dotC* gene disruption vector was constructed using the Multisite Gateway Three-fragment Vector Construction Kit (Invitrogen). The whole cloning procedure was composed of four steps and is outlined in Figs. 4.1 and 4.2.

4.2.1 Step 1: Producing *att*B attached PCR products

As shown in Fig. 4.1, the 5'element and 3'element regions that flank the *dotC* gene were amplified by PCR, using *D. septosporum* strain NZE8 genomic DNA as the template. The nucleotide sequence of the two primer sets is shown in Table 2.2 and the precise location of these primers is shown in Fig. 4.1A. For amplifying the 5' element region of the *dotC* gene, an *att*B4 site was attached to the 5' end of the primer dotC5'fwd and an *att*B1 site was added to the 5' end of the primer dotC5'rev (see step 1 in Fig. 4.2). Thus, a 1.1 Kb DNA fragment (Fig. 4.1B, lane 1), which included a 48 bp DNA fragment at the 5' end of the *dotC* open reading frame (ORF), was obtained by PCR amplification using Platinum® *Taq* DNA Polymerase High Fidelity (Invitrogen). For amplifying the 3' element region of the *dotC* gene, *att*B2 and *att*B3 sites were also added to the 5' ends of the primers dotC3'fwd and dotC3'rev, respectively (step 1 in Fig. 4.2). Then a 1 Kb DNA PCR product (Fig. 4.1B, lane 2), which included a 456 bp DNA fragment at the 3' end of the *dotC* ORF was obtained. Since the whole ORF of *dotC* gene is about 1.9 Kb in length, if the 48 bp 5' arm and the 456 bp 3' arm keep intact in the subsequent recombination reaction in *D. septosporum*, the remaining approximately 1.4 Kb coding region of the *dotC* will be replaced by the hygromycin (*hph*) gene cassette (the selectable marker).

Figure 4.1: PCR products of 5'and 3' elements of the *dotC* gene.

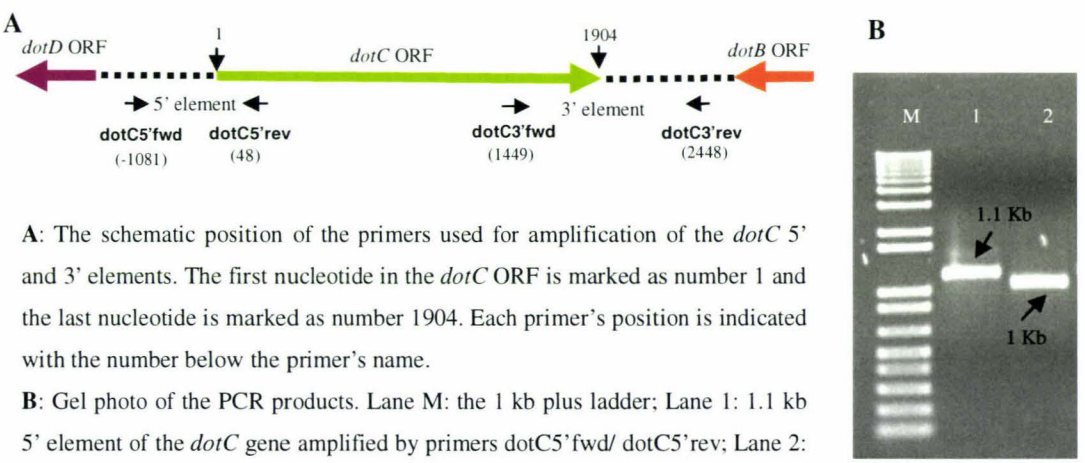

A: The schematic position of the primers used for amplification of the *dotC* 5' and 3' elements. The first nucleotide in the *dotC* ORF is marked as number 1 and the last nucleotide is marked as number 1904. Each primer's position is indicated with the number below the primer's name.

B: Gel photo of the PCR products. Lane M: the 1 kb plus ladder; Lane 1: 1.1 kb 5' element of the *dotC* gene amplified by primers dotC5'fwd/ dotC5'rev; Lane 2: 1 kb 3' element of the *dotC* gene amplified by primers dotC3'fwd/ dotC3'rev.

Figure 4.2: Experimental procedure for constructing the disruption

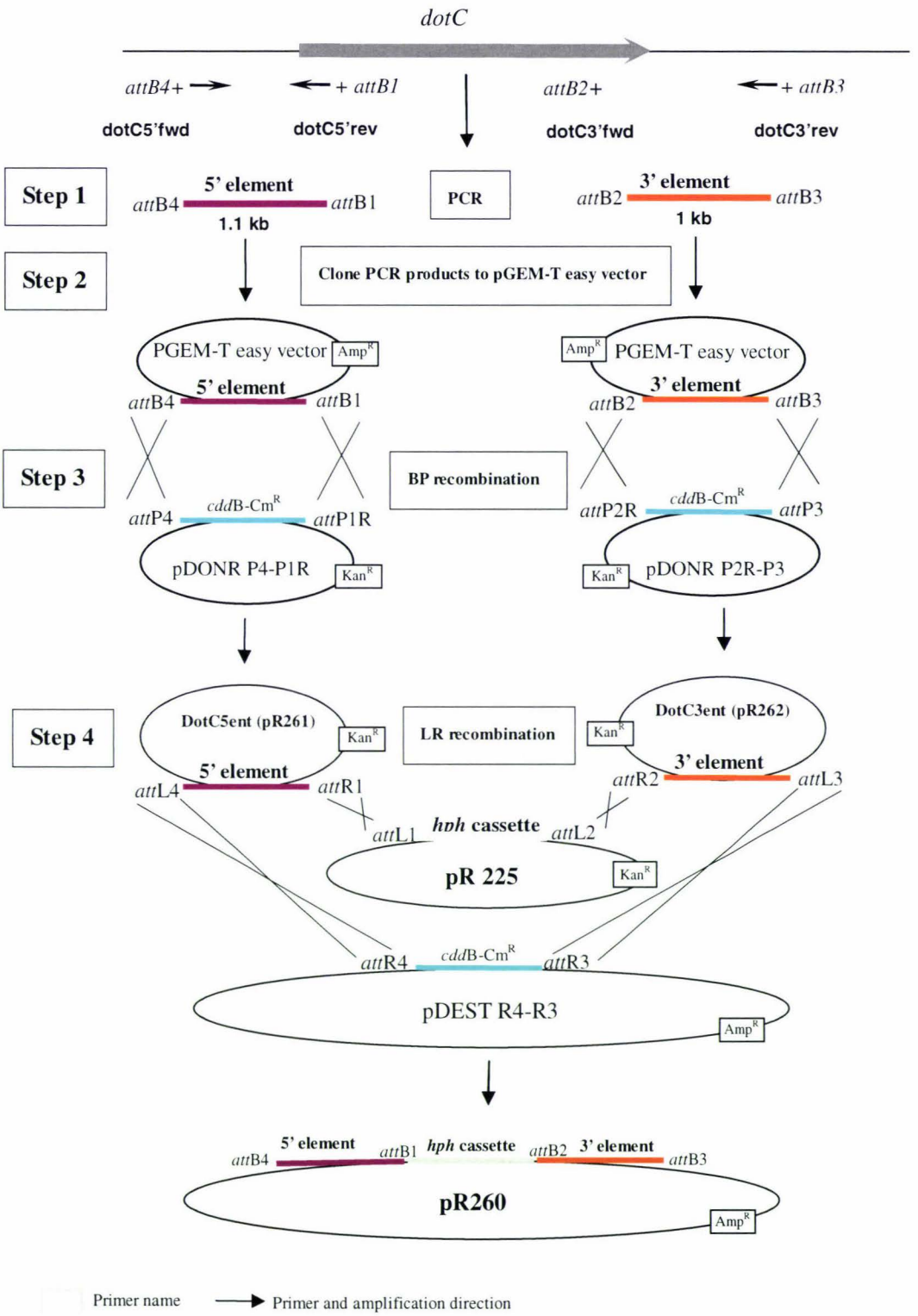

4.2.2 Step 2: Cloning the 5'and 3'elements into the pGEM®-T Easy vector

The PCR products of 5' and 3' elements of the *dotC* gene were then purified using a PCR purification kit (Qiagen) and ligated individually into the pGEM®-T Easy vector (Promega) prior to BP recombination (step 2 in Fig. 4.2). The plasmids containing the 5' and 3' elements were isolated individually and sent for DNA sequencing to confirm that the correct 5' and 3' elements had been cloned into the pGEM®-T Easy vector.

4.2.3 Step 3: BP (*att*B: *att*P) recombination to generate entry clones

The vectors containing the 5' and 3' elements flanked with the *att*B sites were subsequently recombined with their corresponding pDONR™ vectors by BP recombination reactions (Section 2.4.3.1; Fig. 4.2 step 3). Table 4.1 shows the corresponding vector pairs in the BP reactions and the names of the final entry clones. After BP reactions, the mixtures were cleaned using a PCR purification kit (Qiagen) and eluted into 30 µl elution buffer (Qiagen). An aliquot of 1µl of either the 5' element or 3' element purified BP reaction product was transformed into Top 10 *E. coli* competent cells (Section 2.5.1.1) using kanamycin (final 50 µg/ml concentration in each LB plate) as a selectable marker. Positive control (pMS/GW vector, which is supplied within the Invitrogen Gateway kit) and negative control (no DNA) transformations were also included. All transformants were screened by colony PCR (Section 2.6.5) using the same primer sets used for amplifying the 5' and 3' elements. In the 5' element colonies, three colonies were identified with positive results out of a total of four colonies. In the 3' element colonies, all three colonies tested were positive transformants. The plasmid DNA of those colonies was isolated and reconfirmed by PCR with the same primer sets again (results not shown). Therefore, the entry clones with the 5' and 3' elements of the *dotC* gene had been prepared.

The selectable gene entry clone, pR225, had been constructed by Teddy (Teddy, 2004). This vector was generated by amplifying the hygromycin (*hph*) gene with *att*B1 and *att*B2 attached primers followed by recombination into the donor vector pDONR 221.

Table 4.1: Construction of the *dotC* 5' and 3' elements containing entry clones.

PCR products (in pGEM®-T Easy vector)	Donor vectors (antibiotic resistance)	Entry clones
*att*B4-5' element-*att*B1	p DONR P4-P1R (Kana^r)	DotC5ent(pR261)
*att*B2-3' element-*att*B3	p DONR P2R-P3 (Kana^r)	DotC3ent(pR262)

4.2.4 Step 4: LR recombination to obtain the final disruption vector

The LR recombination reaction was carried out as described in Section 2.4.3.2. The homologous *att* site recombination occurred as shown in Fig. 4.2, step 4. An aliquot of 2 µl purified LR recombination product was transformed into Top 10 *E. coli* competent cells (Section 2.5.1.1) and ampicillin (final 100 µg/ml concentration) was added to the LB plates for selection. The transformants were screened using a rapid restriction endonuclease (*Xba*I) digestion method which involves digestion of DNA in a crude cell lysate (Section 2.4.1). From the plasmid map of the final disruption vector (Fig. 4.3A and Fig. 4.4), two *Xba*I sites were expected to give two DNA fragments (2.4 Kb and 4.6 Kb) after digestion. Thus, as shown in Fig. 4.3B, five transformants (No. 13, 19, 26, 27 and 28) were identified which matched the expected digestion results. In this gel photo, each transformant actually showed four bands. Besides the two expected fragments, the top band (the largest fragment) was genomic DNA of *E. coli* cells, whilst the second largest band, (approximately 7 Kb) was probably due to partial digestion of the vector (considering the digestion time only was 30 minutes for this rapid screening method). The digestion time was 30 minutes maximum in this screening method because longer digestion may increase the background when the genomic DNA was digested, preventing clear visualization of plasmid DNA.

The transformants No.19 and 26 were selected and purified by streaking on fresh ampicillin-containing LB plates and the plasmid DNA was subsequently isolated. The isolated plasmids DNA were reconfirmed by PCR, with the primer sets shown in Fig. 4.3A, and results indicated that the two transformants had the correct PCR products (Fig.

4.3C). Moreover, the sequencing result of the plasmid from transformant 19 showed that the 5' element, *hph* gene and 3' element all had been cloned into the final vector with an appropriate order and it was selected for further use as the *dotC* disruption vector pR260.

Figure 4.3: LR recombination

A. Diagram of the expected LR recombination products and the location of primers.

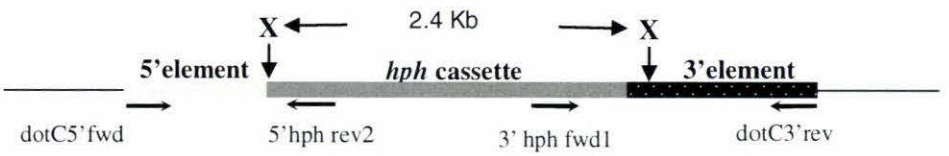

Approximate positions of primers used for screening the transformants are indicated by the lower pairs of arrows. X indicates the two *Xba*I sites.

B. The enzyme digestion results for screening the LR transformants

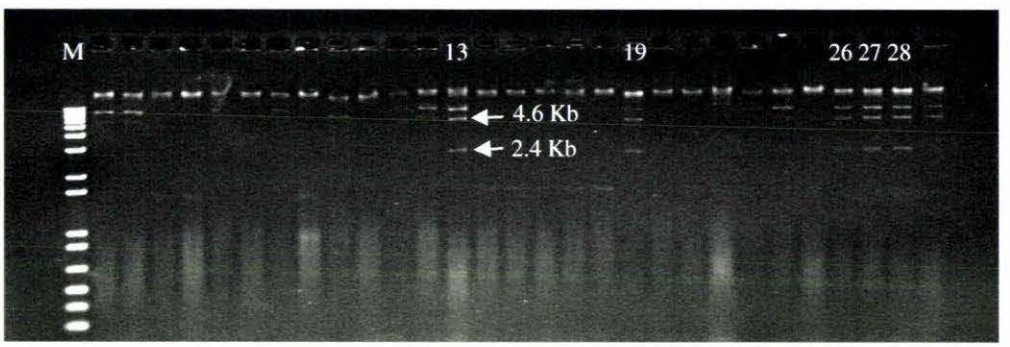

DNA in *E. coli* cell lysate was digested with *Xba*I. The 2.4 Kb fragment represents the *hph* cassette and the 4.6 Kb fragment represents the remaining of the *dotC* disruption plasmid.

C. The PCR results for confirmation of plasmid DNA from transformants No. 19 and 26

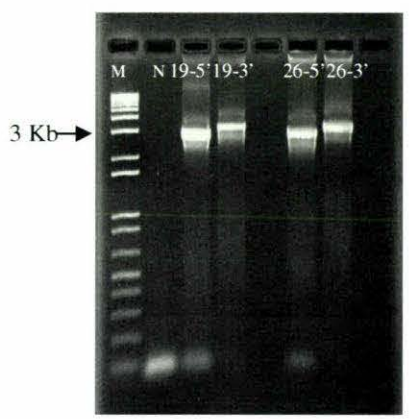

The 19-5' and 26-5' PCR products were amplified by primers dotC5'fwd/5' hph rev2. The two bands were about 2.7 Kb in size, which matched the expected results based on the plasmid map.

The 19-3' and 26-3' PCR products were amplified by primers dotC3'rev/3' hph fwd1. The two bands were about 3 Kb in size, which also matched the expected results.

Lane M : 1 Kb^{+} ladder ; Lane N: negative control without template DNA.

4.3 TARGETED DELETION OF THE *DOTC* GENE IN *D. SEPTOSPORUM*

The *dotC* gene was disrupted by transforming vector pR260 into *D. septosporum* wild type strain NZE10 (Section 2.5.2). The NZE10 is the latest isolated *D. septosporum* strain and it was chosen for the transformation due to its consistent production of dothistromin in the laboratory.

D. septosporum transformation was carried out as described in Section 2.5.2. Hundreds of tiny colonies were observed after 7 days incubation at 22°C. However, only a few of these continued to grow up to a size of approximately 5-10 mm upon the agar. These larger colonies were likely to be true transformants. Approximately 100 larger colonies (20 per plate) were transferred onto fresh hygromycin-containing DM or PDA plates, which had cellophane on the surface of agar. After two weeks incubation, only 26 colonies out of 100 had eventually grown up to a size of approximately 15 mm diameter. These were likely to be stable transformants in which pR260 had integrated into the genome.

4.3.1 Screening of *dotC* deletion mutants by PCR

The 26 transformants were subsequently screened by PCR. The colony of each transformants was divided into two parts using a sterile scalpel and forceps. The smaller part of mycelia was sub-cultured into another DM plate and incubated at 22°C; the larger part of mycelia was freeze-dried to extract its genomic DNA (Section 2.3.1), which was used as the template for PCR screening. In order to check the reliability of the genomic DNA isolated directly from colonies, test PCR reactions were firstly set up using primer sets applied to originally amplify the 5' element of the *dotC* gene. PCR products were obtained from these templates (results not shown), however, two DNA samples only worked after purifying the genomic DNA with a PCR purification kit

(Qiagen).

As mentioned in Section 4.2.1, the partial (~1.4 Kb) *dotC* coding region would be replaced with the *hph* cassette (~2.4 Kb) only when a double crossover (both in 5' end and 3' end) happened by homologous recombination. The two primer sets, which were designed to examine homologous recombination both in the 5' element region and 3' element region, are shown in Fig. 4.5A. Primer 5'dotD RACE (in the *dotD* coding sequence region) and primer 5'hphout (in the *hph* gene region) were used to identify 5' end recombination by producing a 2.1 Kb PCR product as an indication. Primer 3'hphout (in the *hph* gene region) and primer 100downdotC-Rep3 (100 bp downstream of the 3' element of the *dotC*) were applied to detect the 3' end recombination by acquiring a 1.3 Kb PCR product. The *dotC* gene disrupted mutant strain(s) should have PCR products with correct sizes for both the 5' end and 3' end. In contrast with the mutant, the wild type *D. septosporum* genomic DNA was used as a template for the PCR reaction with the same primer sets; no PCR products should be observed since no *hph* gene had been integrated into *D. septosporum* genome in the wild type.

The isolated genomic DNA (4-10 ng/ul, usually 1 ul DNA per PCR reaction) of each transformant was directly used as a template for PCR screening. In the first round of screening, 22 transformants produced the 5' region PCR products, while, only five of these produced the 3' region PCR products. This result indicated that five transformants were possible double-crossover gene replacement mutants since they had the correct PCR products both at the 5' and 3' end. Four of these putative *dotC* disrupted mutants (FJT15, FJT16, FJT19 and FJT46) were selected for further study (one transformant was eliminated since it had a very weak 3' end PCR product). In addition to these, two transformants (FJT42 and FJT43) only had 5' region PCR products and two transformants (FJT79 and FJT80) that had no PCR products in either 5' or 3' regions (ectopics) were also chosen for further characterization. All eight transformants were subcultured into the DSM plates to undergo the single spore purification process (Section 2.2.2.2). This step is essential as primary transformants can often be mixed

cultures or heterokaryons. Then, the genomic DNA of those purified cultures was extracted and subjected to the second round PCR screening. As shown in the Fig. 4.5B, this second round PCR results showed that only FJT15 and FJT16 out of the four putative *dotC* disrupted mutants still had correct PCR products both in the 5' region and 3' region. The transformant FJT19 kept its 3' region product but no longer had a 5' region product, which indicated that it may be a 3' single cross-over mutant. The rest of the five transformants all appeared to be ectopic transformants since they did not show any products in either the 5' region or in 3' the region. The negative control (lane 1) without DNA template did not show any products in the 5' region and in the 3' region as expected. Another control (lane 2, top panel) using NZE10 WT genomic DNA as the template showed a few smaller size PCR products in the 5' region. Those products were thought to be non-specific PCR products since they did not fit the expected size and all the transformants also had these same size PCR products. Overall, two *dotC* disrupted mutants (FJT15 and FJT16) were identified out of 26 transformants by PCR.

Figure 4.4: The plasmid map of the *dotC* disruption vector pR260.

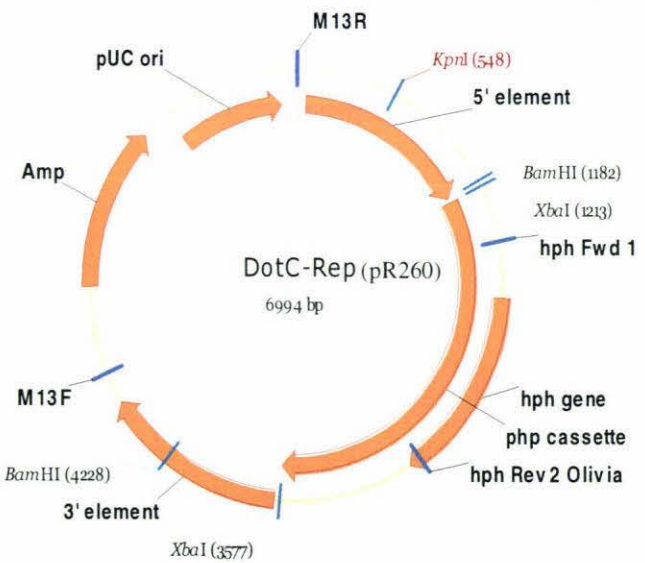

Figure 4.5: PCR screening of the purified *dotC* disrupted transformants

A. Schematic map of PCR screening of *dotC* transformants

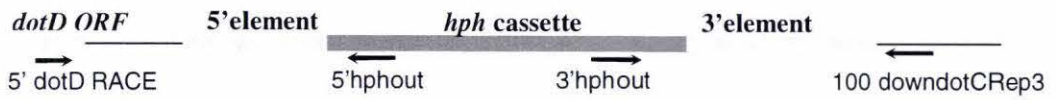

Primers' positions indicated by arrows.

B. PCR screening results of the purified transformants

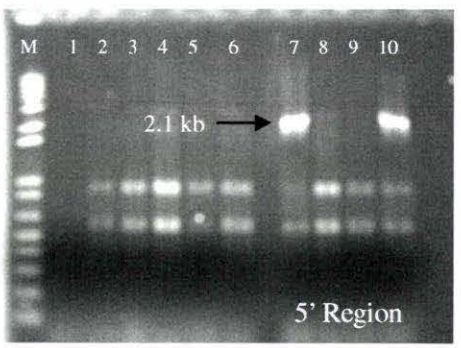

The top panel shows the PCR results for checking the 5' region recombination. The primer sets used were 5' *dotD* RACE and 5' *hph*out. Transformants FJT15 and FJT16 had the expected 2.1 Kb PCR products, which indicated correct insertion at the 5' end of *dotC*.

The bottom panel shows the PCR results for checking the 3' region recombination. The primer sets used were 3' *hph*out and 100downdotCRep3. Transformants FJT15, FJT 16 and FJT19 had the 1.3 Kb PCR products, which indicated correct insertion at the 3' of *dotC*.

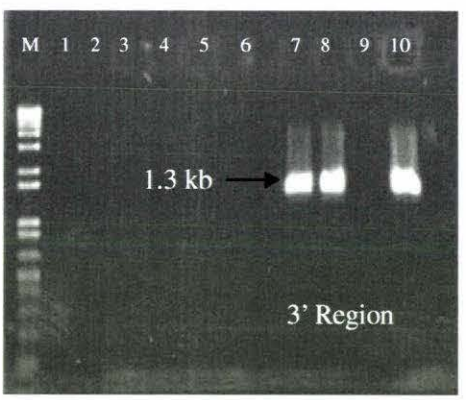

Only FJT15 and FJT16 had PCR products in both 5' and 3' ends.

Lane M: 1 Kb^+ ladder Lane 1: negative control (no DNA);
Lane 2: NZE10 wild type DNA as template
Lane 3: FJT43 Lane 4: FJT42
Lane 5: FJT79 Lane 6: FJT80
Lane 7: FJT16 Lane 8: FJT19
Lane 9: FJT41 Lane 10: FJT15

4.3.2 Confirmation of *dotC* disrupted mutants by Southern blotting analysis

Using the PCR method, two *dotC* disrupted mutants (FJT15 and FJT16) had been identified; however, they still needed to be reconfirmed using other reliable methods to make sure they were the true mutants. Therefore, Southern blot hybridization was applied to further verify whether the 5' and 3' region double-crossover had happened in the *dotC* disrupted mutants, and to indicate the copy number of the *dotC* gene in *D. septosporum* wildtype genome. Three ectopic transformants (FJT42, 79, 80) and one 3' *dotC* integrated transformants (FJT19) were included as controls along with the wild type (NZE10).

The genomic DNA of each transformant or WT were extracted and purified as described in Section 2.3.1 and 2.6.6. The DIG-labelled hybridization probe was a 2.1 Kb PCR product amplified with primers DotCSE920 and MF4152P2 using NZE10 genomic DNA as the template. This probe included the whole *dotC* ORF region and an extra 165 nucleotides upstream of the *dotC* ORF and 70 nucleotides downstream (Fig. 4.6). Individual enzyme digestions by *Kpn*I and *Bam*HI were applied to examine changes in their digestion pattern before and after homologous recombination. Approximately 2 μg digested genomic DNA of each sample was loaded in the agarose gel. The details of Southern hybridization are described in Section 2.8 and the expected patterns of hybridizing fragments are shown in Fig. 4.6.

Fig. 4.7A (right panel) shows the Southern hybridization results for *Kpn*I digestion. Lanes 2 and 3 are the WT samples, an expected 3.5 Kb band can be observed in these two lanes. Lanes 4 (FJT16) and lane 9 (FJT15) show a 4.5 Kb band as expected for a *dotC* gene replacement, and confirm the PCR screening results from the last section. Ectopic transformants showed a wild type 3.5 Kb hybridization band as well as additional band(s) of variable size, suggesting that *dotC* was still intact in these stains. There was no unexpected band observed in WT, FJT15 and FJT16, therefore, the copy number of the *dotC* gene in the *D. septosporum* genome was considered to be one.

For *Bam*HI digestion (Fig. 4.7B), there are four *Bam*HI digestion sites. The fragment sizes between each of the digestion site are shown in Fig. 4.6. The site B3 is deleted when homologous recombination happens to replace the *dotC* gene. Then the two fragments B2-B3 (0.3 Kb) and B3-B4 (1.7 Kb) are "merged", but since the *hph* gene cassette (2.4 Kb) is 1 Kb larger than the replaced *dotC* coding sequence, thus, after homologous recombination, the B2-B4 distance expands to 3 Kb. In terms of the hybridization results, two fragments, B2-B3 (0.3 Kb) and B3-B4 (1.7 Kb) should be detected after hybridization with the DIG-labelled probe in WT and they would be replaced by a 3 Kb fragment in the *dotC* disrupted mutant after recombination. As shown in Fig. 4.7B (right panel), two bands of 0.3 Kb and 1.7 Kb were observed in the WT (lane 2) as expected. In lane 3 (FJT16) and lane 8 (FJT 15), as expected, a 3 Kb band was found instead of the two 0.3 Kb and 1.7 Kb bands. This result confirmed that the FJT15 and FJT16 were the two *dotC* disrupted mutants. The 7.5 Kb band was the B1-B2 fragment which was present in all samples. An unexpected 2.2 Kb band in WT (lane 2) may be due to non specific hybridization or it could be the product of partial digestion (although this band is a little bigger than the B2-B4 fragment). However, when the WT genomic DNA was again digested with *Bam*HI and hybridized with the same probe, the 2.2 Kb fragment disappeared (results not shown). Ectopic strains showed the WT band (1.7 Kb) and some of them also showed a 3 Kb fragment indicative of section B2-B4 of the vector having integrated elsewhere into the genome.

Figure 4.6: Schematic outline of expected Southern blot hybridization patterns

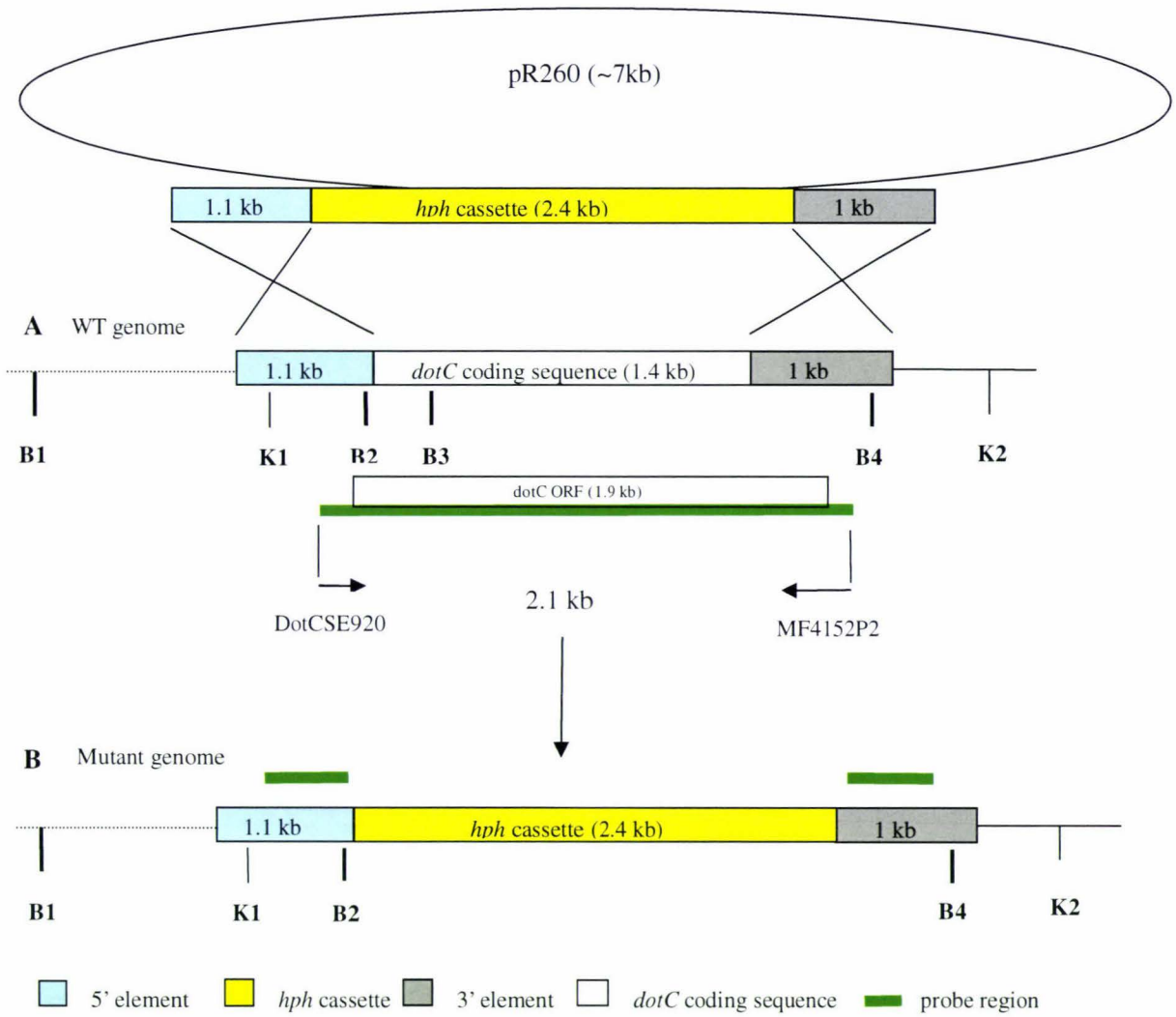

K: *Kpn*I digestion sites **B**: *Bam*HI digestion sites.

The hybridization probe was amplified using primers DoctSE920/ MF4152P2. This probe included the whole *dotC* ORF region and extra 165 nucleotides upstream of the *dotC* ORF and 70 nucleotides downstream.

Expected hybridization fragment sizes:

	*BamH*I	*Kpn*I
A Wild type:	B1-B2: 7.5 Kb	K1-K2: 3.5 Kb
	B2-B3: 0.3 Kb	
	B3-B4: 1.7 Kb	
B The *dotC* disrupted mutant:	B1-B2: 7.5 Kb	K1-K2: 4.5 Kb
	B2-B4: 3 Kb	

Figure 4.7: Southern blot results to confirm the identified *dotC* mutants.

A. *Kpn*I digestion to confirm the *dotC* mutants

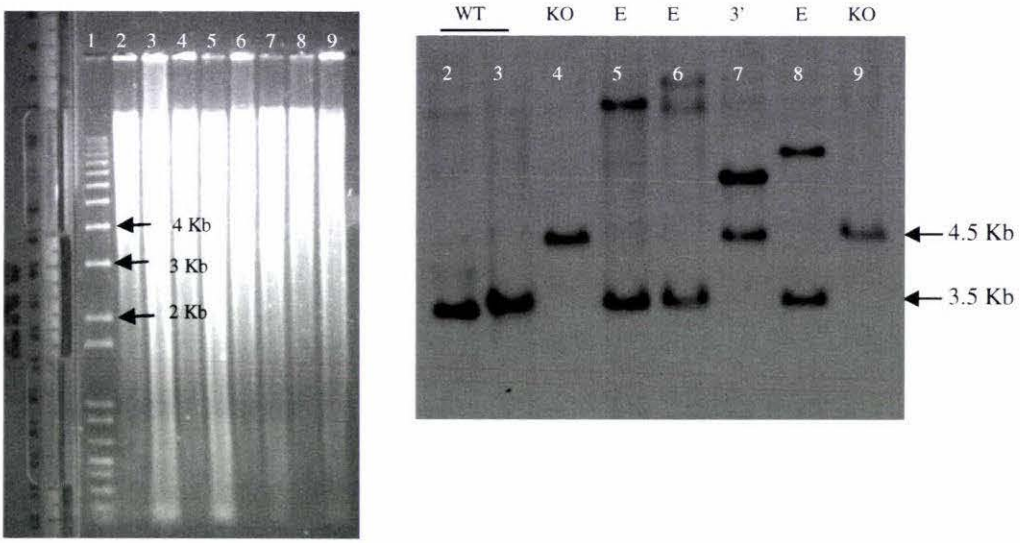

Lane1: 1 Kb$^+$ ladder Lane2: WT (NZE10) Lane3: WT (NZE10)

Lane4: FJT16 (KO) Lane5: FJT79 (E) Lane6: FJT80 (E)

Lane7: FJT19 (3') Lane8: FJT42 (E) Lane9: FJT15 (KO)

Left panel: Southern blot gel; Right panel: Southern hybridization X-ray film

KO: *dotC* disrupted mutant; E: ectopic mutant; 3': 3' end cross-over mutant.

B. *BamH*I digestion to confirm the *dotC* mutants

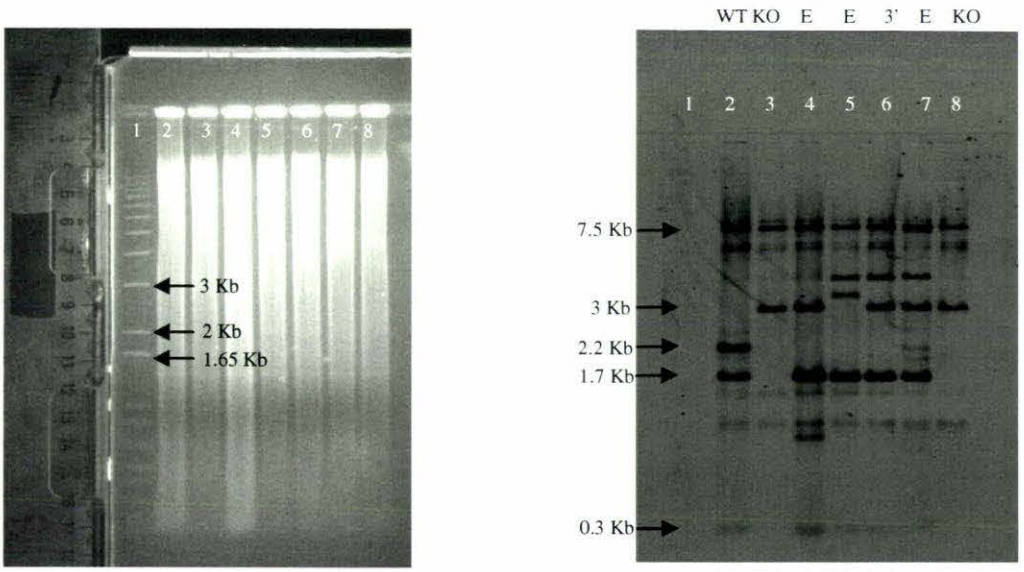

Lane1: 1 Kb$^+$ ladder Lane2: WT (NZE10) Lane3: FJT16 (KO)

Lane4: FJT79 (E) Lane5: FJT80 (E) Lane6: FJT19 (3')

Lane7: FJT42 (E) Lane8: FJT15 (KO)

Left panel: Southern blot gel; Right panel: Southern hybridization X-ray film

4.4 CHARACTERIZATION OF THE DOTC DISRUPTED MUTANTS

Once the *dotC* disrupted mutants had been obtained, their phenotypes were characterized by comparing with the *D. septosporum* wild type strain. The *dotC* gene is a putative MFS transporter encoding gene and possibly participates in secreting the dothistromin toxin and as a self-protection function for the fungus to resist its own toxin. Therefore, the toxin production and toxin resistance of the *dotC* mutants needed to be examined to testify whether the *dotC* gene was truly involved in toxin efflux and the effects of the toxin to the mutants. Meanwhile, growth rate and sporulation rate of the mutants were measured to check any side effects of the disruption of the *dotC* gene.

4.4.1 Growth rate of the *dotC* mutants

The radial growth rates of the *dotC* mutants and WT were measured as described in Section 2.12. Two *dotC* disrupted mutants (FJT15 and FJT16), three ectopic mutants (FJT79, FJT80 and FJT42), one possible 3' single cross-over mutant (FJT19) and one WT strain (NZE10) were selected to test their growth rate. The results are shown in Table 4.2. From day 5 to 28, the radial growth of each mutant compared to the WT was analyzed by an unpaired T-test (http://www.graphpad.com/quickcalcs/ttest1.cfm).

The WT encountered a lag-phase of growth till day 11, since its colony size was significantly ($p<0.0001$) smaller than any of the other strains (except FJT16 at day 11). The FJT15 grew remarkably faster ($p<0.0001$) than the WT from day 5 to day18, however, from day 18 to 28 there was no difference between FJT15 and WT. The FJT16 *dotC* mutants also showed no difference to the WT during these growth periods after day 5. FJT79 showed faster growth from day 5 to day 18, but eventually it had the similar colony size with the WT. The FJT19, FJT42 and FJT80 all grew slower than the WT by the end of the day 28, although some of them also grew faster than the WT in

the early stage due to its lag-phase. In general, two *dotC* disrupted mutants did not show statistically significant growth difference to the WT over the 28 days.

Table 4.2 Radial growth of *dotC* mutants

Strains	5days	11days	18days	24days	28days
	Mean ± SD (mm)	Mean ± SD (mm)	Mean ± SD (mm)	Mean ± SD (mm)	Mean ± SD (mm)
NZE10 (wild type)	3.68 ± 0.24	7.27 ± 0.76	13.33 ± 0.67	19.25 ± 1.53	22.76 ± 1.58
FJT15 (double *dotC* cross-over)	*4.76 ± 0.26	*9.67 ± 0.57	*16.05 ± 0.87	20.52 ± 0.66	23.32 ± 1.03
FJT16 (double *dotC* cross-over)	*4.47 ± 0.44	7.90 ± 0.79	14.04 ± 1.23	18.68 ± 1.18	21.27 ± 1.45
FJT19 (3' single cross-over)	*4.60 ± 0.30	*8.18 ± 0.72	*14.15 ± 0.76	19.35 ± 1.28	*21.26 ± 1.41
FJT42 (ectopic)	*4.48 ± 0.22	*8.69 ± 0.73	*14.39 ± 0.71	19.25 ± 1.28	*21.31 ± 1.18
FJT79 (ectopic)	*4.92 ± 0.31	*8.42 ± 0.98	*14.55 ± 0.53	19.18 ± 1.42	21.75 ± 1.59
FJT80 (ectopic)	*4.53 ± 0.48	*8.02 ± 0.39	13.02 ± 0.35	*17.79 ± 0.87	*20.61 ± 1.33

All strains had 9 replicates, except FJT79 (8 replicates).

*: indicates the data statistically significant ($p \leq 0.05$) when comparing mutants to wild type within each column.

4.4.2 Dothistromin production of *dotC* mutants

The dothistromin production of the *dotC* mutants is a critical phenotype, which indicates whether the DotC protein is involved in toxin efflux and also implicates whether dothistromin biosynthesis is affected in a *dotC* mutant. By observing the *dotC* mutants and WT colonies on DM plates, as shown in Fig. 4.8, there was much less red pigment around the *dotC* disrupted mutant (FJT15) than the WT and two ectopic mutants (FJT79 and FJT42). Both WT and ectopic mutants had a strong red halo around their colonies. Since the red pigment is indicative of dothistromin, the *dotC* disrupted mutants seemed to be secreting much less toxin than the WT and ectopic mutants.

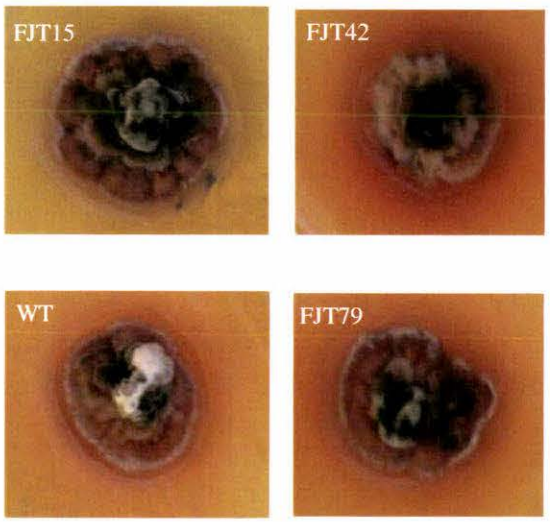

Figure 4.8: The *dotC* mutants' phenotype

FJT15: the *dotC* disrupted mutant.

FJT42 and FJT79: ectopic mutants.

However, visual assessment was not quantitative and did not distinguish between reduced biosynthesis or reduced secretion of dothistromin. Thus, competitive ELISA (Section 2.10) was applied to quantify the production of dothistromin in the *dotC* mutants FJT15, FJT16, ectopic mutant FJT79 and WT strain (NZE10) both intracellular (the dothistromin concentration in mycelia) and extracellular (the toxin concentration from the filtrate in liquid media) of the fungus. To examine the toxin stored in the fungus, the corresponding mycelia of each strain were collected and then freeze-dried and their dry weights determined using a fine balance. The toxin was extracted from the freeze-dried mycelia using acetone, re-suspended in 100 µl DMSO (Section 2.9) and then quantified with ELISA. To test the secreted toxin concentration, the filtrate of each strain was collected as described in Section 2.2.2.3 and the dothistromin concentration was analysed using ELISA directly.

The dothistromin concentrations of filtrates and extracts from each strain are listed in Table 4.3A. Data for the three biological replicates of each strain are shown in this table to indicate the wide variability between replicates. Mean data for the toxin concentration (ng dothistromin /mg dry mycelium weight) are shown in Table 4.3B. From the unpaired T-test (comparing each mutant to WT), the two *dotC* disrupted mutants, FJT15 and FJT16 showed significantly lower toxin concentration both in filtrates (7 fold lower of FJT15 and 19 fold of FJT16) and mycelia (9 fold lower of

FJT15 and 19 fold of FJT16) than WT. However, the ectopic mutant (FJT79) produced significantly more toxin than the WT both in filtrates and mycelia.

Since different methods were used to collect toxin from filtrates and mycelia, the toxin concentrations from these could not be directly compared. It means although the dothistromin concentration of each strain in filtrates is remarkably higher than in mycelia as shown in Table 4.3B, this might be only due to the inefficient extraction method from mycelia. Therefore, the toxin secreted into the filtrate was extracted using the same method as used to extract the toxin from mycelia. This trial experiment was carried out with strains FJT79 and WT. Five ml of filtrate from each sample was freeze-dried overnight and dothistromin extracted by adding acetone. The dothistromin was finally re-suspended into 100 µl DMSO (Section 2.9). In order to account for background caused by the DMSO in ELISA assay, a negative control using DMSO only was set up, which was diluted with MilliQ water to the same dilution as the DMSO used to re-suspend toxin solution during this ELISA assay. The toxin concentrations of the filtrates that were quantified using two different extraction methods are shown in the Table 4.3C. The dothistromin concentration in filtrates measured directly by ELISA had a much higher toxin concentration (~ 150 fold of WT and 340 fold of FJT79) than the identical filtrate after acetone extraction. This experiment indicated that most of dothistromin in filtrate was degraded or lost during the freeze-dry step or acetone extraction procedure. However, when pigments were visualized in filtrate before freeze-drying and in the acetone suspension after freeze-drying, the toxin seemed more likely degraded in the freeze-dry step.

Table 4.3: The dothistromin production of the *dotC* mutants.

A. Replicates data: dothistromin concentration quantified from filtrates and mycelia.

Strain	Dothistoomin from filtrates			Dothistromin from mycelia		
	Dothistromin (ng/ml LDB)	*Dry weight(mg)	Dothistromin (ng/mg DW)	Dothistromin (ng/ml DMSO)	#Dry weight(mg)	Dothistromin (ng/mg DW)
FJT15-1	2973.8	102.2	727.45	7350.5	39.0	18.85
FJT15-2	1714.3	155.0	276.50	4800.1	80.0	6.00
FJT15-3	2219.8	122.1	454.50	4747.1	57.5	8.26
FJT16-1	2326.5	345.7	168.25	3420.6	61.0	5.61
FJT16-2	2164.8	317.2	170.62	3091.6	61.3	5.04
FJT16-3	2864.9	345.4	207.36	2317.5	52.1	4.45
FJT79-1	59614.3	100.9	14770.64	249336.3	87.4	285.28
FJT79-2	50478.9	114.7	11002.38	258853.7	91.5	282.90
FJT79-3	52728.3	110.6	11918.69	163687	93.6	174.88
WT(NZE10)-1	22595.8	173.3	3259.64	57317.1	54.5	105.17
WT(NZE10)-2	26236.9	139.2	4712.09	48304.8	52.8	91.49
WT(NZE10)-3	13046.9	125.6	2596.91	50229.0	58.8	85.42

*: Dry weight (mg, DW) of mycelia per 25 ml LDB broth; #: dry weight of mycelia for dothistromin extraction.

The dothistromin concentration (ng/mg, DW) was calculated as:

Dothistromin (ng/mg, DW) = Dothistromin (ng/ml media) × 25 ml (the volume of original inoculation LDB broth) / the dry weight of mycelia

B. The mean dothistromin production per mg mycelium.

Strain	Toxin from filtrates			Toxin from mycelia		
	Dothistromin production Mean ± SD (ng/mg, DW)	*T*	*p*	Dothistromin production Mean ± SD (ng/mg, DW)	*T*	*p*
FJT15	486.15 ± 227.13	4.7580	0.0089	11.03 ± 6.86	11.7599	0.0003
FJT16	182.97 ± 21.93	5.3474	0.0059	5.03 ± 0.58	15.2118	0.0001
FJT79	12563.90 ± 1965.24	6.9804	0.0022	247.69 ± 62.06	4.1670	0.0141
WT(NZE10)	3522.88 ± 1081.88	-	-	94.03 ± 10.11	-	-

Each *dotC* mutant's toxin concentration was compared to the WT by an unpaired T-test

C. ELISA estimates of dothistromin concentration in the same filtrate using different extraction methods

Strain*	Dothistromin (ng/ml media) Directly measured	Dothistromin(ng/ml media) Measured after acetone extraction
WT(NZE10)-1	22596	145
FJT79-1	59614	172

*: The tested strains were the replicate number one of each strain (refer to Table 4.3A).

4.4.3 Dothistromin resistance of *dotC* mutants

Based on the results shown in Section 4.4.2, the FJT15 and FJT16 *dotC* disrupted mutants were found to produce much less dothistromin than the WT strain. Besides the toxin efflux ability, the *dotC* gene is also postulated to exert a self-protection function for the fungus to resist its own toxin or compete with toxin secreted from other organisms. In this section, the radial growth of the *dotC* mutants (FJT15, FJT16 and FJT79) was measured in dothistromin containing media to observe any inhibition of the mutants. The WT (NZE10) was measured as a control under same conditions as the mutants (Section 2.14).

When the experiment was in process, an unexpected contamination by another fungus happened in some plates. However, this contamination provided a hint that the *dotC* gene may have a role in *D. septosporum* competing with other organisms. Fig. 4.9 was taken after approximately 5 days growth of the *dotC* mutants and WT in a plate containing 14 μM dothistromin. The contaminating fungus appeared to have started near the FJT15 inoculum, and totally overgrew the other disrupted mutant FJT16. However, the WT and ectopic mutant FJT79 retained their own territory and inhibited the growth of the competitor.

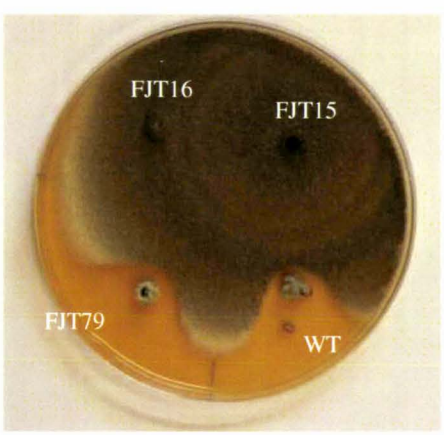

Figure 4.9: Resistance of the *dotC* mutants (FJT15 and 16), ectopic strain (FJT79) and WT (NZE10) to a contaminating fungus.

Due to the contamination, there were four replicates of each strain finally counted in the radial growth analysis in this dothistromin resistance assay (Table 4.4A and B). Table 4.4C shows the mean value of growth rate from day 14 to 27 for each strain. These values were also analyzed by unpaired T-tests between the same strain in different dothistromin concentration plates (indicated by "△") and between each mutant to WT in 14 μM dothistromin (the highest concentration tested) and control plates (no dothistromin), respectively (indicated by "*", Table 4.4C). The *dotC* disrupted mutants FJT15 and FJT16 had significantly slower growth rate in dothistromin-containing plates than the control plates (refer "△" in Table 4.4C). The ectopic mutant and WT did not show any growth differences between them.

In 14 μM dothistromin plates, the *dotC* disrupted mutant FJT16 showed a statistically significantly slower growth rate than the WT from day 14 to day 27 (refer "*" in Table 4.4C). The other *dotC* disrupted mutant FJT15 grew significantly slower than the WT at the day 14 time point (Table 4.4A). However, from days 20 to day 27, although the mean radial growth values of FJT15 were smaller than the WT, this was not quite statistically significant (at day 20, the P value is 0.0604; at day 27, the P value is 0.0903). The ectopic mutant (FJT79) showed a significantly slower growth rate than WT from day 6 to 27 (Table 4.4A), while its growth rate did not show difference between them from day 14 to 27 (Table 4.4C). This implied that the ectopic grew slower than WT during day 6 to 14. In control DM plates, there was no growth difference between any mutants and WT (Table 4.4B).

Table 4.4: The radial growth of *dotC* mutants in dothistromin containing media.

A. Radial growth of strains in 14 µM dothistromin.

Strains	6days	14days	20days	27days
	Mean ± SD (mm)	Mean ± SD (mm)	Mean ± SD (mm)	Mean ± SD (mm)
NZE10 (wild type)	4.59 ± 0.50	12.85 ± 0.95	17.00 ± 0.67	22.25 ± 1.89
FJT15 (double cross-over)	4.50 ± 0.47	*10.25 ± 1.49	14.65 ± 1.93	18.96 ± 2.65
FJT16 (double cross-over)	*4.40 ± 0.30	*9.10 ± 0.96	*12.54 ± 1.12	*16.31 ± 0.46
FJT79 (ectopic)	4.60 ± 0.34	*9.71 ± 0.54	*14.40 ± 0.76	*18.01 ± 0.89

*: indicates the data statistically significant when comparing mutants to wild type within each column. (n=4).

Each *dotC* mutant's radial growth was compared to the WT by an unpaired T-test from day 6 to day 27.

B. Radial growth of strains in control (0 µM dothistromin)

Strains	6days	14days	20days	27days
	Mean ± SD (mm)	Mean ± SD (mm)	Mean ± SD (mm)	Mean ± SD (mm)
NZE10 (wild type)	4.65 ± 0.33	11.58 ± 1.36	16.84 ± 2.85	21.84 ± 1.87
FJT15 (double cross-over)	4.88 ± 0.47	11.00 ± 0.98	16.45 ± 1.66	21.54 ± 1.55
FJT16 (double cross-over)	5.04 ± 0.65	10.82 ± 2.91	14.98 ± 3.80	19.71 ± 3.85
FJT79 (ectopic)	5.07 ± 0.29	10.73 ± 0.87	14.80 ± 1.72	19.18 ± 2.11

Each *dotC* mutant's radial growth value was compared to the WT by an unpaired T-test from day 6 to day 27. No significant differences were seen. (n=4).

C. The growth rate of each strain from day 14 to 27.

Day 14-27	Growth rate	Mean ± SD (mm/day)
Strain	14 µM dothistromin	0 µM dothistromin
FJT15 (double cross-over)	0.67 ± 0.09	0.80 ± 0.04△
FJT16 (double cross-over)	*0.55 ± 0.08	0.75 ± 0.12△
FJT79 (ectopic)	0.64 ± 0.10	0.67 ± 0.11
WT (wild type)	0.72 ± 0.10	0.81 ± 0.08

*: indicates the data statistically significant when comparing mutants to wild type within each column. (n=4).

△: indicates the data statistically significant when comparing the same strain (different dothistromin concentration) in the same row. (n=4).

4.4.4 Sporulation of *dotC* mutants

In order to test for any effects of the *dotC* mutation on sporulation rate, the sporulation of two *dotC* disrupted mutants (FJT15 and FJT16), one ectopic mutant and WT (NZE10) were examined (Section 2.13). This experiment was repeated three times. In experiments one and two, three colony plugs from the same strain were put into each DSM plate, and totally six replicates of each strain in two DSM plates were checked (due to the contamination was observed in some plugs, five replicates of each strain were finally counted for spores) . In experiment three, one WT, one ectopic mutant and one *dotC* mutant were put in the same DSM plate and seven replicate plates were made. In experiment one (Table 4.5), FJT15 produced significantly more spores than the WT, while FJT16 produced significantly less. However, this finding was not repeated in experiment two and three. Combining all the data from the three experiments, there was no difference between the mutants and WT. Overall, the *dotC* mutations had no significant effect on the sporulation, however, this could be due to the high standard deviation between replicates.

Table 4.5: Sporulation of the *dotC* mutants

Strain	Spores $\times 10^4$ per ml (Mean ± SD)			
	Experiment 1	Experiment 2	Experiment 3	Experiment 1-3 (combined)
FJT15	*263.8 ± 99.6	164.4 ± 101.5	64.5 ± 126.7	147.6 ± 136.6
FJT16	*7.20 ± 7.19	159.8 ± 118.8	164.3 ± 115.5	116.8 ± 117.7
FJT79	568.8 ± 645.9	203.6 ± 161.5	53.86 ± 78.95	249.4 ± 403.0
WT	96.2 ± 45.5	119.2 ± 114.1	163.3 ± 164.8	132.4 ± 124.9

*: indicates the data statistically significant when comparing mutants to wild type within each column.
(Experiments one and two, n=5; experiment three, n=7)

4.5 DISCUSSION

4.5.1 Construction of the *dotC* mutants

In this project, the MultiSite Gateway system provided a reliable and efficient cloning method to construct the *dotC* disruption vector. In terms of the construction method, a few aspects are discussed as follows:

1) Length of the homologous region. The 1.1 Kb (5' element) and 1 Kb (3' element) homologous regions used for construction of the *dotC* mutants only gave two mutants obtained out of 26 transformants. Previous research found that the recombination efficiency was related to the length of the homologous region of the circular vector DNA. The longer homologous region used in the disruption vector, the more correctly targeted mutants could be obtained (Bird and Bradshaw, 1997). For instance, Choquer *et al* reported that 16 mutants out of 41 transformants were obtained when the 2.6 Kb and 1.6 Kb homologous regions had been used for *CTB1* gene disruption (Choquer *et al.*, 2005).

2) Position of the homologous region. As mentioned in Chapter one, the *dotC* gene is located in mini cluster one and flanked with two putative dothistromin biosynthetic genes, *dotB* and *dotD* (Fig. 1.3). In this case, none of the *dotC*-associated homologous regions used in the replacement vector overlapped with coding sequences of *dotB* and *dotD*, due to sufficient length of the flanking sequence of the *dotC* ORF (Fig. 4.2A). This was good because the possibility of other genes being affected during the homologous recombination was reduced. In some circumstances, if homologous regions are inevitably overlapped with other genes, they must be precisely amplified and sequence checked to avoid any nucleotide changes of other genes after homologous recombination due to PCR amplification errors.

3) Modifications of the construction method. Differing to the manufacturer's

instructions, the 5' and 3' elements of the *dotC* were ligated into the pGEM®-T Easy vector prior to BP recombination (Section 2.4.3.1). This alteration is due to a previous study (Teddy, 2004), which indicated that recombination between circular DNA was more efficient than with linear DNA. In addition, based on the optimization study by Jin (2005), a PCR purification kit was used instead of adding proteinase K to stop the BP and LR recombination reactions.

4.5.2 Characterization of the *dotC* mutants

4.5.2.1 Dothistromin production

The reduction of dothistromin production was the most predominant phenotype of the two *dotC* disruption mutants (FJT15 and FJT16). Compared to the wild type, the dramatic dothistromin reduction was observed not only in the filtrates but also in the toxin extracted from mycelia. This result provides evidence to suggest that the *dotC* gene product may have a role in dothistromin secretion. In addition, it also indicates that reduction of toxin secretion raised a negative feedback signal to decrease the toxin production in fungus. However, unlike the *pksA* (a polyketide synthase gene) disruption mutant in *D. septosporum*, which totally blocked the synthesis of dothistromin (Bradshaw *et al.*, 2006), the *dotC* mutants still have detectable toxin secreted out of, and accumulated in, the fungus. This confirmed that the *dotC* gene product, a putative MFS transporter, was not essential for dothistromin synthesis.

In this experiment, the ectopic mutant (FJT79) showed a significant increase in toxin secretion and accumulation in fungus. The reason is unclear since in ectopic mutants, the exact effects of the randomly integrated vector are hard to predict.

Although the toxin concentration cannot be directly compared between the filtrates and mycelia as mentioned in Section 4.4.2, their relationship still can be estimated by a ratio of dothistromin concentration in filtrate to mycelium (Table 4.6). This value fluctuated

from 36 to 50 in these four stains, which implied that the dothistromin accumulated in the fungus maintained a relatively constant range over the toxin secreted out the fungus. Furthermore, comparing the toxin concentration of each strain to WT both in filtrate and mycelium (Table 4.6), the two *dotC* mutants had a similar level of toxin reduction in both filtrate and mycelium (7.2 and 8.5 of FJT15; 19.3 and 18.7 of FJT16). While, the ectopic mutant (FJT79) had a similar level of toxin increase in filtrate and mycelium (0.28 and 0.38). Overall, Table 4.6 suggests that the *dotC* mutants still keep a biological homeostasis in dothistomin amount between intracellular and extracellular environment. Possibly the accumulation of the toxin in cells subsequently raised a negative feedback signal to reduce toxin production. Finally the toxin amount both in mycelium and in filtrate dropped to a corresponding level. Meantime, the amount of toxin accumulated in and secreted out maintained a relatively constant ratio. In contrast to the *dotC*, in the AF gene cluster, a MFS transporter encoding gene (*aflT*) deleted mutant produced comparable aflatoxin to the *aflT*-non-deleted strain (Chang *et al.*, 2004).

Table 4.6: Ratios of dothistromin levels WT: mutant.

Strain	Doth of WT : each mutant (in filtrate)	Doth of WT : each mutant (in mycelium)	Doth filtrate : mycelium of each strain
FJT15	7.2	8.5	44
FJT16	19.3	18.7	36
FJT79	0.28	0.38	50
WT	1	1	37

4.5.2.2 Dothistromin resistance

The radial growth is a straightforward phenotype, which indicates a common response of fungal species to their environmental conditions. Based on the results from Section 4.4.1, two *dotC* disrupted mutants did not show significant growth differences to the WT. Similar results were also found in the *pks*A mutants (Jin, 2005). These findings suggested no matter what strains (i.e: WT, the *dotC* mutants and the *pks*A mutants), the

dothistromin production did not affect the growth of the fungus, at least in the laboratory under the conditions used. This result further confirms that dothistromin truly belongs to the secondary metabolites, which are "non-essential for growth and reproduction of the organisms that produce them" (Martin *et al.*, 2005).

In addition to functioning as an efflux pump, some MFS proteins also possess a self-protection function to resist its own toxin. An example exists in the fungal genus *Cercospora*. The *cfp* (cercosporin facilitator protein) encodes a putative MFS transporter; targeted disruption of the *cfp* resulted in a drastic reduction in cercosporin production and increased sensitivity to exogenous cercosporin (Callahan *et al.*, 1999). To examine the sensitivity of the *dotC* mutants to exogenous dothistromin, the radial growth was used again as an indicator to test any inhibition of fungus growth under dothistromin stress. The results from Section 4.4.3 showed that the *dotC* mutant (FJT16) had a significantly slower growth rate than WT in 14 μM dothistromin containing over day 14 to 27, while another *dotC* mutant (FJT15) only had a significantly slower growth rate from on day 14. Moreover, the two *dotC* mutants grown in exogenous dothistromin containing plates both showed a significantly slower growth rate than the mutants grown in control plates (no dothistromin) from day 14 to 27. These results implied that the *dotC* mutants showed more sensitivity to dothistromin than WT and also showed sensitivity to dothistromin when their growth rate was compared to the control plates (Table 4.4C). Although the FJT79 (ectopic mutant) grew slower than WT in dothistromin containing plates over day 14 to 27, it did not show significantly slower growth in dothistromin plates compared to control plates.

4.5.2.3 Sporulation

Secondary metabolites sometimes participate in sporulation processes in microorganisms, including fungi. Their association with sporulation can be as an active factor or simply by being secreted by growing colonies at the approximate time of sporulation (Calvo *et al.*, 2002). The *pksA* mutants showed a significant (60%-70%)

reduction of sporulation compared to WT (Jin, 2005). This result indicated that there is indeed a relationship between dothistromin production and sporulation rate in *D. septosporum*. However, although the *dotC* mutants had a dramatic reduction in dothistromin production, a consistent reduction in sporulation rate could not be observed in this project. However there was a high variability of spore counts in biological replicates of the same sample, hence none of the mutants had statistically significant differences compared to WT (Table 4.5).

4.5.3 The role of the *dotC* in *D. septosporum*

The ABC and MFS transporters are the two major classes of transporters found in bacteria to higher eukaryotes. In filamentous fungi, the most common function of these membrane proteins is to transport a wide range of natural and synthetic toxic products of either endogenous or exogenous origin in survival mechanisms. In plant pathogens, these transporters can play a role as a critical virulence factor by providing protection against plant defence compounds or mediating the secretion of host-specific toxins (Del Sorbo *et al.*, 2000; Stergiopoulos *et al.*, 2002).

The *dotC* gene is located in the dothistromin synthetic mini cluster one between the putative oxidase gene *dotB* and the putative thioesterase gene *dotD* of *D. septosporum*. It is considered to encode a MFS transporter, which may assist in secretion of dothistromin and provide protection against endogenous or exogenous toxins. Numerous studies of the functions of MFS transporters have been reported in different species, and their functions were not always the same. Table 4.7 summarizes a few MFS transporters' functions.

Table 4.7: Examples of the MFS transporters' function.

Name	Species	Function	References
mgMfs1	*Mycosphaerella graminicola*	Strong protectant against natural toxic compounds and fungicides	(Roohparvar *et al.*, 2007)
bcmfs1	*Botrytis cinerea*	Provides tolerance towards the camptothecin, cercosporin and fungicides	(Hayashi *et al.*, 2002)
smt	*Gibberella fujikuroi*	Not involved in gibberellin secretion	(Voss *et al.*, 2001)
ctb4	*Cercospora nicotianae*	Responsible for cercosporin toxin accumulation and fungal virulence	(Choquer *et al.*, 2007)
aflT	*Aspergillus parasiticus*	Does not have a significant role in aflatoxin secretion	(Chang *et al.*, 2004)
cfp	*Cercospora kikuchii*	Required for cercosporin production, resistance and virulence	(Callahan *et al.*, 1999)
toxA	*Cochliobolus carbonum*	No *toxA*-disrupted mutants obtained.	(Pitkin *et al.*, 1996)

The biological functions of DotC were investigated by targeted gene disruption in this chapter. The copy number of *dotC* was determined by Southern analysis and the result indicated that only a single copy of *dotC* is present in the *D. septosporum* genome. The reduction of dothistromin production of *dotC* mutants suggested that the *dotC* may have a role in dothistromin production or secretion. The dothistromin resistance assay also suggested that the *dotC* might be involved in secretion of exogenously supplied dothistromin toxin. If the DotC did play a role in toxin secretion, however, this role might not be unique. The detectable dothistromin secreted by *dotC* mutants indicated that some other transporter(s) also may participate in the secretion of dothistromin in cooperation with the DotC. S. Zhang identified another putative MFS-like transporter (DS28, Table 1.1) in the dothistromin synthetic mini cluster three , but the role of this transporter is not yet known (Zhang *et al.*, 2007).

CHAPTER FIVE: NOVEL DOTHISTROMIN GENES

5.1 INTRODUCTION

Dothistromin shares biosynthetic pathway steps with aflatoxin (AF) /sterigmatocystin (ST) and *D. septosporum* contains homologous toxin biosynthetic genes to the AF/ST biosynthetic genes. Previous researchers have found nine genes that are homologous to their corresponding genes in the AF/ST gene clusters and possibly involved in dothistromin biosynthesis. However, in contrast to all 25 AF biosynthetic genes tightly clustered in one region of the genome, the dothistromin gene clusters are separated into three mini-clusters (Fig. 1.3). The aim of the work described in this chapter was to further identify novel dothistromin biosynthetic genes. This was achieved *via* PCR using degenerate primers designed from the amino acid sequences of AF/ST biosynthetic proteins. Inverse PCR was applied to identify the flanking sequence of the known DNA sequence from degenerate PCR products. These sequences were subsequently used to screen a partial *D. septosporum* genomic library; then positive clones were sequenced by primer walking.

5.2 IDENTIFICATION OF NOVEL DOTHISTROMIN SYNTHETIC GENES

5.2.1 Design of degenerate PCR primers

The degenerate PCR primers were designed according to the multiple amino acid alignments of the AF/ST synthetic gene products, NorA (AflE)/StcV and VerB (AflL)/StcL. The names *norA* and *verB* were the original ones used to describe the AF/ST synthetic genes. Now, these genes all have their corresponding "*afl*" and "*stc*" names in AF and ST producing species *Aspergillus parasiticus* and *A. nidulans*,

respectively (see Chapter one). In this chapter, only the original names are used to avoid confusion. The alignment of *norA* encoded proteins was obtained from *A. nidulans* (GenBank accession number: XP_681074), *A. nomius* (AAS90055), *A. oryzae* (BAC15569) and *A. parasiticus* (Q00258). The alignment of *verB* encoded proteins was obtained from *A. nidulans* (XP_681082), *A. nomius* (AAS90059), *A. oryzae* (BAE71326) and *A. parasiticus* (AAS66013). Fig. 5.1 shows the alignment results.

Before designing degenerate PCR primers, the locations of the intron regions in each protein's coding sequence were firstly identified to avoid primers spanning the intron region. As shown in Fig. 5.1, the highly conserved amino acid sequences are highlighted with the darkest color and position of each primer is marked under the corresponding amino acid sequences. The intron positions of each stain were marked with "^" using different colors. Table 5.1 shows the details of each degenerate primer used in this project. For each gene, two sets of primers were designed to increase the chance of success.

Table 5.1: Degenerate primers for amplifying the *norA* and *verB* genes.

Primer name	Amino acid sequence	Nucleotide sequence (5'-3')	Degeneracy	Tm°C
DgNorA-fwd1	GNFIDV/TAN	GGCAACTTCATHGAYRYNGCNAA	384	68°C
DgNorA-fwd2	DV[illegible]ANFYQG	GATGTNGCNAAYTTYTAYCARGG	256	66°C
DgNorA-rev3	YVHMWDFTT	GTAGTRAARTCCCACATRTGNACRTA	64	74°C
DgNorA-rev4	PYVFPVIG	CCGATCACIGGRAA IACRTAIGG	256	68°C
DgVerB-fwd1	HQKYGDTV	CACCARAARTAYGGNGAYACNGT	256	68°C
DgVerB-fwd2	YFNMAIFD	TACTTYAAYATGGCNATHTTYGA	96	60°C
DgVerB-rev3	PWVDAIHK	TTATGAATNGCRTCNACCCANGG	128	68°C
DgVerB-rev4	MYPAVPGQ	TGGCCTGGNACNGCNGGRTACAT	128	70°C

H: A+T+C; Y: C+T; R: A+G; N: A+G+T+C

Figure 5.1: The multiple amino acid alignments of the NorA and VerB proteins.

NorA ▪▪▪▪ : The position of the primers; → : the direction of primer extension.

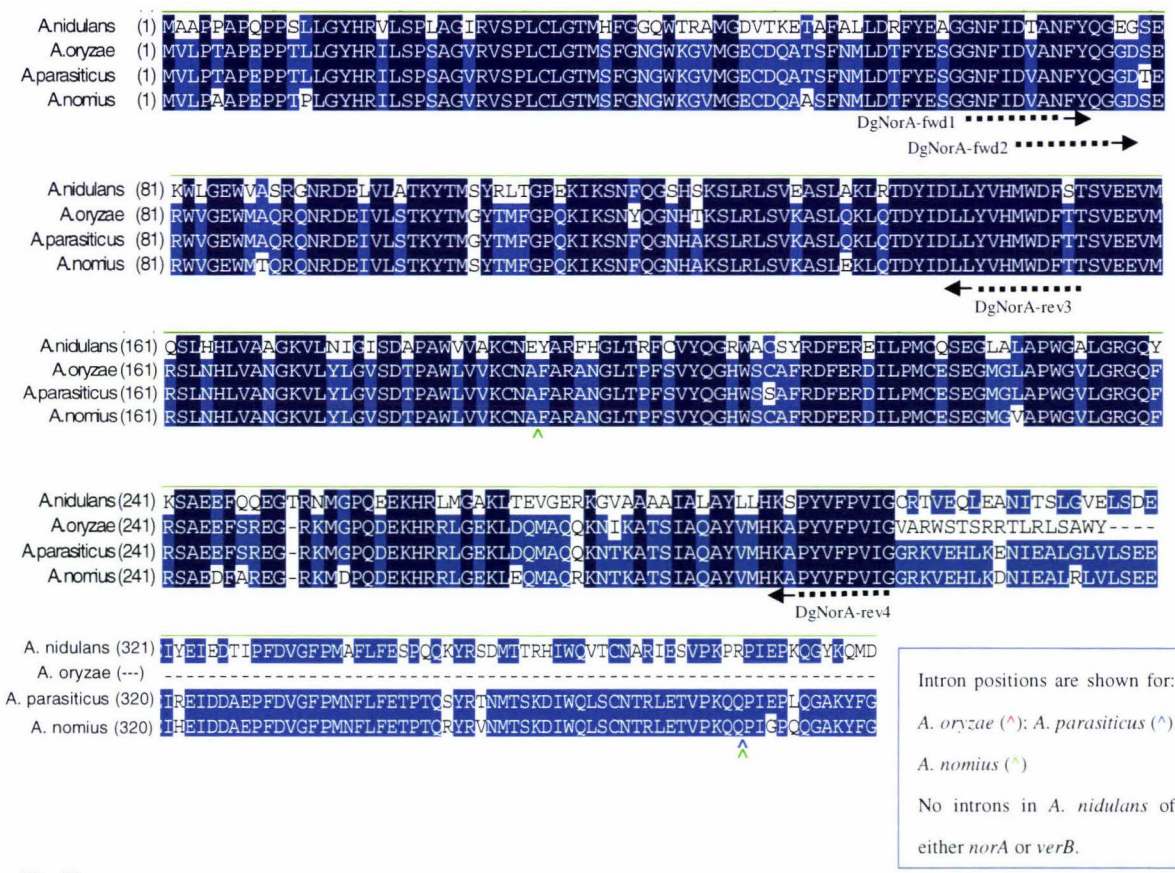

Intron positions are shown for: *A. oryzae* (^); *A. parasiticus* (^) *A. nomius* (^)

No introns in *A. nidulans* of either *norA* or *verB*.

VerB

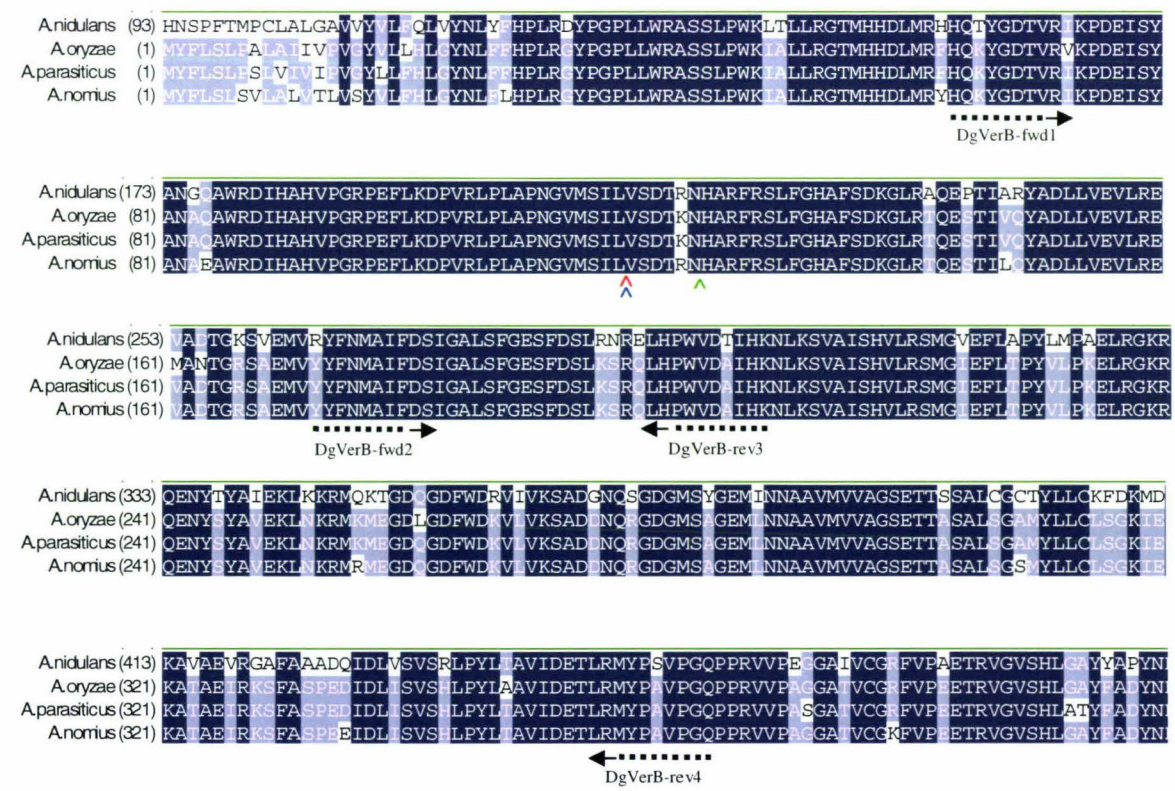

5.2.2 Touchdown PCR using degenerate primers

The touch-down PCR was carried out as described in Section 2.6.4.1 using NZE10 genomic DNA as the template. The two forward primers and two reverse primers in the *norA* or *verB* gene could give four combinations with different forward-reverse primer sets; but only one of the primer combinations gave products of the expected size for each of the genes. As shown in Fig. 5.2A, two bands (~0.6 Kb and 0.7 Kb) were amplified with primer set DgNorA-fwd1 and DgNorA-rev4 (expected size 0.7 Kb) with a final 2.5 μM magnesium concentration. Primer set DgVerB-fwd2 and DgVerB-rev3 amplified just an expected 100 bp product with 3 μM $MgCl_2$ (Fig. 5.2B). All three fragments (100 bp, 0.6 Kb, 0.7 Kb) were purified from the gel (Section 2.3.4) and then ligated into the pGEM®-T Easy vector (Section 2.4.2). All other primer combinations did not show any expected PCR products and the negative result was clean (not shown in Fig. 5.2).

Figure 5.2: Touch-down PCR results using degenerate primers.

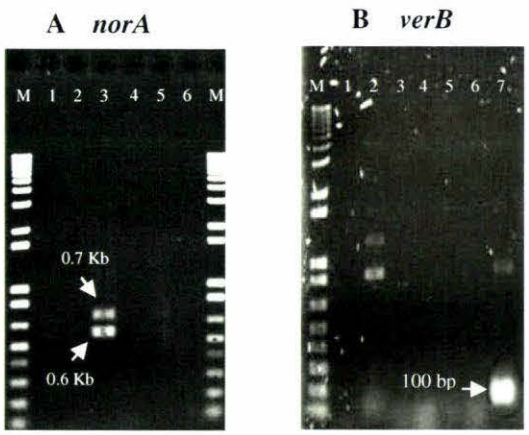

A. Using degenerate primers to amplify the putative *NorA* gene. Two PCR products (0.7 Kb and 0.6 Kb) in lane 3 were amplified with primers DgNorA-fwd1/DgNorA-rev4.

B. Using degenerate primers to amplify the putative *VerB* gene. The 100 bp product was amplified with primers DgVerB-fwd2/ DgVerB-rev3 in lane 7.

In Fig. A and B, all other lanes were PCR using different primer combinations. However, none of them had the expected products.

Lane M: 1 Kb plus ladder; the negative was clear (not shown).

DNA sequencing was carried out with primers M13 fwd and M13 rev (Section 2.7) and the sequences of those three inserts were subsequently submitted into BLASTX to compare with the database (http://www.ncbi.nlm.nih.gov/BLAST/). BLASTX results illustrated that the partial sequences of the *norA* (or *norB*) and *verB* in *D. septosporum*

had been successfully amplified by PCR using the degenerate primers. The 700 bp insert (ligated into pGEMT-easy vector as plasmid pR266) produced significant alignments with both the *norB* encoded protein in *A. flavus* (AAS89996.1; Score: 296; E value: 6e-79) and the *norA* encoded protein in *A. flavus* (AAS90040.1; Score: 223; E value: 9e-57) as well. The 100 bp insert (ligated into pGEMT-easy vector as plasmid pR267) showed alignment with the *verB* encoded protein in *A. nomius* (AAS90102; Score: 57.8; E value: 2e-07). However, the 600 bp insert matched a TIM-barrel enzyme family protein from *A. clavatus*, (XP_001269251; Score: 173; E value: 4e-42) which indicated it was only a non-specific PCR product. The 700 bp fragment aligned with both the NorA and NorB proteins, since the *norA* and *norB* both encode a dehydrogenase and have 47.1% identity in their amino acid sequences. Therefore, the term "*norA/B*" was used in the following stages of this research to indicate this novel gene in *D. septosporum*, although it was more similar to the *norB*.

5.2.3 Inverse PCR to determine the whole sequences of the *norA/B* and *verB*

Once the partial sequences of the *norA/B* and *verB* were obtained, the flanking sequences of these known DNA fragments could be achieved by Inverse PCR (Section 2.6.4.2).

The inverse PCR process is illustrated in Fig. 5.3B schematically (using enzyme *EcoR*I as an example). *D. septosporum* NZE8 genomic DNA was digested individually with four restriction enzymes: *BamH*I, *EcoR*I, *Sal*I and *Sca*I. These enzymes were chosen because there was no recognition site of these enzymes in the two identified *norA/B* and *verB* sequences. This was critical since the existence of a recognition site would split the internal fragment after the corresponding enzyme digestion and result in failure of PCR due to the separation of the primer set. After purification, the digested DNA fragments were ligated using T4 DNA ligase and used as templates (2.5 ng DNA per μl) for PCR. Inverse PCR was carried out with primer set Inv-NorAfwd1 and Inv-NorArev1 (the approximate position and direction of the primers shown in Fig.

5.3A, left panel) to determine the rest of the *norA/B* sequence and the primers Inv-VerBfwd1/Inv-VerBrev1 (Fig. 5.3A, right panel) to characterize the flanking sequence of the *verB*, using standard PCR conditions (Section 2.6.2).

Fig. 5.3C and D show the Inverse PCR results for the *norA/B* and *verB* respectively. The negative control PCR was set up with no template (not shown in this figure and free of amplified products). For the n*orA/B*, (Fig. 5.3C), two bands (0.85 Kb and 0.75 Kb) in the *EcoR*I lane and one band (0.7 Kb) in *Sal*I were recovered from the gel (Section 2.3.4). For the *verB* (Fig. 5.3D), one band (1.5 Kb) in the *Sal*I lane and one band (2.5 Kb) in *Sca*I were quite clear and thus purified from the gel. Some bands (Fig. 5.3D, in red circle) with the same size were observed in all enzyme fractions, they probably were non-specific PCR products. The five DNA fragments were then ligated into the pGEM®-T Easy vector (Section 2.4.2), cloned in *E.coli* cells and submitted for DNA sequencing of the isolated plasmid DNA with universal primers from one end of the insert (Section 2.3.2 and Section 2.7). However, the 0.7 Kb fragment of *norA* did not successfully ligate into the vector. Thus sequences of the remaining four fragments were compared with BLASTX and results indicated that the 0.85 Kb and 0.75 Kb fragments had a significant alignment with the NorA/B protein of *Aspergillus* species. Table 5.2 summarizes the BLASTX results of these five fragments.

Due to the time limitation in this project, the optimization of Inverse PCR for characterization of the *verB* gene did not carry on further. For the same reason, in the next section, screening the *D. septosporum* genomic library using the DIG-labeled probe of the *verB* also did not proceed.

Figure 5.3: Inverse PCR results.

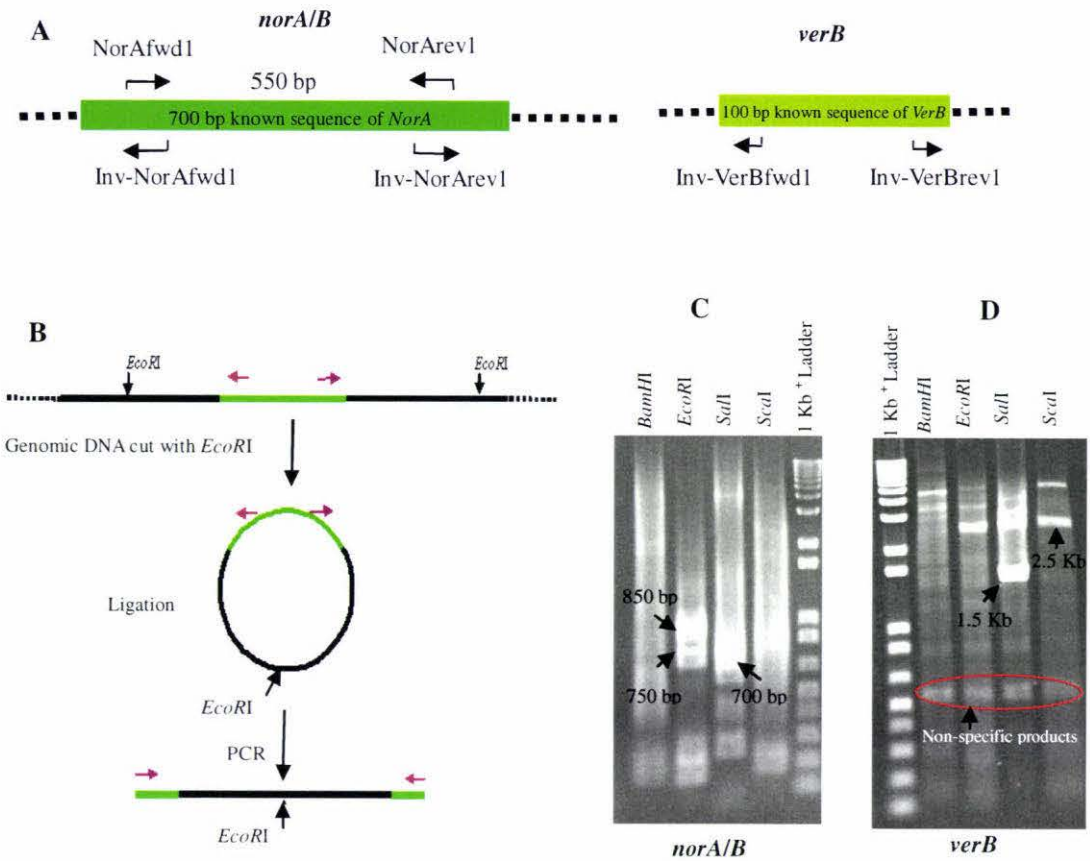

A. The primers' positions are indicated as arrows.

B. The Schematic process of the Inverse PCR, using *EcoR*I as an example.

C. Inverse PCR products of the *norA/B*. Three bands (0.85 Kb and 0.75 Kb from *EcoR*I; 0.7 Kb from *Sal*I) were purified from gel for DNA sequencing.

D. Inverse PCR products of the *verB*. Two bands (1.5 Kb from *Sal*I and 2.5 Kb from *Sca*I) were purified from gel for DNA sequencing.

Table 5.2: BLASTX results of inverse PCR products.

Gene	Digestion Enzyme	Fragment Size (Kb)	Aligned protein (Best match)	Score	E value	Genbank accession number
norA/B	*EcoR*I	0.85 Kb	NorB (*A. nomius*)	128	4e-28	AAS90044.1
			NorA(*A. nomius*)	89.4	2e-16	AAS90055.1
norA/B	*EcoR*I	0.75 Kb	NorB (*A. flavus*)	111	4e-23	AAS89996.1
			NorA(*A. nomius*)	89.4	2e-16	AAS90055.1
verB	*Sal*I	2.5 Kb	hypothetical protein (*A. nidulans*)	195	3e-48	XP_661236.1
verB	*Sca*I	1.5 Kb	hypothetical protein (*A. nidulans*)	41.2	4e-06	XP_662946.1

5.2.4 Screening the *D. septosporum* genomic library with a *norA/B* probe

In this section, a DIG-labeled probe, which hybridized to the *norA/B* gene, was used to screen an existing size fractionized sub-genomic library of *D. septosporum* (constructed by S. Zhang in this laboratory) to discover some positive clones, which could contain potential dothistromin biosynthetic genes clustered with the *norA/B*. In this project, the library screening was carried out in parallel with the inverse PCR to increase the possibility to obtain the *norA/B* gene, and because the inverse PCR described in the previous section did not give the full gene sequence.

The partial genomic library was constructed by cleaving *D. septosporum* genomic DNA with *BamH*I and *Xba*I, recovering 10 to 20 Kb DNA fractions from the gel and then cloning them into the pBluescript KS (+) vector (construction details see Zhang *et al.*, 2007). The probe was a 550 bp DNA fragment derived from a PCR product amplified with primers NorAfwd1/NorArev1 (Fig. 5.3A) and labeled using the DIG-random primer labeling kit (Section 2.8.1).

The sub-genomic library contained 10 differently sized DNA fractions (7 from *BamH*I digestion and 3 from *Xba*I), which were screened by PCR with primers NorAfwd1 and NorArev1 to determine if they contained fragments with the *norA/B* gene. The templates were prepared by pipetting 10 µl *E. coli* cells from each fraction to a microcentrifuge tube and boiling to release DNA as described in Section 2.6.5. As shown in Fig. 5.4A, positive PCR results were found for six of the ten fractions.

The *E. coli* cells of three fractions (two *BamH*I fractions B1 and B2; one *Xba*I fraction X3) out of six with positive PCR results were plated. The colony lifts (four replicates of each fraction) were prepared as described in Section 2.8.3 and the hybridization step was mentioned in Section 2.8.5. After immunological detection (Section 2.8.6), the positive colony regions could be determined. However, it still was hard to locate the single colony position since the positive dots on the film were usually bigger than one

colony, particularly since some of the library plates had about 800-1000 colonies. Thus, all the colonies in the positive region were transferred into a microcentrifuge tube and incubated in 1 ml LB broth (Amp^R) at 37°C overnight. The *E. coli* cells were diluted and spread on LB agar plates to make approximately 20-50 colonies in one plate, and then another set of colony lifts was prepared as described in Section 2.8.3. The hybridization and detection steps were repeated as above. This time, a single positive colony was easy to pick up according to the location of the positive dots on the film.

Finally, all positive colonies were confirmed by PCR individually using primers NorAfwd1/NorArev1. As shown in Fig. 5.4B, one clone containing plasmid pR268 from *Xba*I fraction (X3) was eventually identified.

Figure 5.4: PCR results of screening the *D. septosporum* genomic library.

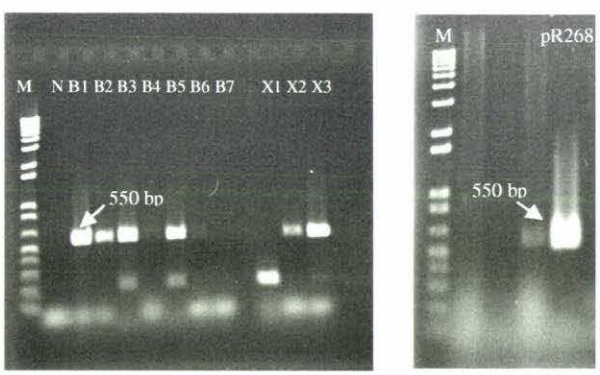

B: *BamH*I; X: *Xba*I ; Lane M: 1 Kb plus ladder; Lane N: negative control.

A. Preliminary PCR screen of the *D. septosporum* genomic library. PCR was carried out with primers NorAfwd1/NorArev1. A 550 bp band indicated which fractions had the *norA/B* fragment. Six fractions (B1, B2, B3, B5, X2, X3) had the positive results.
B1-B7 were the seven differently sized genomic library with *BamH*I digestion. X1-X3 were the three differently sized genomic library with *Xba*I digestion

B. Verifying the probe hybridized colonies with PCR. The same PCR reactions were carried out as above. Only one colony (pR268) gave the 550 bp *norA/B* PCR product out of 15 colonies. Negative control was clear (not shown in this figure).

5.2.5 Sequencing the isolated clone pR268.

The pR268 plasmid that hybridized to *norA/B* had an approximate 13 Kb insert, thus primer walking sequencing was carried out to determine the whole DNA sequence of this insert. The *norA/B* region was sequenced on both strands, the other regions were sequenced only on one strand. All primers used for sequencing are listed in Table 2.2.

The sequencing result and GC content are shown in Fig. 5.5. There was only one putative dothistromin biosynthetic gene (*norA/B*) found in this ~13 Kb fragment. One ATP dependent RNA helicase and two hypothetical proteins were also identified in the pR268 (Table 5.3). High GC content was observed in the putative ATP dependant RNA helicase ORF. The nucleotide and amino acid sequence of the putative NorA/B protein, ~ 1.5 Kb upstream region and ~ 0.5 Kb downstream region are shown in Fig. 5.6. Moreover, Fig. 5.7 shows the alignment results of the putative NorA/B of *D. septosporum* with other NorA/B proteins of *Aspergillus* species. The initiation codon of the putative NorA/B was predicated based on the alignment results and no intron region was identified. RACE (Rapid amplification of cDNA ends) can be used to determine the 5' and 3' untranslated regions of the gene.

Figure 5.5: The sequencing result of pR268.

A. Schematic positions of each identified protein at pR268.

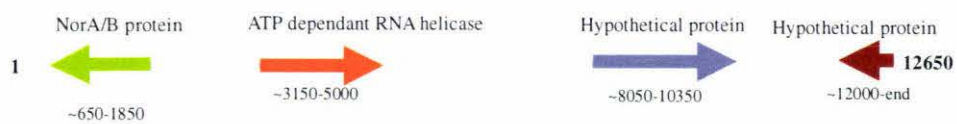

B. The GC content of the pR268.

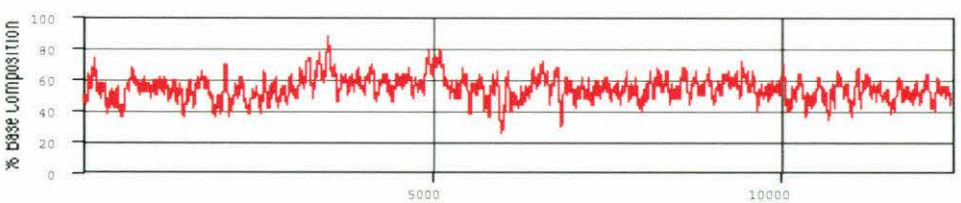

A. Arrows represent the ORF region and translation direction of each putative protein. The numbers indicate the approximate position of the proteins.

B. The GC content was calculated by R. Bradshaw using the program MacVector. The "%GC" is indicated on the Y axis. The calculation window was every 50 nucleotides.

Table 5.3 BLASTX results of pR268.

Gene position	Aligned protein*	Score	E value	Genbank accession number
~650-1,850	NorB (*A. flavus*)	490	7e-137	AAS89996.1
	NorA (*A. flavus*)	369	2e-100	AAS90040.1
~3,150-5,000	ATP dependant RNA helicase (*A. terreus*)	813	0	XP_001214616.1
~8,050-10,350	hypothetical protein (*A. terreus*)	399	4e-109	XP_001214619.1
~12,000-end	hypothetical protein (*A. niger*)	50.4	1e-04	XP_001395156.1

*: Both NorA and NorB are shown for comparison. Other matches represent top hits.

Figure 5.6: Nucleotide and amino acid sequences of the putative *norA/B*.

```
   1 GCTCTTTACTTACTTGGCTTGACCTGGAGTCGGGTAGCCGTTGGCGCCGTCAAGGCCGTTGGGCGCTGCG  70
  71 CCAGGTACTGGGCCTGGTGCTGGGCCTGGTGCTGGACCACGAGTAGACCCTCTCATGTGTGGTGGAATGT 140
 141 AGGCGGAGCGACCAGCGCCAAAGCCATTTTGCTGTGGGCCTGCGCCGTTCTGTGGAGCGTGCTGCGAATC 210
 211 CTGGAGGGACAGACCGTTCATGTTCAGTTGATCAGCCATATTGGTCTCCTGCCTGTACGGGTCTTCTGGT 280
 281 GGTGTGTTGAGTGTGAATAGAGGTGGTGGGTGAGTGAGTGAACGTCGTTCGGTGAGCGCGCGCGTGTATC 350
 351 GCTGCTAGTAATGTCGATGCCTCTGCTGCAAGAAACAACCTGCAAAAAGAGACGAAAGGAAGAAGCGACG 420
 421 AGTGCGTTCAGTGTCGAACGGAGCGTTGTAAAGACACACGATGGTGGTGGTGATGGTTTTGGAGGAGGAT 490
 491 GTGTTGTACGAAGGCGGACTTCACAAAGTTGTGAGAAAATCTTGGGAAGGGACTGTTCAGCACGCGGCCC 560
 561 GCTCCCCGGAACCTTAATATATGGCGAATCAGAAGCCTTGTCGTGCTTGCCTGCCACCTCAGCACTTCTT 630
 631 CGTGACTGTTTTCCATTCTCTCCTCCTACCAAACATTATCGCTACACTTTGCAGAGCACAGGTCCTGGCA 700
 701 GTCGGGCGACTTACATACGCGGCTGGTCTCGCACACGCATTTTTAACAGAAGCGAACAAAACATGGTCAA 770
 771 CTTCAGCTATTCGCTGCAAGTTTCCGATAACGCCACTGACAGAGAACGTTGAACGCTTTCGCGCTGCTGA 840
 841 CGTATTCCGATAACTGCTTCAACATCAGTCTGCTACGCTCGCATCGAGAAGCCGTGATAGCAAGCATGGA 910

                                                  Putative AflR binding site
 911 GATAATGAAACAGTATATGGGACAGGATATCGTTGCCTGAATGCTTTCGATGTACGACAAATGACAATCT 980

Putative AflR binding site
 981 GATCGGTATCACGACCATCTGACGCCTTGAGATCAGTCCAGCGTTATCTCAGAGAGCTCAGCTGCGGGTC 1050
1051 CTTGGTCCTGTCTCGGACGATGTCGATGCATCGAAGGGACTTCTTCAGGTGTGTCTGATACGACACGAAG 1120
1121 CGTCGTCAAGTCGGATGGCGAGACCAAATCTGCATTCAGCGTCGAGGAATTATTCTGTTTGGAGCGATCT 1190
1191 TCGCAGAGCAACTACTATCTTTGTGCTACGAAGTCGTAATGTTACTGTAAACCGAATGAGAGATTCCGCG 1260
1261 CGCGGCCGCGTCTAAGCGCGTTGCCGACCGAATGGCGATCACTGTACAAGGCAGACCCACATGATGTAAC 1330
1331 AATATGTTACAAGAGTCCAGACATCAAACGCTATGTCCAGCTAACTCCGTCGGTGTTTAGCATCGATTCT 1400
1401 CCAATTATAGGCTCGATAGATTGTCTTGCATTCCAACCCTTCTTGATTTCATCAGCCTTGCTCTACACTC 1470

                                  Kozak consensus sequence; initiation of the norA/B ORF
1471 TACTGACGGTCCTTCCTCCATCAACACTTTCAGCACAatggcgtctctccgccgaggcttcggctctgat 1540
   1                                  M  A  S  L  R  R  G  F  G  S  D    11
```

1541 cagacgacagcttcagacaccaagatgcactaccggcaactcgctccaacggcatcagtccgcgtctccc 1610
12 Q T T A S D T K M H Y R Q L A P T A S V R V S P 35
1611 ctctctgcttgggagccatgaacttcggtgaagctcacaaagctcgctacggcgagtgcagcaaggagac 1680
36 L C L G A M N F G E A H K A R Y G E C S K E T 58
1681 cgcgttctcgatcatggactactttattcccaaggtggcaacttcatcgacacagcaaatggctatcaa 1750
59 A F S I M D Y F Y S Q G G N F I D T A N G Y Q 81
1751 gctggagagtccgagcagtgggtcggcgaatggatgaaatctcgcgacaaccgagatgagattgtgcttg 1820
82 A G E S E Q W V G E W M K S R D N R D E I V L A 105
1821 cgacgaaatattcgaccggctacatgaaccatgaaaaggataagatccaaatcaactatggtggcaattc 1890
106 T K Y S T G Y M N H E K D K I Q I N Y G G N S 128
1891 ggcaaagagcatgaaggtctctgtcgcggcgtcgctcaagaaactccaaacgaactacatcgacattctc 1960
129 A K S M K V S V A A S L K K L Q T N Y I D I L 151
1961 tacatccactggtgggactactcaacctcgatcccggagctgatgcacagcctgaacgatctggtcgtct 2030
152 Y I H W W D Y S T S I P E L M H S L N D L V V S 175
2031 ctggtcaagtgctatatcttggagtctctgacactccagcgtgggttgtatcgaaggcaaatcaatacgc 2100
176 G Q V L Y L G V S D T P A W V V S K A N Q Y A 198
2101 ccgcgaccacggtctgcgccaattcgtcatctaccaaggcatgtggaatgcagccatgcgggatttcgag 2170
199 R D H G L R Q F V I Y Q G M W N A A M R D F E 221
2171 cgcgatatcattcccatgtgtcgcgacgagggcatgggtttggctccatatggcacactcggacaaggtt 2240
222 R D I I P M C R D E G M G L A P Y G T L G Q G S 245
2241 ccttccagactgaagaaggccgaaagcagcgcgagaaggataatccggggcgcaagtttggtgcgaagtc 2310
246 F Q T E E G R K Q R E K D N P G R K F G A K S 268
2311 attgccatacgtcgaagtctcgaaagtgctggagaagctggcgaacgccaaggggaaagccattacagat 2380
269 L P Y V E V S K V L E K L A N A K G K A I T D 291
2381 gtcgcgttggcatacgtcctgcagaagacgccgtacgtcttcccgatcgtcggtggtcgtaagctggaac 2450
292 V A L A Y V L Q K T P Y V F P I V G G R K L E H 315
2451 acatccaaggcaatgtagcagcactccaggtggctttgtcagaggcggaagtggaggaaattgaggctgc 2520
316 I Q G N V A A L Q V A L S E A E V E E I E A A 338
2521 gtatcccttcgatgccgggtttccccacacgttcctcagtgggacgctattcgacggtgcaaagccgacg 2590
339 Y P F D A G F P H T F L S G T L F D G A K P T 361
2591 gcagcgcaagggccaggggatgtgttcttgacgaagtggcaaggcgatattgattgggtggaggcaccga 2660
362 A A Q G P G D V F L T K W Q G D I D W V E A P K 385
2661 aggcgatcagaccgagtggtcagtgaAAAGACATGCTCTGAAGATTACGACAGTATTTCGGAGAGCATTC 2730
386 A I R P S G Q * 392
2731 GATCAGGAATACGATAAATGCTCAATTCAGTATGTATGTGTAGCGCCGCTTTTAGTAAGCCTTGCGGAAC 2800
2801 GGCCGTAGAAGCAAGCTTGATGCTGAAGGATCAACTTCAAGCTCTGTATCTCTTGACCCAATTTGGCACC 2870
2871 ACCCAGCACCTCATCCTACGGAAGTTCTTTTTCCATATTGCCACTCCGCCACTACCTCTCAATCTTTGTA 2940
2941 CTCTGATAACTCAAGCCAACGATATCTCACAATGTCCCTCCCTCCCGTCCTCGAGGCAATGCTCTAGTCA 3010
3011 ATCGAGGTAAGCATCGTCCCCCTCTACCAAAGCTCACATTGACCCTCCACAACCAGTGCCTCTTCTCCCT 3080
3081 TATCCTCGCCAGACTCCCATGAAAACTCCTCGCCCTCAGCCTCTCCCGCAGCGGAACCGACTCCCTCCGC 3150
3151 CTTGCCCTTTCAACCCTCAGCACCAAGACATATGCCACAGCCCAACCGTTGCCGGCTCCTCTCCTTCCTG 3220

Figure 5.7: The amino acid alignments of the putative NorA/B and partial VerB proteins.

NorA/B

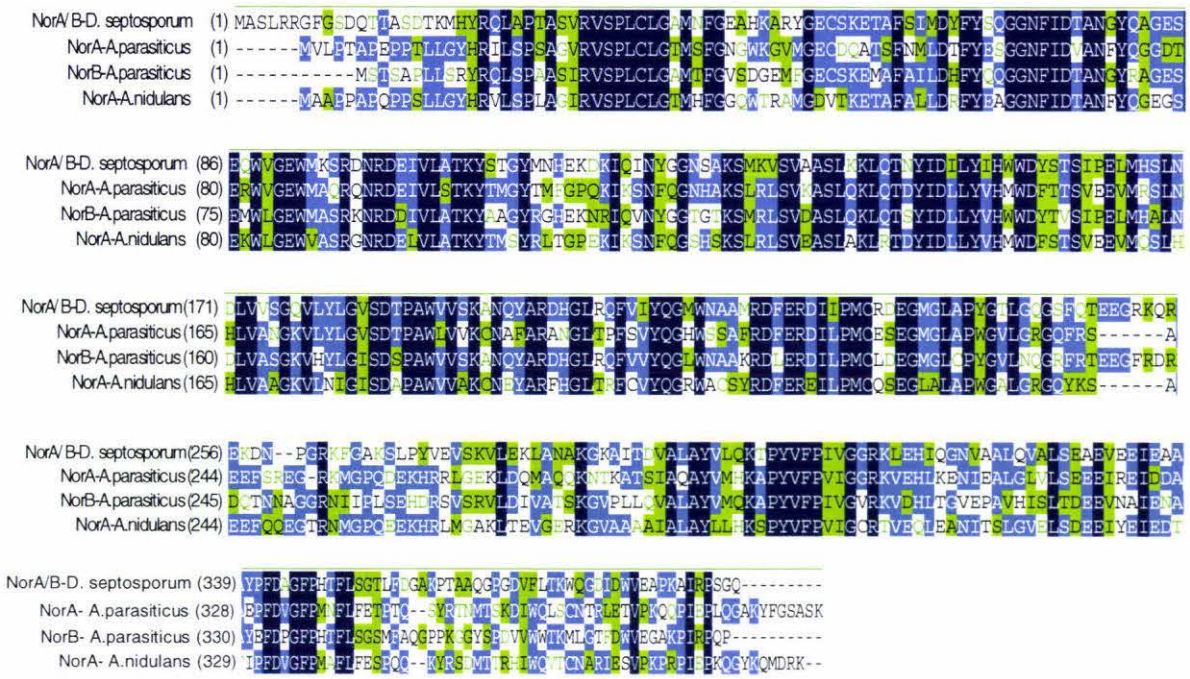

The initiation codon of the NorA/B was predicated based on the alignment results.

Partial VerB

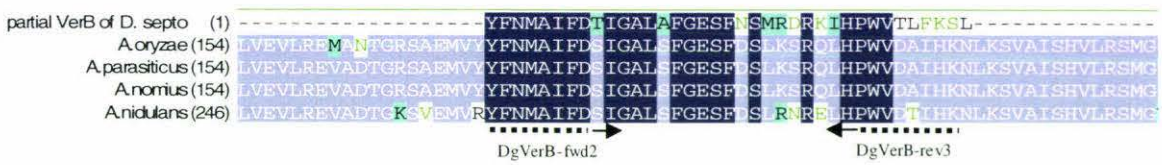

▪▪▪▪ : The position of the primers; →: the direction of primer extension.

5.3 DISCUSSION

5.3.1 Obtaining the novel dothistromin biosynthetic genes

By using degenerate PCR and *D. septosporum* genomic library screening, two novel DOTH biosynthetic genes, *norA/B* and *verB* (partial sequence) have been identified.

For *norA/B*, when comparing the sequence results from inverse PCR and the degenerate PCR clone pR268, inverse PCR did not obtain the whole putative ORF region of the *norA/B*. However, the identified nucleotide sequences of the *norA/B* from inverse PCR exactly matched the *norA/B* sequences from pR268. From the BLASTX results from Table 5.2 and 5.3, the NorA/B protein of *D. septosporum* had more similarity to the NorB protein than NorA. This was further confirmed by comparison of amino acid identity between this putative NorA/B protein to NorA/B proteins of other *Aspergillus* species (Table 5.4). The NorA/B of *D. septosporum* has 60.7% amino acid identity to the NorB of *A. parasiticus*, only 45.9% identity to NorA of *A. parasiticus* and 43.4% identity to NorA of *A. nidulans*. These findings suggest that the newly found *norA/B* gene is more likely the *norB* and not the *norA*. So far, no evidence supports that *D. septosporum* has both NorA and NorB protein. This is similar to the *A. nidulans*, only *norA* has been identified in the ST synthetic cluster (Yu *et al.*, 2004b).

Table 5.4: Amino acid identity of NorA/B between *D. septosporum* and *Aspergillus* species

Amino acid identity	NorA/B of *D. septosporum*	NorA of *A. nidulans*	NorB of *A. parasiticus*
NorA of *A. parasiticus*	45.9%	65.3%	47.1%
NorB of *A. parasiticus*	60.7%	45.6%	
NorA of *A. nidulans*	43.4%		

For *verB*, the degenerate PCR product was only 100 bp, however, it still had high amino acid similarity with other VerB proteins of *Aspergillus* species in the short amplified region between the PCR primers (Fig. 5.7). Inverse PCR did not achieve any products to

extend this 100 bp fragment and this is possibly due to the sub-optimal PCR conditions and DNA amount used in ligation. An early report demonstrated that the outcome of ligation is affected by the expected DNA size and the amount used in ligation (Dugaiczyk *et al.*, 1975). Therefore, further optimization of ligation and PCR conditions should be tried. Once a longer fragment of the *verB* is obtained, the probe can be designed to screen the genomic library as same as the *norA/B*. In this project, inverse PCR usually gave quite a few products (Fig. 5.3C, D) and their sizes were variable between each independent PCR (results not shown). Only two PCR products from them had been cloned and sequenced (Section 5.2.3, Table 5.2) and further characterization of other products could be done. However, using the probe derived from the known 100 bp *verB* fragment to screen the genomic library directly is still an option.

5.3.2 The possible roles of the *norA/B* and *verB* in dothistromin biosynthesis

The putative NorA/B in *D. septosporum* has high amino acid identity to its homologous proteins in *Aspergillus* species. Therefore, the possible function of the NorA/B in *D. septosporum* can be predicted by studying NorA and NorB proteins in *Aspergillus* species. In the AF biosynthetic pathway (Fig. 5.8), NORA is converted to AVN by reductase/ dehydrogenase enzymes. NorA and NorB participate in the reaction along with reductase, Nor-1. Deletion of *norA* and *norB* in *A. parasiticus,* showed no effects on the NORA to AVN reaction or on aflatoxin production. Yu *et al.* (2004b) postulated that this might be due to the redundancy and compensation by the other two NOR reductase/dehydrogenases. However, in *A. nidulans*, disruption of *norA* (stcV) did not impact ST production (McDonald *et al.*, 2005) either. Therefore, if the NorA/B in D. *septosporum* functions as its homologues in *Aspergillus* species, deletion of the NorA/B possibly would not affect dothistromin production. Indeed, more solid experimental evidence is required to characterize the true function of the *norA/B* in *D. septosporum.*

The *verB* gene encodes a desaturase (P450 monooxygenase), which converts VERB to VERA in the AF biosynthetic pathway (Fig. 5.8). Kelkar *et al.* (1997) demonstrated that

deletion of *verB* in *A. nidulans* prevented ST synthesis and resulted in the accumulation of VERB. Therefore, they suggested that the P450 monooxygenase was required for ST synthesis. In *D. septosporum*, the complete ORF sequences of the *verB* gene need to be identified and its function can then be determined by targeted gene disruption.

Figure 5.8: The schematic AF biosynthetic pathway

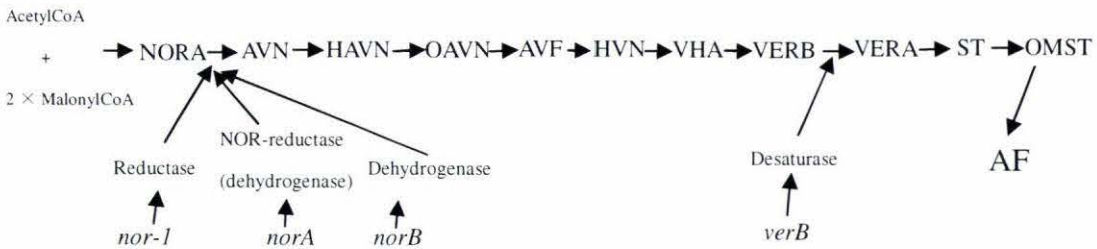

NOR, norsolorinic acid; AVN, averantin; HAVN, hydroxyaverantin; OAVN, oxoaverantin; AVF, averufin; HVN, hydroxyversicolorone; VHA, versicolorone hemiacetal acetate; VERB, versicolorin B; VERA, versicolorin A; ST, sterigmatocystin; OMST: o-methyl sterigmatocystin; AF, aflatoxin

5.3.3 The dothistromin biosynthetic clusters

Different to the highly clustered AF/ST biosynthetic genes, the dothistromin gene clusters are separated into three mini-clusters (Fig 1.3). The dothistromin genes are separated by other "non-dothistromin" genes. Real time PCR analysis of the expression of dothistromin genes and "non-dothistromin" genes revealed that they had different expression patterns and thus indicated that they were possibly under different regulation mechanisms (Zhang *et al.*, 2007).

The *norA/B* containing clone pR268 is the fourth mini gene cluster isolated from a *D. septosporum* genomic library. Three "non-dothistromin" genes have been identified upstream of the putative *norA/B* ORF. The protein AflR is considered as an important factor to regulate the expression of AF/ST genes. Two possible AflR binding motifs have been found upstream of the *norA/B* (Fig. 5.6), as also found in most of the other dothistromin genes. However, only approximate 0.6 Kb sequence downstream of the

norA/B ORF was obtained. This short fragment could not provide enough information to determine if other dothistromin genes are adjacent to *norA/B*. Sequence analysis did not show any overlapping of the pR268 to the other three mini-clusters. Whether pR268 is an independent cluster and whether it is located on the 1.3 Mb mini-chromosome along with the other mini-clusters will be the focus of future work.

CHAPTER SIX: CONCLUSIONS AND FUTURE WORK

In this research, the subcellular localization of DotC was observed by constructing *dotC-egfp* transformed *D. septosporum* mutants and the *dotC* biological function was characterized by targeted gene disruption. Two putative dothistromin biosynthetic genes, *norA/B* and *verB* (partial sequence) were also identified in the *D. septosporum* genome.

6.1 LOCALIZATION OF THE DOTC PROTEIN

Based on the similarity of DotC amino acid sequence to other fungal MFS transporters and the typical MFS feature (14 predicted TMDs) existing in the DotC protein, *dotC* is proposed to encode a MFS membrane transporter. The confocal microscopy images of two *dotC-egfp* integrated mutants (FJT73 and FJT75) provided evidence that the DotC protein is mainly targeted to the plasma membrane. Green fluorescence was condensed in the margins and septa of the hyphae, particularly in FJT73. The cross section images of FJT73 clearly showed that green fluorescence formed a hollow circle, which indicated that the DotC-eGFP fusion proteins were targeted to the plasma membrane. In contrast to FJT73, much stronger fluorescence was observed in FJT75, possibly in vesicles, vacuoles or peroxisomes. Based on the Southern analysis, the different fluorescence distribution between the FJT73 and FJT75 was possibly due to the different integration patterns (i.e. copy numbers or location) of the *dotC-egfp* constructs.

Although real-time PCR showed that the *dotC* gene is constitutively expressed, the green fluorescence was also observed in the margin of the *dotC-egfp* colonies at a high level. This suggested that more active metabolism was occurring in the young hyphae or alternatively the post-transcriptional regulation occurred so that the DotC protein was not constitutively translated.

Future work will be focused on more intensive studies of the microscopy images by comparing the FJT73 and FJT75 and with other *dotC-egfp* integrated mutants (with different integrated patterns) and using some particular stains (e.g FM4-64) to determine what those strong fluorescence dots are. More phenotypes of those mutants can be further examined since FJT73 and FJT75 had multiple copies of integrated *dotC-egfp* fusion gene. Therefore, the dothistromin production, the toxin resistance ability and the virulence ability of those mutants are all interesting parameters to further evaluate the *dotC* gene's function.

6.2 TARGETED DISRUPTION OF THE DOTC GENE

The biological function of the *dotC* gene was characterized by targeted gene disruption. As a MFS transporter encoding gene, the *dotC* may be involved in secreting the dothistromin and/or as a self-protection function against its own toxin.

The Southern blotting analysis indicated that *dotC* was present in a single copy in the *D. septosporum* genome. Two *dotC* disrupted mutants (FJT15 and FJT16) did not show significant growth difference to the WT over the 28 days and also had no significantly different sporulation rate to the WT. For the toxin production assay of these two mutants, a dramatic dothistromin reduction was observed both in the filtrates and in the toxin extraction from the mycelia when compared to the WT. Furthermore, the two *dotC* mutants had a similar level of toxin reduction in both filtrate and mycelium. FJT15 had ~ 14% toxin yield in filtrate than the WT and ~12% in mycelia. FJT16 had only ~5.2% toxin yield in filtrate and ~5.3% in mycelia. No toxin accumulation was observed in mycelia of the mutants. This is necessary for fungal survival since too high a toxin concentration accumulated in the cell would be lethal. These results did not provide evidence to indicate that DotC protein is involved in toxin secretion, while, it did implicate *dotC* with a role in dothistromin production. At this stage, it is still unknown whether DotC protein has a direct effect on the synthesis of the toxin or whether

reduced toxin secretion in *dotC* mutants results in a decreased toxin production due to a feedback process.

The dothistromin resistance assay showed that FJT15 and FJT16 had significantly slower growth in the exponential phase in the presence of dothistromin than in the non-toxin control condition. In addition, FJT16 showed significantly slower growth than the WT with dothistromin. Although FJT15 had average smaller colony size than WT in the exponential phase, this difference was not quite statistically significant (the P value was over 0.05 but less than 0.1). These findings suggested that the *dotC* may be involved in secretion of exogenously supplied dothistromin toxin.

To further characterize the biological function of *dotC*, future work could be carried out as follows:

1) Examine the expression of other dothistromin genes in *dotC* mutants by real-time PCR to determine any effects on other dothistromin genes due to the *dotC* disruption.
2) Repeat the dothistromin resistance assay with more biological replicates and using a wide range of dothistromin concentrations to get more accurate experimental data.
3) Competition assay can be done by inoculating the *dotC* mutants with other fungal species to check any inhibition that would be observed in the *dotC* mutants when comparing with the WT. A previous similar experiment showed that the dothistromin deficient mutant (the *pksA* mutant) was remarkably inhibited in its growth by other fungal species (Schwelm, 2007).
4) Repeat the dothistromin quantification by inoculating samples on agar plates in order to directly compare levels of dothistromin in mycelium with levels in the agar. Acetone extraction can be used to purify dothistromin from agar or from mycelium (Chang *et al.*, 2004). Then, the dothistromin concentration can be directly compared using thin layer chromatography (TLC) or ELISA (since the TLC is a semi-quantitative method). Recently, a MFS transporter-like gene *ctb*4 in *Cercospora nicotianae* has been reported that was responsible for secretion and

accumulation of cercosporin. In this research, the TLC was successfully applied to quantify the toxin production (Choquer *et al.*, 2007).

6.3 THE NOVEL DOTHISTROMIN SYNTHETIC GENES

By using degenerate PCR, the partial sequences of two novel dothistromin biosynthetic genes (*norA/B* and *verB*) were isolated from *D. septosporum* genome. The subsequent inverse PCR and *D. septosporum* genomic library screening identified the putative ORF of the *norA/B*. However, the attempts to expand the *verB* sequence by inverse PCR were not successful.

The putative NorA/B is a 393-amino acid-protein postulated to encode a dehydrogenase which converts norsolorinic acid to averantin in the early stage of DOTH/AF/ST synthesis. The putative NorA/B of *D. septosporum* has 60.7% amino acid identity to the NorB (AflF) of *A. parasiticus*, but only 45.9% identity to NorA (AflE) of *A. parasiticus* and 43.4% identity to NorA (StcV) of *A. nidulans*.

Two possible *aflR* regulatory binding sites were found at the upstream of the *norA/B* as in most of the other dothistromin genes. This suggests that the *norA/B* is co-regulated with other dothistromin genes by an AflR-like protein, although an *aflR*-like gene has not been identified in *D. septosporum* genome. The genomic library screening result showed that the *norA/B* was located in one end of an isolated ~13 Kb clone pR268. Three non-dothistromin genes have been found based on the primer walking sequence. Sequence analysis did not show any overlapping of the pR268 to the other three mini clusters; this finding suggests that the pR268 may be the fourth independent mini-cluster and further confirmed that the dothistromin genes are fragmented rather than clustered.

The *verB* is a putative desaturase encoding gene, which converts versicolorin B to

versicolorin A in the AF biosynthetic pathway. The identified partial sequence from degenerate PCR showed high amino acid similarity with other VerB proteins of *Aspergillus* species.

The identification of two novel putative dothistromin genes reinforces the similarity of the dothistromin biosynthetic pathway genes to these of AF/ST. The separation of dothistromin genes by non-dothistromin genes possibly suggests that the dothistromin clusters represent an ancestral form to the AF/ST (Cary and Ehrlich, 2006). The future work will firstly be to identify the ORF of the *verB* by screening the genomic library or by optimized inverse PCR. Secondly, to identify the downstream sequence of the *norA/B* will be very helpful to further study the arrangement of the dothistromin genes. Finally, the biological function of these two novel genes can be characterized by targeted gene disruption.

REFERENCES:

Albano, C. R., Lu, C. H., Bentley, W. E., and Rao, G. (2001). High throughput studies of gene expression using green fluorescent protein-oxidative stress promoter probe constructs - The potential for living chips. Journal of Biomolecular Screening *6*, 421-428.

Alexander, N. J., McCormick, S. P., and Hohn, T. M. (1999). TRI12, a trichothecene efflux pump from *Fusarium sporotrichioides*: gene isolation and expression in yeast. Molecular and General Genetics *261*, 977-984.

Ames, G. F., Nikaido, K., Groarke, J., and Petithory, J. (1989). Reconstitution of periplasmic transport in inside-out membrane vesicles energization by ATP. Journal of Biological Chemistry *264*, 3998-4002.

Azzaria, M., Schurr, E., and Gros, P. (1989). Discrete mutations introduced in the predicted nucleotide-binding sites of the *mdr1* gene abolish its ability to confer multidrug resistance. Molecular and Cellular Biology *9*, 5289-5297.

Barnes, I., Crous, P. W., Wingfield, B. D., and Wingfield, M. J. (2004). Multigene phylogenies reveal that red band needle bight of *Pinus* is caused by two distinct species of *Dothistroma, D. septosporum* and *D. pini*. Studies in Mycology *50*, 551-565.

Barron, N. (2006). Optimizing *Dothistroma septosporum* infection of *Pinus radiata* and the development of red-band disease. MSc thesis, Massey University, New Zealand.

Bassett, C., Buchanan, M., Gallagher, R. T., and Hodges, R. L. (1970). A toxic difuroanthraquinone from *Dothistroma pini*. Chemistry and Industry *26*, 1659-1660.

Bauer, B. E., Wolfger, H., and Kuchler, K. (1999). Inventory and function of yeast ABC proteins: about sex, stress, pleiotropic drug and heavy metal resistance. Biochimica Et Biophysica Acta-Biomembranes *1461*, 217-236.

Bear, C. A., Waters, J. M., and Waters, T. N. (1972). Crystal structure and absolute configuration of a derivative of dothistromin, a fungal toxin implcated in pine-needle blight. Journal of the Chemical Society-Perkin II, 2375-2378.

Bennett, J. W. (1979). Aflatoxins and anthraquinones from diploids of *Aspergillus parasiticus*. Journal of General Microbiology *113*, 127-136.

Bird, D., and Bradshaw, R. E. (1997). Gene targeting is locus dependent in the filamentous fungus *Aspergillus nidulans*. Molecular and General Genetics *255*, 219-225.

Bradshaw, R. E. (2004). Dothistroma (red-band) needle blight of pines and the dothistromin toxin: a review. Forest Pathology *34*, 163-185.

Bradshaw, R. E. (2006). From protoplasts to gene clusters. Mycologist *20*, 133-139.

Bradshaw, R. E., Bhatnagar, D., Ganley, R. J., Gillman, C. J., Monahan, B. J., and Seconi, J. M. (2002). *Dothistroma pini*, a forest pathogen, contains homologs of aflatoxin biosynthetic pathway genes. Applied and Environmental Microbiology *68*, 2885-2892.

Bradshaw, R. E., Bidlake, A., Forester, N., and Scott, D. B. (1997). Transformation of the fungal forest pathogen *Dothistroma pini* to hygromycin resistance. Mycological Research *101*, 1247-1250.

Bradshaw, R. E., Jin, H. P., Morgan, B. S., Schwelm, A., Teddy, O. R., Young, C. A., and Zhang, S. G. (2006). A polyketide synthase gene required for biosynthesis of the aflatoxin-like toxin, dothistromin. Mycopathologia *161*, 283-294.

Bullock, W. O., Fernandez, J.M., and Short, J.M. (1987). XL-1-Blue: a hihg efficiency plasmid transfroming *recA Escherichia coli* strain with b-galactosidase selection. Biotechniques *5*, 376-378.

Bulman., L. S., Gadgil., P. D., Kershaw., D. J., and Ray, J. W. (2004). Assessment and control of Dothistroma needle blight. Forest Resrarch Bulletin *229*.

Callahan, T. M., Rose, M. S., Meade, M. J., Ehrenshaft, M., and Upchurch, R. G. (1999). CFP, the putative cercosporin transporter of *Cercospora kikuchii*, is required for wild type cercosporin production, resistance and virulence on soybean. Molecular Plant Microbe Interactions *12*, 901-910.

Calvo, A. M., Wilson, R. A., Bok, J. W., and Keller, N. P. (2002). Relationship between secondary metabolism and fungal development. Microbiology and Molecular Biology Reviews *66*, 447-459.

Capecchi, M. R. (1989). Altering the genome by homologous recombination. Science *244*, 1288-1292.

Carson, S. D., and Carson, M. J. (1989). Breeding for resistance in forest trees, a quantitative genetic approach. Annual Review of Phytopathology *27*, 373-395.

Cary, J. W., and Ehrlich, K. C. (2006). Aflatoxigenicity in *Aspergillus*: molecular genetics, phylogenetic relationships and evolutionary implications. Mycopathologia *162*, 167-177.

Chalfie, M., Tu, Y., Euskirchen, G., Ward, W. W., and Prasher, D. (1994). Green fluorescent protein as a marker for gene expression. Science *263*, 802-805.

Chang, P. K., Yu, J. J., and Yu, J. H. (2004). *aflT*, a MFS transporter-encoding gene located in the aflatoxin gene cluster, does not have a significant role in aflatoxin secretion. Fungal Genetics and Biology *41*, 911-920.

Chiou, C. H., Lee, L. W., Owens, S. A., Whallon, J. H., Klomparens, K. L., Townsend, C. A., and Linz, J. E. (2004). Distribution and sub-cellular localization of the aflatoxin enzyme versicolorin B synthase in time-fractionated colonies of *Aspergillus parasiticus*. Archives of Microbiology *182*, 67-79.

Chiou, T. J., and Bush, D. R. (1996). Molecular cloning, immunochemical localization to the vacuole, and expression in transgenic yeast and tobacco of a putative sugar transporter from sugar beet. Plant Physiology *110*, 511-520.

Choquer, M., Dekkers, K. L., Chen, H. Q., Cao, L. H., Ueng, P. P., Daub, M. E., and Chung, K. R. (2005). The *ctb1* gene encoding a fungal polyketide synthase is required for cercosporin biosynthesis and fungal virulence of *Cercospora nicotianae*. Molecular Plant-Microbe Interactions *18*, 468-476.

Choquer, M., Lee, M. H., Bau, H. J., and Chung, K. R. (2007). Deletion of a MFS transporter-like gene in Cercospora nicotianae reduces cercosporin toxin accumulation and fungal virulence. Febs Letters *581*, 489-494.

Chung, K. R., Ehrenshaft, M., and Daub, M. E. (2002). Functional expression and cellular localization of cercosporin-resistance proteins fused with the GFP in *Cercospora nicotianae*. Current Genetics *41*, 159-167.

Danks, A. V., and Hodges, R. (1974). Polyhydroxyanthraquinones from *Dothistroma pini*. Australian Journal of Chemistry *27*, 1603-1606.

Debnam, P., Narayan, R., Cranshaw, N., Jones, W. T., Nicol, M., and Reynolds, P. H. S. (1994). Role of the fungal toxin dothistromin in resistance towards Dothistroma needle blight in *Pinus radiata*. Paper presented at: 1994 Annual meeting American Society of Plant Physiologists. (Portland, Oregon, USA).

Del Sorbo, G., Schoonbeek, H., and De Waard, M. A. (2000). Fungal transporters involved in efflux of natural toxic compound and fungicides. Fungal Genetics and Biology *30*, 1-15.

DelSorbo, G., Andrade, A. C., VanNistelrooy, J. G. M., VanKan, J. A. L., Balzi, E., and DeWaard, M. A. (1997). Multidrug resistance in *Aspergillus nidulans* involves novel ATP-binding cassette transporters. Molecular General Genetics *254*, 417-426.

deWaard, M. A. (1997). Significance of ABC transporters in fungicide sensitivity and resistance. Pesticide Science *51*, 271-275.

Dick, A. M. P. (1989). Control of Dothistroma needle blight in the *Pinus radiata* stands of Kinleith forest. New Zealand Journal of Forestry Science *19*, 171-179.

Dodge, M. A., Waller, R. F., Chow, L. M. C., Zaman, M. M., Cotton, L. M., McConville, M. J., and Wirth, D. F. (2004). Localization and activity of multidrug resistance protein 1 in the secretory pathway of *Leishmania parasites*. Molecular Microbiology *51*, 1563-1575.

Doyle, J. J., and Doyle, J. L. (1987). A rapid DNA isolation procedure for small quantities of fresh leaf tissue. Phytochemical Bulletin *19*, 11-15.

Du, W. L., Huang, Z. Y., Flaherty, J. E., Wells, K., and Payne, G. A. (1999). Green fluorescent protein as a reporter to monitor gene expression and food colonization by *Aspergillus flavus*. Applied and Environmental Microbiology *65*, 834-836.

Dubin, H. J., and Walper, S. (1967). *Dothistroma pini* on *Pseudotsuga menziesii*. Plant Disease Reporter *51*, 454.

Dugaiczyk, A., Boyer, H. W., and Goodman, H. M. (1975). Ligation of *EcoR*I endonuclease-generated DNA fragments into linear and circular structures. Journal of Molecular Biology *96*, 171-184.

Edwards, D. W., and Walker, J. (1978). Dothistroma needle blight in Australia. Australian Forest Research *8*, 125-137.

Elliott, G. S., Mason, R. W., Ferry, D. G., and Edwards, I. R. (1989). Dothistromin risk assessment for forestry workers. New Zealand Journal of Forestry Science *19*, 163-170.

Ferguson, L. R., Parslow, M. I., and McLarin, J. A. (1986). Chromosome damage by dothistromin in human peripheral-blood lymphocyte cultures -a comparison with aflatoxin B-1. Mutation Research *170*, 47-53.

Franich, R. A., Carson, M. J., and Carson, S. D. (1986). Synthesis and accumulation of benzoic acid in *Pinus radiata* needles in response to tissue injury by dothistromin, and correlation with resistance of *Pinus radiata* families to *Dothistroma pini*. Physiological and Molecular Plant Pathology *28*, 267-286.

Gadgil, P. D. (1984). Dothistroma needle blight. Forest Pathology in New Zealand *5*, 1-8.

Gadgil, P. D., and Holden, G. (1976). Effect of light intensity on infection *Pinus radiata* by *Dothistroma pini*. New Zealand Journal of Forestry Science *6*, 67-71.

Gallaghe, R. T., and Hodges, R. (1972). Chemistry of Dothistromin, a Difuroanthraquinone from *Dothistroma pini*. Australian Journal of Chemistry *25*, 2399-2407.

Gardiner, D. M., Jarvis, R. S., and Howlett, B. J. (2005). The ABC transporter gene in the sirodesmin biosynthetic gene cluster of *Leptosphaeria maculans* is not essential for sirodesmin production but facilitates self-protection. Fungal Genetics and Biology *42*, 257-263.

Gibson, I. (1972). Dothistroma blight of *Pinus radiata*. Annual Review of Phytopathology *10*, 51-72.

Gibson, I. (1974). Impact and control of Dothistroma blight of pines. European Journal of Forest Pathology *4*, 89-100.

Gilmour, J. W. (1981). The effect of season on infection of *Pinus radiata* by *Dothistroma pini*. European Journal of Forest Pathology *11*, 265-269.

Griffith, J. K., Baker , M. E., rouch , D. A., Page , M. G., Skurray, R. A., Paulsen, I. T., Chater, K. F., Baldwin , S. A., and Henderson , P. J. (1992). Membrane transport proteins: implications of sequence comparisons. Current Opinion in Cell Biology *4*, 684-695.

Hayashi, K., Schoonbeek, H. J., and De Waard, M. A. (2002). *Bcmfs1*, a novel major facilitator superfamily transporter from *Botrytis cinerea*, provides tolerance towards the natural toxic compounds camptothecin and cercosporin and towards fungicides. Applied and Environmental Microbiology *68*, 4996-5004.

Higgins, C. F., and Linton, K. L. (2001). The xyz of ABC transporters. Science *293*, 1782-1784.

Hotter, G. S. (1997). Elicitor-induced oxidative burst and phenylpropanoid metabolism in *Pinus radiata* cell suspension cultures. Australian Journal of Plant Physiology *24*, 797-804.

Ivory, M. H. (1967). A new variety of *Dothistroma pini* in Kenya. Transactions of the British Mycological Society *50*, 289-297.

Ivory, M. H. (1972). Resistance to Dothistroma needle blight induced in *Pinus radiata* by maturity and shade. Transactions of the British Mycological Society *59*, 205-212.

Jin, H. P. (2005). Further characterization of dothistromin genes in the fungal forest pathogen *Dothistroma septosporum*. MSc thesis, Massey University, New Zealand.

Jones, W. T., Harvey, D., Jones, S. D., Fielder, S., Debnam, P., and Reynolds, P. H. S. (1993). Competitive ELISA employing monoclonal antibodies specific for dothistromin. Food and Agricultural Immunology *5*, 187-197.

Karadzic, D. (1989). *Scirrhia pini* Funk et Parker. Life cycle of the fungus in plantations of *Pinus nigra* Arn in Serbia. European Journal of Forest Pathology *19*, 231-236.

Kelkar, H. S., Skloss, T. W., Haw, J. F., Keller, N. P., and Adams, T. H. (1997). *Aspergillus nidulans stcL* encodes a putative cytochrome P-450 monooxygenase required for bisfuran desaturation during aflatoxin/sterigmatocystin biosynthesis. Journal of Biological Chemistry *272*, 1589-1594.

Keller, N. P., and Hohn, T. M. (1997). Metabolic pathway gene clusters in filamentous fungi. Fungal Genetics and Biology *21*, 17-29.

Kuwayama, H., Obara, S., Morio, T., Katoh, M., Urushihara, H., and Tanaka, Y. (2002). PCR-mediated generation of a gene disruption construct without the use of DNA ligase and plasmid vectors. Nucleic Acids Research *30*.

Lee, L. W., Chiou, C. H., Klomparens, K. L., Cary, J. W., and Linz, J. E. (2004). Subcellular localization of aflatoxin biosynthetic enzymes Nor-1, Ver-1, and OmtA in time-dependent fractionated colonies of *Aspergillus parasiticus*. Archives of Microbiology *181*, 204-214.

Lorang, J. M., Tuori, R. P., Martinez, J. P., Sawyer, T. L., Redman, R. S., Rollins, J. A., Wolpert, T. J., Johnson, K. B., Rodriguez, R. J., Dickman, M. B., and Ciuffetti, L. M. (2001). Green fluorescent protein is lighting up fungal biology. Applied and Environmental Microbiology *67*, 1987-1994.

Magnani, E., Bartling, L., and Hake, S. (2006). From Gateway to MultiSite Gateway in one recombination event. Bmc Molecular Biology *7*.

March, J. C., Rao, G., and Bentley, W. E. (2003). Biotechnological applications of green fluorescent protein. Applied Microbiology and Biotechnology *62*, 303-315.

Martin, J. F., Casqueiro, J., and Liras, P. (2005). Secretion systems for secondary metabolites: how producer cells send out messages of intercellular communication. Current Opinion in Microbiology *8*, 282-293.

McDonald, T., Hammond, T., Noordermeer, D., Zhang, Y. Q., and Keller, N. (2005). The sterigmatocystin cluster revisited: lessons from a genetic model. Aflatoxin and Food Safety CRC/Taylor&Francis,Boca Raton,pp, 117-136.

Monahan, B. J. (1998). Identification of putative dothistromin genes. MSc thesis, Massey University, New Zealand.

Muller, T., Benjdia, M., Avolio, M., Voigt, B., Menzel, D., Pardo, A., Frommer, W. B., and Wipf, D. (2006). Functional expression of the green fluorescent protein in the ectomycorrhizal model fungus *Hebeloma cylindrosporum*. Mycorrhiza *16*, 437-442.

Nelissen, B., DeWachter, R., and Goffeau, A. (1997). Classification of all putative permeases and other membrane plurispanners of the major facilitator superfamily encoded by the complete genome of Saccharomyces cerevisiae. Fems Microbiology Reviews *21*, 113-134.

Ninomiya, Y., Suzuki, K., Ishii, C., and Inoue, H. (2004). Highly efficient gene replacements in *Neurospora* strains deficient for nonhomologous end-joining. Proceedings of the National Academy of Sciences of the United States of America *101*, 12248-12253.

Oliver, R. P., Roberts, I. N., Harling, R., Kenyon, L., Punt, P. J., Dingemanse, M. A., and Vandenhondel, C. (1987). Transformation of *Fulvia fulva*, a Fungal Pathogen of Tomato, to Hygromycin-B Resistance. Current Genetics *12*, 231-233.

Pao, S. S., Paulsen, I. T., and Saier, M. H. (1998). Major facilitator superfamily. Microbiology and Molecular Biology Reviews *62*, 1-34.

Peterson, G. W. (1973). Infection of Austrian and Ponderosa pines by *Dothistroma pini* in eastern Nebraska. Phytopathology *63*, 1060-1063.

Peterson, G. W. (1984). Resistance to *Dothistroma pini* within geographic seed sources of *Pinus ponderosa*. Phytopathology *74*, 956-960.

Pitkin, J. W., Panaccione, D. G., and Walton, J. D. (1996). A putative cyclic peptide efflux pump encoded by the *toxA* gene of the plant-pathogenic fungus *Cochliobolus carbonum*. Microbiology-Uk *142*, 1557-1565.

Prasher, D. C., Eckenrode, V. K., Ward, W. W., Prendergast, F. G., and Cormier, M. J. (1992). Primary structure of the *Aequorea victoria* green fluorescent protein. Gene *111*, 229-233.

Punt, P. J., and Vandenhondel, C. (1992). Transformation of filamentous fungi based on hygromycin B and phleomycin resistance markers. Methods in Enzymology *216*, 447-457.

Reimann, S., and Deising, H. B. (2005). Inhibition of efflux transporter-mediated fungicide resistance in Pyrenophora tritici-repentis by a derivative of 4 '-hydroxyflavone and enhancement of fungicide activity. Applied and Environmental Microbiology *71*, 3269-3275.

Rekangalt, D., Verner, M. C., Kues, U., Walser, P. J., Marmeisse, R., Debaud, J. C., and Fraissinet-Tachet, L. (2007). Green fluorescent protein expression in the symbiotic basidiomycete fungus *Hebeloma cylindrosporum*. FEMS Microbiology Letters *268*, 67-72.

Roohparvar, R., De Waard, M. A., Kema, G. H. J., and Zwiers, L. H. (2007). MgMfs1, a major facilitator superfamily transporter from the fungal wheat pathogen *Mycosphaerella graminicola*, is a strong protectant against natural toxic compounds and fungicides. Fungal Genetics and Biology *44*, 378-388.

Schwelm, A. (2007). Investigations of dothistromin gene expression in *Dothistroma septosporum* and the putative role of dothistromin toxin. PhD Thesis, Massey University, New Zealand.

Schwelm, A., Barron, N., Zhang, S. G., and Bradshaw, R. E. (2007). Early expression of aflatoxin-like dothistromin genes in the forest pathogen *Dothistroma septosporum*. Mycological Research *doi:10.1016/j.mycres.2007.03.018*.

Seconi, J. M. (2001). Confirmation of the presence of a dothistromin biosynthetic gene cluster in the fungal forest pathogen *Dothistroma pini*. MSc thesis, Massey University, New Zealand.

Shain, L., and Franich, R. A. (1981). Induction of Dothistroma blight symptoms with dothistromin. Phytopathology *71*, 254-254.

Shaw, G. J., Chick, M., and Hodges, R. (1978). C-13 NMR-study of biosynthesis of anthraquinone dothistromin by *Dothistroma pini*. Phytochemistry *17*, 1743-1745.

Shimazu, M., Sekito, T., Akiyama, K., Ohsumi, Y., and Kakinuma, Y. (2005). A family of basic amino acid transporters of the vacuolar membrane from *Saccharomyces cerevisiae*. Journal of Biological Chemistry *280*, 4851-4857.

Skinnider, L., Stoessl, A., and Wang, J. (1989). Increased frequency of sister-chromatid exchange induced by dothistromin in Cho Cells and human-lymphocytes. Mutation Research *222*, 167-170.

Skory, C. D., Chang, P., and Linz, J. E. (1993). Regulated expression of the *nor-1* and *ver-1* genes associated with aflatoxin biosynthesis. Applied and Environmental Microbiology *59*, 1642-1646.

Southern, E. M. (1975). Detection of specific sequences among DNA fragments separated by gel electrophoresis. Journal of Molecular Biology *98*, 503-517.

Stergiopoulos, I., Zwiers, L. H., and De Waard, M. A. (2002). Secretion of natural and synthetic toxic compounds from filamentous fungi by membrane transporters of the ATP-binding cassette and major facilitator superfamily. European Journal of Plant Pathology *108*, 719-734.

Stoessl, A., and Stothers, J. B. (1985). Minor anthraquinonoid metabolites of *Cercospora arachidicola*. Canadian Journal of Chemistry-Revue Canadienne De Chimie *63*, 1258-1262.

Teddy, O. R. (2004). Further characterization of the dothistromin gene cluster of *Dothistroma pini*. MSc thesis, Massey University, New Zealand.

Tenreiro, S., Rosa, P. C., Viegas, C. A., and Sa-Correia, I. (2000). Expression of the *azr1* gene (ORF YGR224w), encoding a plasma membrane transporter of the major facilitator superfamily, is required for adaptation to acetic acid and resistance to azoles in *Saccharomyces cerevisiae*. Yeast *16*, 1469-1481.

Trail, F., Mahanti, N., and Linz, J. (1995). Molecular biology of aflatoxin biosynthesis. Microbiology *141*, 755-765.

Tsien, R. Y. (1998). The green fluorescent protein. Annual Review of Biochemistry *67*, 509-544.

Upchurch, R. G., Rose, M. S., Eweida, M., and Callahan, T. M. (2002). Transgenic assessment of CFP-mediated cercosporin export and resistance in a cercosporin-sensitive fungus. Current Genetics *41*, 25-30.

Vanderpas, J. B. (1981). Reduced early growth rates of *Pinus radiata* caused by *Dothistroma pini*. New Zealand Journal of Forestry Science *11*, 210-220.

Vollmer, S. J., and Yanofsky, C. (1986). Efficient cloning of genes of *Neurospora crassa*. Proceedings of the National Academy of Sciences of the United States of America *83*, 4869-4873.

Voss, T., Schulte, J., and Tudzynski, B. (2001). A new MFS-transporter gene next to the gibberellin biosynthesis gene cluster of *Gibberella fujikuroi* is not involved in gibberellin secretion. Current Genetics *39*, 377-383.

Walker, D., Htun, H., and Hager, G. L. (1999). Using inducible vectors to study intracellular trafficking of GFP-tagged steroid/nuclear receptors in living cells. Methods-a Companion to Methods in Enzymology *19*, 386-393.

Walker, J. E., Saraste, M., Runswick, M. J., and Gay, N. J. (1982). Distantly Related Sequences in the Alpha-Subunits and Beta-Subunits of Atp Synthase, Myosin, Kinases and Other Atp-Requiring Enzymes and a Common Nucleotide Binding Fold. Embo Journal *1*, 945-951.

Whyte, A. G. D. (1976). Spraying pine plantations with fungicides - the manager's dilemma. Forest Ecology and Management *1*, 7-19.

Woods, A. J. (2003). Species diversity and forest health in northwest British Columbia. Forestry Chronicle *79*, 892-897.

Woods, A. J., Coates, K. D., and Hamann, A. (2005). Is an unprecedented Dothistroma needle blight epidemic related to climate change? Bioscience *55*, 761-769.

Yelton, M. M., Hamer, J. E., and Timberlake, W. E. (1984). Transformation of *Aspergillus nidulans* by using a *trpC* plasmid. Proceedings of the National Academy of Sciences of the United States of America-Biological Sciences *81*, 1470-1474.

Youngman, R. J., and Elstner, E. F. (1984). Photodynamic reductive mechanisms of oxygen activation by the fungal phytotoxins, cercosporin and dothistromin. Oxygen Radicals in Chemistry and Biology Ed by WBors and M Saran Berlin,New York,Walter de Gruyter and Co, 501-508.

Yu, J. H., and Keller, N. (2005). Regulation of secondary metabolism in filamentous fungi. Annual Review of Phytopathology *43*, 437-458.

Yu, J. J., Bhatnagar, D., and Cleveland, T. E. (2004a). Completed sequence of aflatoxin pathway gene cluster in *Aspergillus parasiticus*. Febs Letters *564*, 126-130.

Yu, J. J., Chang, P. K., Ehrlich, K. C., Cary, J. W., Bhatnagar, D., Cleveland, T. E., Payne, G. A., Linz, J. E., Woloshuk, C. P., and Bennett, J. W. (2004b). Clustered pathway genes in aflatoxin biosynthesis. Applied and Environmental Microbiology *70*, 1253-1262.

Yuk, I. H. Y., Wildt, S., Jolicoeur, M., Wang, D. I. C., and Stephanopoulos, G. (2002). A GFP-based screen for growth-arrested, recombinant protein-producing cells. Biotechnology and Bioengineering *79*, 74-82.

Zhang, S., Schwelm, A., Jin, H. P., Collins, L. J., and Bradshaw, R. E. (2007). A fragmented aflatoxin-like gene cluster in the forest pathogen *Dothistroma septosporum*. Fungal Genetics and Biology *doi:10.1016/j.fgb.2007.06.005*.

Zhong, J., Karberg, M., and Lambowitz, A. M. (2003). Targeted and random bacterial gene disruption using a group II intron (targetron) vector containing a retrotransposition-activated selectable marker. Nucleic Acids Research *31*, 1656-1664.

Zimmer, M. (2002). Green fluorescent protein (GFP): applications, structure, and related photophysical behavior. Chemical Reviews *102*, 759-781.

APPENDIX I: MEDIA

All media were prepared with Milli-Q water and sterilized by autoclaving at 121 °C for 15 minutes. Media were cooled to approximately 50°C before addition of antibiotics.

A1.1 *E. coli* Media

Luria Broth (LB) (g/L): Tryptone (Becton, Dickison and company), 10; NaCl, 5; Yeast extract (Becton, Dickison and company), 5.

LB solid media (g/L): Tryptone, 10; NaCl, 5; Yeast extract, 5; Agar, 15.

Selective LB media

Supplements were added at the following final concentrations.

(μg/mL) Ampicillin, 100; Kanamycin sulphate, 50; isopropylthio-β-D-galactoside (IPTG), 30; 5-bromo 4-chloro 3-indolyl-β-D-galactoside (X-gal), 60.

A1.2 *D. septosporum* Media

***D. septosporum* medium (DM)**

(g/L) Malt extract (Oxoid), 50.0; Nutrient agar (Oxoid), 28.0.

Low *D. septosporum* Broth (LDB)

(g/L) Nutrient broth (Oxoid), 23; Malt extract (Oxoid), 23.

***D. septosporum* Sporulation Medium (DSM)**

(g/L) Malt extract (Oxoid), 15; Yeast extract (BD), 5; Agar, 20.

Potato Dextrose Medium (PDA)

(g/L) Potato dextrose agar, 39.

A1.3 *D. septosporum* Transformation Media

***D. septosporum* Top media (DM Top)**

(g/L) Malt extract, 50.0; Nutrient Agar, 11.2: Sucrose, 273.9 (0.8 M).

Osmotically Stabilised DM (DM Suc)

(g/l) Malt extract, 50.0; Nutrient Agar, 28.0: Sucrose, 273.9 (0.8 M).

Selective DSM and DM

Media used to select for hygromycin resistant *D. septosporum* transformants contained (μg/ml): Hygromycin B (Sigma), 70.

Appendix II: BUFFERS AND SOLUTIONS

All solutions were prepared with Milli-Q water and sterilized by autoclaving at 121°C for 15 minutes, unless otherwise stated.

A2.1 Common Buffers and solutions

TE Buffer

10 mM Tris-HCl and 1mM Na_2EDTA (TE 10:1) prepared from 1 M Tris-HCl (pH 8.0) and 250 mM Na_2EDTA (pH 8.0) stock solutions

1 x TBE Buffer

89 mM Tris-HCl, 2.5 mM Na_2EDTA and 89 mM Boric acid (pH 8.3).

Ethidium Bromide

Agarose gels were stained in ethidium bromide prepared as follows: 1 µl of 10 mg/ml stock per 10 ml of MilliQ water to give a final concentration of 1 µg/ml.

RNAseA (DNAse free)

10 mg/mL RNAse was dissolved in 0.01M Sodium acetate (pH 5.2) and placed in a boiling water bath for 15 minutes. This was cooled slowly to room temperature and 0.1 volumes of Tris-HCl (pH 7.4) added and stored at -20°C.

Gel Loading Buffer (10x)

2 M Urea, 50% (v/v) glycerol, 50 mM Tris acetate, 0.4% (w/v) bromophenol blue and 0.4% (w/v) xylene cyanol.

1×TNE buffer

10 mM Tris-HCl, 1 mM Na_2EDTA and 100 mM NaCl, pH 7.4.

Green buffer

0.1 M NaCl; 10 mM Tris-HCl; 1 mM EDTA and 0.5%Triton X-100, PH 8.0.

A2.2 Genomic DNA isolation Buffers

Lysis buffer

40 mM Tris-Acetate pH 7.8; 20 mM Sodium Acetate; 1 mM EDTA; 1% SDS.

CTAB buffer

2% CTAB (w/v), 1% PVP40 (w/v), 5 M NaCl, 0.5 M EDTA, 1 M Tris-HCl.

A2.3 Reagents for *D. septosporum* Transformation

OM buffer: 1.4 M $MgSO_4 \cdot 7H_20$, with 10 mM Na_2HPO_4/100 mM NaH_2PO_4 buffer, pH 5.8.

ST buffer: 1.0 M Sorbitol, 100 mM Tris-HCl (pH 8.0).

STC Buffer: 1.0 M Sorbitol, 50 mM Tris-HCl (pH 8.0), 50 mM $CaCl_2$.

40% PEG: 40 g PEG 6000 in 100 ml STC buffer.

Glucanex: 10 mg/ml in OM buffer.

A2.4 Reagents for Southern Blotting and Hybridization

Denaturing Solution: 500 mM NaOH, 500 mM NaCl.

Neutralising Solution: 500 mM Tris (pH 7.4), 2 M NaCl.

20 × SSC: 3 M NaCl, 0.2 M tri-sodium citrate, pH 7.0.

Wash Solution I (low stringency): 2 x SSC, 0.1% SDS.

Wash Solution II (high stringency): 0.5 × SSC, 0.1% SDS.

Buffer I: 100 mM Tris, 150 mM NaCl, pH 7.5.

Buffer II: 1% blocking reagent (Roche Applied Science), in Buffer I.

Buffer III: 100 mM Tris-HCl, 100 mM NaCl, 50 mM $MgCl_2$, pH 9.5.

Antibody solution: Anti-Digoxigenin AP diluted 1:10000 in Buffer II.

Stripping buffer: 0.2 M NaOH, 0.1% (v/v) SDS.

A2.5 Reagents for ELISA

Phosphate-buffered saline (PBS 10X):
8% NaCl (BDH), 2.9% Na_2HPO_4 (BDH), 0.2% KH_2PO_4 (BDH), PH 7.4.

Phosphate-buffered saline plus 0.1% Tween 20 (PBST):
1× PBS and 0.1% Tween 20 (Difco).

Skim milk powder (BSA):
1% skim milk powder (Pams), 1% PBS and 1% thiomersal (BDH).

Dilution buffer (per ELISA plate)
PBS (10 ×) 8 ml, RO water 32 ml, milk powder 0.8 g, Tween 20 80 µl.

Dilution buffer and broth (per ELISA plate)
Dilution buffer: growth media 1:1.

Working buffer (per ELISA plate)
Dilution buffer 10 ml, DMSO 15 µl.

Working buffer and broth (per ELISA plate)
Dilution buffer 20 ml, growth media 20 ml, and DMSO 40 µl.

Labeled peroxidase (per ELISA plate)
Dilution buffer 198 µl, 10C12 (dothistromin antibody) 2 µl makes 100-fold dilution. Add 40 µl of above dilution to 12 ml dilution buffer (make a final 30,000-fold dilution).

APPENDIX III: The DOTC-EGFP SEQUENCE

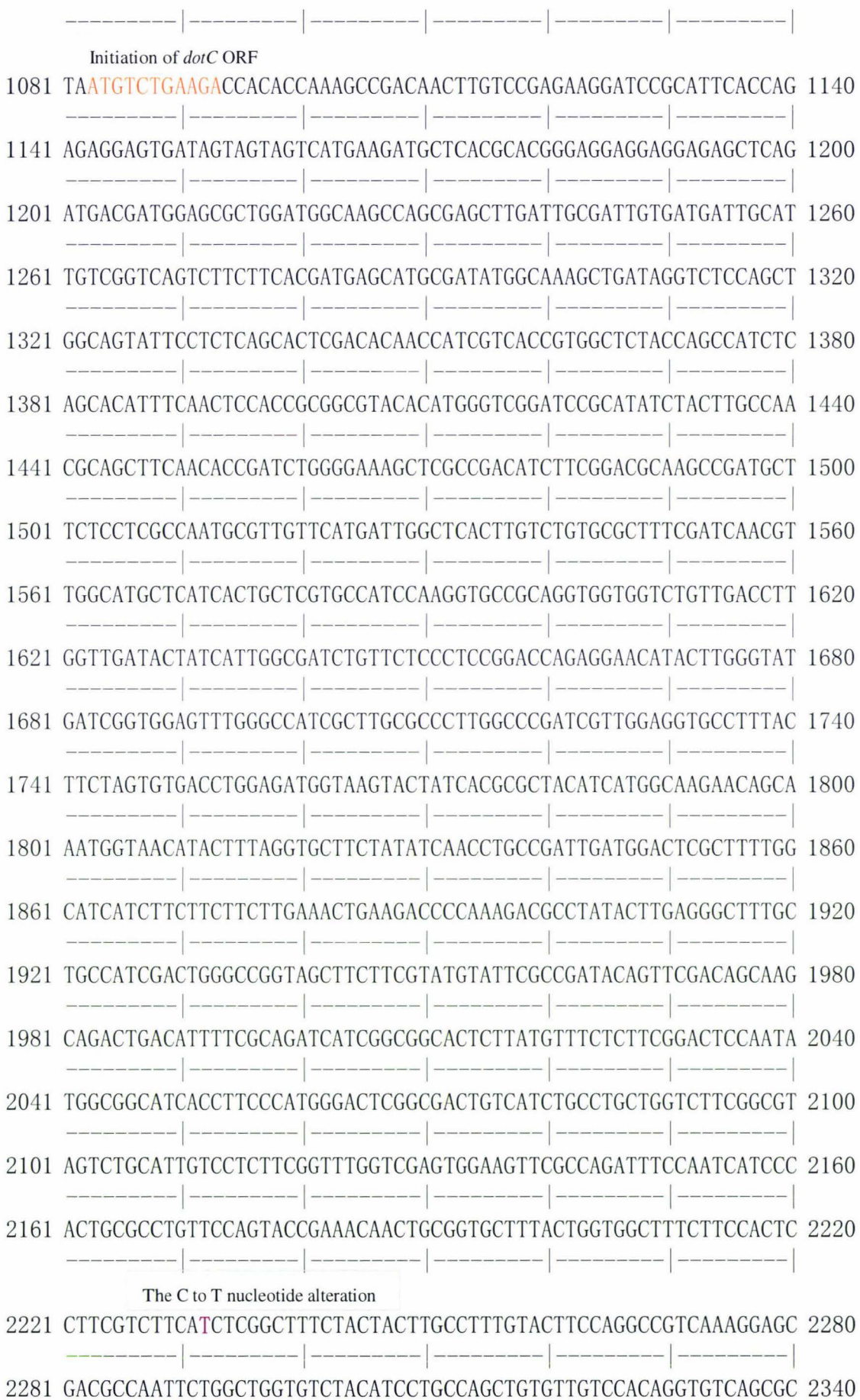
Initiation of *dotC* ORF
1081 TAATGTCTGAAGACCACACCAAAGCCGACAACTTGTCCGAGAAGGATCCGCATTCACCAG 1140
1141 AGAGGAGTGATAGTAGTAGTCATGAAGATGCTCACGCACGGGAGGAGGAGGAGAGCTCAG 1200
1201 ATGACGATGGAGCGCTGGATGGCAAGCCAGCGAGCTTGATTGCGATTGTGATGATTGCAT 1260
1261 TGTCGGTCAGTCTTCTTCACGATGAGCATGCGATATGGCAAAGCTGATAGGTCTCCAGCT 1320
1321 GGCAGTATTCCTCTCAGCACTCGACACAACCATCGTCACCGTGGCTCTACCAGCCATCTC 1380
1381 AGCACATTTCAACTCCACCGCGGCGTACACATGGGTCGGATCCGCATATCTACTTGCCAA 1440
1441 CGCAGCTTCAACACCGATCTGGGGAAAGCTCGCCGACATCTTCGGACGCAAGCCGATGCT 1500
1501 TCTCCTCGCCAATGCGTTGTTCATGATTGGCTCACTTGTCTGTGCGCTTTCGATCAACGT 1560
1561 TGGCATGCTCATCACTGCTCGTGCCATCCAAGGTGCCGCAGGTGGTGGTCTGTTGACCTT 1620
1621 GGTTGATACTATCATTGGCGATCTGTTCTCCCTCCGGACCAGAGGAACATACTTGGGTAT 1680
1681 GATCGGTGGAGTTTGGGCCATCGCTTGCGCCCTTGGCCCGATCGTTGGAGGTGCCTTTAC 1740
1741 TTCTAGTGTGACCTGGAGATGGTAAGTACTATCACGCGCTACATCATGGCAAGAACAGCA 1800
1801 AATGGTAACATACTTTAGGTGCTTCTATATCAACCTGCCGATTGATGGACTCGCTTTTGG 1860
1861 CATCATCTTCTTCTTCTTGAAACTGAAGACCCCAAAGACGCCTATACTTGAGGGCTTTGC 1920
1921 TGCCATCGACTGGGCCGGTAGCTTCTTCGTATGTATTCGCCGATACAGTTCGACAGCAAG 1980
1981 CAGACTGACATTTTCGCAGATCATCGGCGGCACTCTTATGTTTCTCTTCGGACTCCAATA 2040
2041 TGGCGGCATCACCTTCCCATGGGACTCGGCGACTGTCATCTGCCTGCTGGTCTTCGGCGT 2100
2101 AGTCTGCATTGTCCTCTTCGGTTTGGTCGAGTGGAAGTTCGCCAGATTTCCAATCATCCC 2160
2161 ACTGCGCCTGTTCCAGTACCGAAACAACTGCGGTGCTTTACTGGTGGCTTTCTTCCACTC 2220
The C to T nucleotide alteration
2221 CTTCGTCTTCATCTCGGCTTTCTACTACTTGCCTTTGTACTTCCAGGCCGTCAAAGGAGC 2280
2281 GACGCCAATTCTGGCTGGTGTCTACATCCTGCCAGCTGTGTTGTCCACAGGTGTCAGCGC 2340

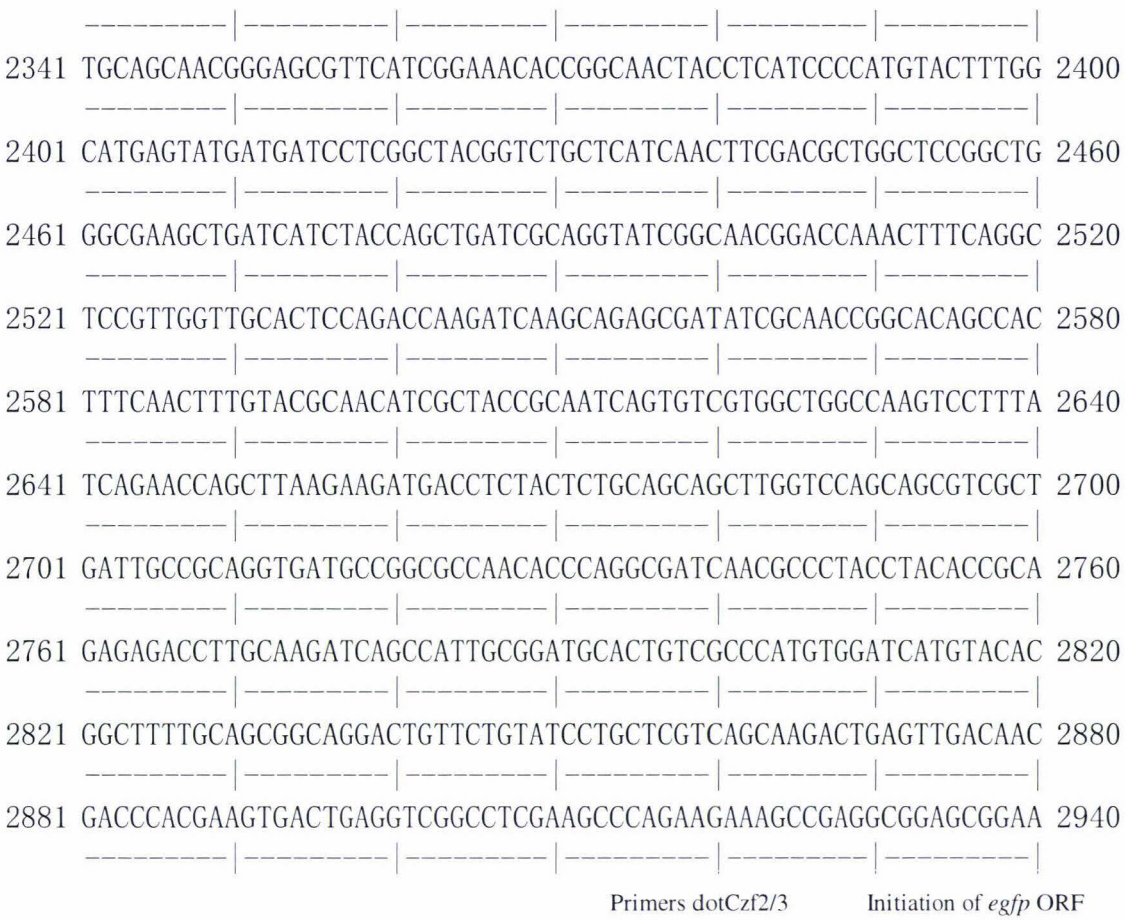
2341 TGCAGCAACGGGAGCGTTCATCGGAAACACCGGCAACTACCTCATCCCCATGTACTTTGG 2400
2401 CATGAGTATGATGATCCTCGGCTACGGTCTGCTCATCAACTTCGACGCTGGCTCCGGCTG 2460
2461 GGCGAAGCTGATCATCTACCAGCTGATCGCAGGTATCGGCAACGGACCAAACTTTCAGGC 2520
2521 TCCGTTGGTTGCACTCCAGACCAAGATCAAGCAGAGCGATATCGCAACCGGCACAGCCAC 2580
2581 TTTCAACTTTGTACGCAACATCGCTACCGCAATCAGTGTCGTGGCTGGCCAAGTCCTTTA 2640
2641 TCAGAACCAGCTTAAGAAGATGACCTCTACTCTGCAGCAGCTTGGTCCAGCAGCGTCGCT 2700
2701 GATTGCCGCAGGTGATGCCGGCGCCAACACCCAGGCGATCAACGCCCTACCTACACCGCA 2760
2761 GAGAGACCTTGCAAGATCAGCCATTGCGGATGCACTGTCGCCCATGTGGATCATGTACAC 2820
2821 GGCTTTTGCAGCGGCAGGACTGTTCTGTATCCTGCTCGTCAGCAAGACTGAGTTGACAAC 2880
2881 GACCCACGAAGTGACTGAGGTCGGCCTCGAAGCCCAGAAGAAAGCCGAGGCGGAGCGGAA 2940
Primers dotCzf2/3
Initiation of egfp ORF
2941 AGCAGAGAGACAAGCCAAGGATTTGGAGAAGGCCCAAAAGTCCATGGTGAGCAAGGGCGA 3000
3001 GGAGCTGTTCACCGGGGTGGTGCCCATCCTGGTCGAGCTGGACGGCGACGTAAACGGCCA 3060
3061 CAAGTTCAGCGTGTCCGGCGAGGGCGAGGGCGATGCCACCTACGGCAAGCTGACCCTGAA 3120
3121 GTTCATCTGCACCACCGGCAAGCTGCCCGTGCCCTGGCCCACCCTCGTGACCACCCTGAC 3180
3181 CTACGGCGTGCAGTGCTTCAGCCGCTACCCCGACCACATGAAGCAGCACGACTTCTTCAA 3240
3241 GTCCGCCATGCCCGAAGGCTACGTCCAGGAGCGCACCATCTTCTTCAAGGACGACGGCAA 3300
3301 CTACAAGACCCGCGCCGAGGTGAAGTTCGAGGGCGACACCCTGGTGAACCGCATCGAGCT 3360
3361 GAAGGGCATCGACTTCAAGGAGGACGGCAACATCCTGGGGCACAAGCTGGAGTACAACTA 3420
3421 CAACAGCCACAACGTCTATATCATGGCCGACAAGCAGAAGAACGGCATCAAGGTGAACTT 3480
3481 CAAGATCCGCCACAACATCGAGGACGGCAGCGTGCAGCTCGCCGACCACTACCAGCAGAA 3540
3541 CACCCCCATCGGCGACGGCCCCGTGCTGCTGCCCGACAACCACTACCTGAGCACCCAGTC 3600


3601 CGCCCTGAGCAAAGACCCCAACGAGAAGCGCGATCACATGGTCCTGCTGGAGTTCGTGAC 3660
The stop codonof egfp
3661 CGCCGCCGGGATCACTCTCGGCATGGACGAGCTGTACAAGTAAAGCGGCCGCACTTAACG 3720
3721 TTACTGAAATCATCAAACAGCTTGACGAATCTGGATATAAGATCGTTGGTGTCGATGTCA 3780
Primer pPN81 2978rev
3781 GCTCCGGAGTTGAGA 3795

APPENDIX IV: SOLVING THE PROBLEMS IN *D. SEPTOSPORUM* TRANSFORMATION

Background

As mentioned in Section 3.3.1, the first attempts of *D. septosporum* transformation had failed due to poor protoplast regeneration. Controls suggested that insufficient protoplasts had regenerated even under non-selective conditions. Therefore, the following experiments were designed to identify the problem(s) that impact protoplast regeneration.

Methods and discussions

Experiment 1:

Instead of incubation of *D. septosporum* mycelia with LDB media in 125 ml flask, the cellophane was firstly covered on the media of two DM and two PDA plates. Mycelia of NZE10 strain were resuspended in 5 ml sterile MilliQ water and then spread on the cellophane. After 7 days incubation at 22°C, the cellophanes covered with mycelia were placed in the Glucanex solution (10 mg/ml in OM buffer, 7 ml in each Petri dish) upside down. To check whether the OM buffer concentration was appropriate for maintaining the protoplast's activity , approximately 1.8 ml sterile MilliQ water was added to one of each DM or PDA dish, thus the final concentration of this diluted OM buffer was about 80% (80% OM) compared with other two undiluted dishes (100% OM). The Petri dishes were incubated overnight at 30°C with shaking at 100 rpm. After 4 hours and overnight enzyme digestion, the protoplast solutions were checked under microscopy to confirm the proper digestion status. The protoplast harvesting process was as same as the previous method except only washing two times with STC buffer. The protoplast concentration was counted before or after floating and the recovery rate was counted as well (Table A4.1). All the recovery rates were quite low,

less than 10%, which indicated that most protoplasts had been lost during harvesting. Also, the ratio of the protoplasts to spores was counted, which are 3.77: 1 and 1.42:1 in the floated protoplasts and the bottom pellet, respectively. This ratio indicated that a considerable amount of protoplasts had been spun down to the bottom as part of the pellet. Protoplasts were plated onto osmotically stabilized DM or PDA media. The "DM 100%" plate showed the highest protoplast concentration and indicated that the proper medium choice and correct OM buffer concentration.

Table A4.1: The protoplasts concentration before/after floating and the recover rate.

	Protoplast concentration before floating (per ml)	Protoplast concentration after floating (per ml)	Recovery rate
DM 100%	1.55×10^8	2.7×10^8	17.42%
DM 80%	5.04×10^7	4.5×10^7	8.9%
PDA 100%	9.6×10^6	9×10^7	93.8%
PDA 80%	1.0×10^7	8×10^7	80%

The "DM 100%" means that the protoplasts were harvested from the plate that mycelia had been grown on DM medium and digested with undiluted OM buffer. The "DM 80%" means that the protoplasts were harvested from the plate that mycelia had been grown on DM medium and digested with diluted 80% OM buffer.

The recovery rate was calculated by the equation as below:

Recovery rate = (Protoplast concentration before floating × volume of the protoplast before floating) / (Protoplast concentration after floating × final volume of the protoplast). In this experiment, the volume of the protoplast before floating was 5 ml; the final volume of the protoplast was 0.5 ml.

Based on the protocol, protoplasts are usually mixed with STC buffer and 40% PEG before transformation. Thus, the STC buffer and PEG are the two most important suspects to impact the protoplasts regeneration. In this experiment, protoplasts (DM 100%, 2.7×10^8 protoplasts/ml) were diluted either with STC buffer or with 40% PEG and 100μl of above dilutions were spread directly or embedded with the DMsuc top agar onto DMsuc medium. Table A4.2 shows the regenerated protoplast counts in those different dilutions. From the results, the 40% PEG appears to affect the regeneration of those protoplasts since all counts in PEG dilutions were much less than in STC buffer dilutions both in the spread or embedded plates. I also found that the counts in the embedded plates were less than the spread plates in the same dilutions. This showed that the lower counts in embedded plates might affect the

Experiment 2:

To further confirm the effect of our stock 40% PEG in the transformation, fresh 40% PEG solution was prepared and further stock was borrowed from another lab for comparing with the old stock PEG. The protoplast harvesting process was as same as the experiment one except the spin speed was reduced to 3000 rpm in both floating and washing steps in order to find the protoplasts yield in different spin speed. The final dilution fold of the protoplasts in usual transformation is less than 0.08 (80 µl protoplast plus 920 µl PEG). A further 10-fold dilution was made with the STC buffer. Table A4.3 shows the protoplasts yield in this experiment. The overall yield of the protoplast was less than in experiment one. Although the spin speed was changed, however, it seemed that the speed did not affect the yield of floated protoplasts (at least between the 5000rpm and 3000rpm) as similar protoplast:spore ratios were seen in both experiments. Table A4.4 clearly shows that the old 40% PEG dramatically decreased the regenerated protoplast counts both in spread and embedded plates. Moreover, the relatively high concentration PEG (12.5-fold) could kill more protoplasts than the lower concentration PEG (125-fold).

Table A4.3: Some general values of the protoplasts in experiment two.

The protoplasts concentration (per ml)		**Protoplasts/ spores ratio**	
Before floating	**After floating**	**Floated protoplasts**	**pellet**
7.9×10^7	6.7×10^7	3.1	1.7
Recover rate: 8.5%			

Table A4.4: Regenerated protoplast counts.

A: Protoplasts spread on DMsuc medium

	Old 40% PEG counts		Fresh 40% PEG counts		Other lab's 40% PEG counts	
Dilution factor	Plate1	Plate2	Plate1	Plate2	Plate1	Plate2
12.5	90	140	Numerous	Numerous	Numerous	Numerous
125	350	400	Numerous	Numerous	400	380
Colonies/ ml	4.7×10^5		-		4.9×10^5	
Regeneration %	0.70		-		0.73	

B: Protoplasts embedded in DMsuc top agar.

	Old 40% PEG counts		Fresh 40% PEG counts		Other lab's 40% PEG counts	
Dilution factor	Plate1	Plate2	Plate1	Plate2	Plate1	Plate2
12.5	None	None	Numerous	Numerous	Numerous	Numerous
125	300		600		500	
Colonies/ ml	3.75×10^5		7.50×10^5		6.25×10^5	
Regeneration %	0.56		1.12		0.93	

Conclusion

From the above two experiments, the 40% old PEG was the crucial factor that decreased the efficiency of protoplast regeneration, particularly at high concentrations of PEG. The embedded protoplasts did not regenerate as well as the spread protoplasts; however, embedding is not the critical factor for transformation.

APPENDIX V: PLASMID MAPS

Maps of plasmids used that were not shown before in this study. Vectors used in "Gateway system" can be referred to manufacturer's instructions.

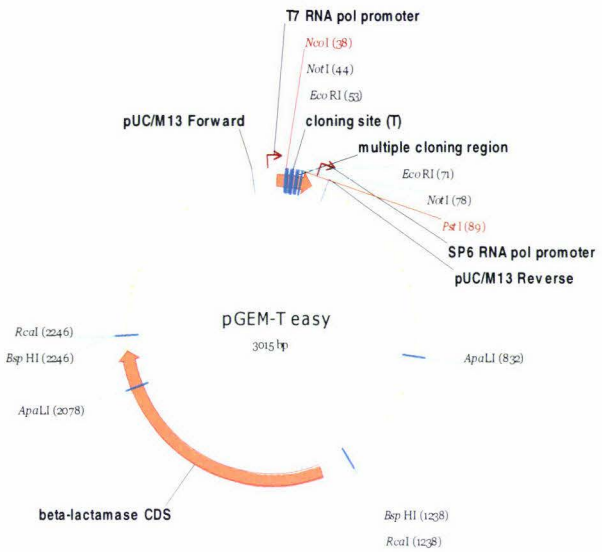

FigureA5.1: pGEMT-easy vector (Promega)

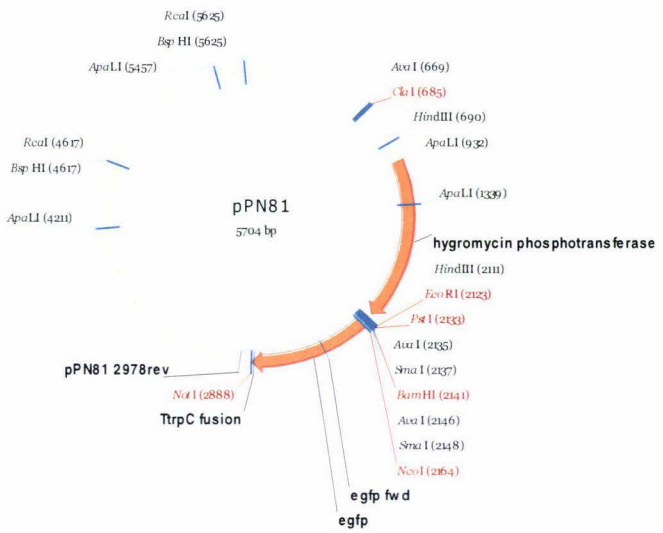

FigureA5.2: eGFP vector pPN81 (Schwelm, 2007)

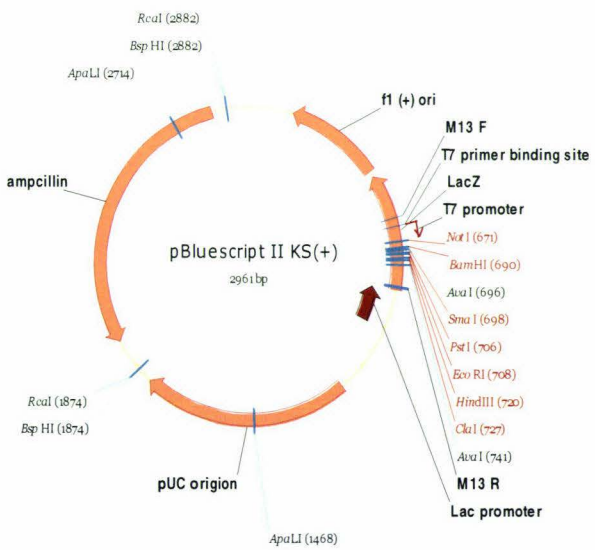

FigureA5.3: pBluescript II KS (+) vector (Stratagene)

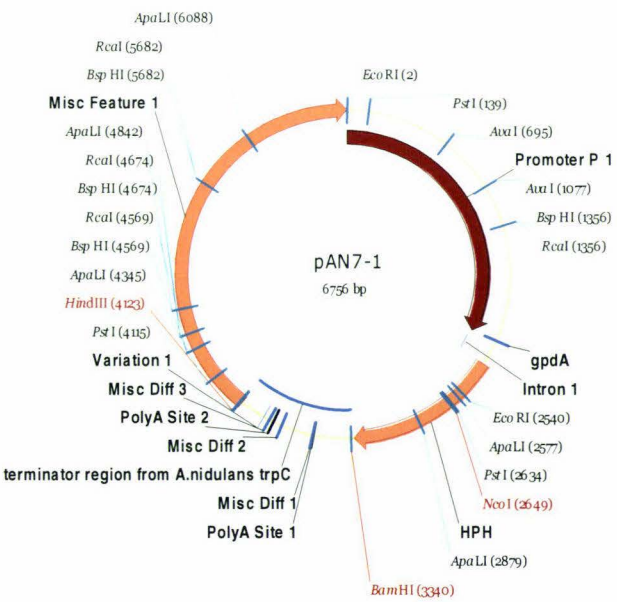

FigureA5.4: pAN7-1vector (Punt and Vandehondel, 1992)